

EPITHELIAL-MESENCHYMAL TRANSITION IN ORAL SQUAMOUS CARCINOMA CELLS

Minna Takkunen

Academic dissertation
Institute of Biomedicine / Anatomy
Faculty of Medicine
University of Helsinki

Helsinki University Biomedical Dissertations No. 137

EPITHELIAL-MESENCHYMAL TRANSITION IN ORAL SQUAMOUS CARCINOMA CELLS

Minna Takkunen

Institute of Biomedicine / Anatomy
Faculty of Medicine
University of Helsinki
Helsinki, Finland

ACADEMIC DISSERTATION

To be presented, with the permission of the Faculty of Medicine of the University of Helsinki, for public examination in Lecture Hall 3, Biomedicum Helsinki, Haartmaninkatu 8, Helsinki, on August 27th, 2010, at 12 noon.

Helsinki 2010

Supervised by:
Professor Ismo Virtanen
Institute of Biomedicine / Anatomy
University of Helsinki

Reviewed by:
Professor Tuula Salo
Department of Diagnostics and Oral Medicine
University of Oulu

Professor Veli-Jukka Uitto
Institute of Dentistry
University of Helsinki

Opponent:
Professor Olli Carpén
Institute of Pathology and Microbiology
University of Turku

Cover: Invadopodia of oral squamous carcinoma cells. Actin filaments (red), cortactin (green), nuclei (blue), overlay (yellow).
ISBN 978-952-92-7605-9 (paperback)
ISBN 978-952-10-6389-3 (PDF)
ISSN 1457-8433
http://ethesis.helsinki.fi
Helsinki University Print
Helsinki 2010

To Mamma and Pappa

Contents

1 LIST OF ORIGINAL PUBLICATIONS **6**
2 ABBREVIATIONS **7**
3 ABSTRACT **9**
4 REVIEW OF THE LITERATURE **11**
4.1. Progression of carcinomas 11
4.2. Oral squamous cell carcinoma (SCC) 12
4.3. Epithelial-mesenchymal transition (EMT) 13
4.3.1. Molecular definition of EMT 15
4.3.2. E- and N-cadherin 15
4.3.3. Transcription factors Snail and Slug 18
4.3.4. Transcription factors ZEB-1 and ZEB-2 20
4.4. Extracellular matrix (ECM) 21
4.5. Basement membrane 22
4.6. Laminins 24
4.6.1. Laminin-332 27
4.6.2. Laminin-511 30
4.6.3. Laminin-411 31
4.7. Laminin receptors 33
4.7.1. Integrins 33
4.7.2. Lutheran 36
4.8. Cell adhesions 37
4.9. Cell migration and invasion 39
4.10. Cell-ECM adhesion and invasion complexes 42
4.10.1. Podosomes 42
4.10.2. Invadopodia 46
5 AIMS OF THE STUDY **49**
6 MATERIALS AND METHODS **50**
6.1. Cell lines and cell culture 50
6.2. Animals 51
6.3. Tissues 51
6.4. Immunocytochemistry, immunohistochemistry and microscopy 52
6.5. Stable and transient transfections 55
6.6. Production of monoclonal antibodies against Snail 56
6.7. Immunoprecipitation 57
6.8. Western blot analysis 58
6.9. Northern blot analysis 59
6.10. Preparation of crude nuclear extracts 60
6.11. Quantitative reverse transcription polymerase chain reaction 61
6.12. Wound-healing assay *in vivo* 61
6.13. Cell morphology and cell invasion assays 61
6.14. Chromatin immunoprecipitation and polymerase chain reaction 62
6.15. Quantitative cell adhesion assay 63
6.16. Wound-healing assay *in vitro* 64

6.17. Random cell migration assay 64
6.18. Analysis of podosomes and invadopodia on different ECM substrata 65
6.19. *In situ* zymography for ECM degradation 65
6.20. Field emission scanning electron microscopy 66
6.21. Live-cell imaging and total internal reflection fluorescence microscopy 66
6.22. Fluorescence recovery after photobleaching 67
6.23. Statistical analysis 68
7 RESULTS 69
7.1. Characterization of EMT in oral SCC cells 69
7.1.1. Endogenous EMT in oral SCC cells 69
7.1.2. Induction of EMT by overexpression of Snail in oral SCC cells 70
7.1.3. Expression of E-cadherin repressors in oral SCC cells 70
7.2. Production and specificity of monoclonal antibodies against Snail 71
7.3. Localization of Snail in human and mouse cell lines and tissues 72
7.3.1. Localization and kinetics of Snail in cell lines 72
7.3.2. Localization of Snail in normal and malignant tissues 73
7.4. Effect of EMT on expression and production of laminins 74
7.4.1. Laminin-332 74
7.4.2. Laminin-511 76
7.4.3. Laminin-411 77
7.5. Expression and distribution of cell surface receptors in EMT 78
7.5.1. Integrin $\alpha_6\beta_4$ 78
7.5.2. Integrin $\alpha_6\beta_1$ 79
7.5.3. Integrin $\alpha_1\beta_1$ 79
7.5.4. Integrin-linked kinase 79
7.5.5. Lutheran glycoprotein 80
7.6. Adhesion of oral SCC cells to different ECM substrata 80
7.7. Effect of EMT on cell invasion, migration and wound-healing 81
7.8. Effect of EMT on structural proteins of podosomes and invadopodia 83
7.8.1. Morphologic and proteolytic differences between podosomes and invadopodia 87
7.8.2. Dynamic differences between podosomes and invadopodia 88
8 DISCUSSION 91
8.1. Snail-dependent and -independent EMT in oral SCC cells 91
8.2. Expression of Snail protein in the tumour-stroma interface 94
8.3. EMT downregulates laminin α5 chain and upregulates laminin α4 chain in oral SCC cells 97
8.4. Podosome-like structures of non-invasive oral SCC cells are replaced in EMT by actin comet-based invadopodia 101
9 CONCLUSIONS 106
10 ACKNOWLEDGEMENTS 108
11 REFERENCES 111
12 ORIGINAL PUBLICATIONS 130

1 LIST OF ORIGINAL PUBLICATIONS

This thesis is based on the following publications, which are referred to in the text by their Roman numerals (I-IV):

I Minna Takkunen, Reidar Grenman, Mika Hukkanen, Matti Korhonen, Antonio García de Herreros, Ismo Virtanen. Snail-dependent and -independent epithelial-mesenchymal transition in oral squamous carcinoma cells. Journal of Histochemistry and Cytochemistry 2006 54:1263-1275.

II Clara Francí, Minna Takkunen, Natàlia Dave, Francesc Alameda, Silvia Gómez, Rufo Rodríguez, Maria Escrivà, Bàrbara Montserrat-Sentís, Teresa Baró, Marta Garrido, Félix Bonilla, Ismo Virtanen, Antonio García de Herreros. Expression of Snail protein in tumor-stroma interface. Oncogene 2006 25:5134-5144.

III Minna Takkunen, Mari Ainola, Noora Vainionpää, Reidar Grenman, Manuel Patarroyo, Antonio García de Herreros, Yrjö T. Konttinen, Ismo Virtanen. Epithelial-mesenchymal transition downregulates laminin α5 chain and upregulates laminin α4 chain in oral squamous carcinoma cells. Histochemistry and Cell Biology 2008 130:509-525.

IV Minna Takkunen, Mika Hukkanen, Mikko Liljeström, Reidar Grenman, Ismo Virtanen. Podosome-like structures of non-invasive carcinoma cells are replaced in epithelial-mesenchymal transition by actin comet-embedded invadopodia. Journal of Cellular and Molecular Medicine 2010 14:1569-1593.

2 ABBREVIATIONS

BM	basement membrane
BMP	bone morphogenetic protein
BP180	bullous pemphigoid protein 180
BSA	bovine serum albumin
ChIP	chromatin immunoprecipitation
Ck	cytokeratin
DIG	digoxigenin
ECM	extracellular matrix
EGF	epidermal growth factor
EGFP	enhanced green fluorescent protein
ELISA	enzyme-linked immunosorbent assay
EMT	epithelial-mesenchymal transition
FAK	focal adhesion kinase
FCS	fetal calf serum
FESEM	field emission scanning electron microscopy
FRAP	fluorescence recovery after photobleaching
GAPDH	glyceraldehyde-3-phosphate dehydrogenase
GFP	green fluorescent protein
GSK3β	glycogen synthase kinase 3β
GST	glutathione S-transferase
HD1	hemidesmosomal protein 1/ plectin
HRP	horseradish peroxidase
IgG	immunoglobulin G
ILK	integrin-linked kinase
KGM-1	keratinocyte growth medium 1
MAb	monoclonal antibody
MET	mesenchymal-epithelial transition
MMP	matrix metalloproteinase
M_r	relative molecular mass
MT1-MMP	membrane-type 1 matrix metalloproteinase
NA	numerical aperture

PBS	phosphate-buffered saline
PCR	polymerase chain reaction
PMSF	phenylmethylsulfonyl fluoride
RPMI	Roswell Park Memorial Institute
RT	room temperature
RT-PCR	reverse transcriptase polymerase chain reaction
SCC	squamous cell carcinoma
SD	standard deviation
SDS	sodium dodecyl sulphate
SDS-PAGE	sodium dodecyl sulphate polyacrylamide gel electrophoresis
SEM	standard error of the mean
SPARC	secreted protein, acidic and rich in cysteine
TGF-β	transforming growth factor β
TIRF	total internal reflection fluorescence

3 ABSTRACT

In epithelial-mesenchymal transition (EMT), epithelial cells acquire traits typical for mesenchymal cells, dissociate their cell-cell junctions and gain the ability to migrate. EMT is essential during embryogenesis, but may also mediate cancer progression. Basement membranes are sheets of extracellular matrix that support epithelial cells. They have a major role in maintaining the epithelial phenotype and, in cancer, preventing cell migration, invasion and metastasis. Laminins are the main components of basement membranes and may actively contribute to malignancy.

We first evaluated the differences between cell lines obtained from oral squamous cell carcinoma and its recurrence. As the results indicated a change from epithelial to fibroblastoid morphology, E-cadherin to N-cadherin switch, and change in expression of cytokeratins to vimentin intermediate filaments, we concluded that these cells had undergone EMT. We further induced EMT in primary tumour cells to gain knowledge of the effects of transcription factor Snail in this cell model. The E-cadherin repressors responsible for the EMT in these cells were ZEB-1, ZEB-2 and Snail, and ectopic expression of Snail was able to augment the levels of ZEB-1 and ZEB-2.

We produced and characterized two monoclonal antibodies that specifically recognized Snail in cell lines and patient samples. By immunohistochemistry, Snail protein was found in mesenchymal tissues during mouse embryonal development, in fibroblastoid cells of healing skin wounds and in fibromatosis and sarcoma specimens. Furthermore, Snail localized to the stroma and borders of tumour cell islands in colon adenocarcinoma, and in laryngeal and cervical squamous cell carcinomas.

Immunofluorescence labellings, immunoprecipitations and Northern and Western blots showed that EMT induced a progressive downregulation of laminin-332 and laminin-511 and, on the other hand, an induction of mesenchymal laminin-411. Chromatin immunoprecipitation revealed that Snail could directly bind upstream to the transcription start sites of both laminin α5 and α4 chain genes, thus regulating their expression. The levels of integrin $\alpha_6\beta_4$, a receptor for laminin-332, as well as the hemidesmosomal complex proteins HD1/plectin and BP180 were downregulated in EMT-experienced cells.

The expression of Lutheran glycoprotein, a specific receptor for laminin-511, was diminished, whereas the levels of integrins $\alpha_6\beta_1$ and $\alpha_1\beta_1$ and integrin-linked kinase were increased. In quantitative cell adhesion assays, the cells adhered potently to laminin-511 and fibronectin, but only marginally to laminin-411. Western blots and immunoprecipitations indicated that laminin-411 bound to fibronectin and could compromise cell adhesion to fibronectin in a dose-dependent manner.

EMT induced a highly migratory and invasive tendency in oral squamous carcinoma cells. Actin-based adhesion and invasion structures, podosomes and invadopodia, were detected in the basal cell membranes of primary tumour and spontaneously transformed cancer cells, respectively. Immunofluorescence labellings showed marked differences in their morphology, as podosomes organized a ring structure with HD1/plectin, αII-spectrin, talin, focal adhesion kinase and pacsin 2 around the core filled with actin, cortactin, vinculin and filamin A. Invadopodia had no division between ring and core and failed to organize the ring proteins, but instead assembled tail-like, narrow actin cables that showed a talin-tensin switch. Time-lapse live-cell imaging indicated that both podosomes and invadopodia were long-lived entities, but the tails of invadopodia vigorously propelled in the cytoplasm and were occasionally released from the cell membrane. Invadopodia could also be externalized outside the cytoplasm, where they still retained the ability to degrade matrix. In 3D confocal imaging combined with in situ gelatin zymography, the podosomes of primary tumour cells were large, cylindrical structures that increased in time, whereas the invadopodia in EMT-driven cells were smaller, but more numerous and degraded the underlying matrix in significantly larger amounts. Fluorescence recovery after photobleaching revealed that the substructures of podosomes were replenished more rapidly with new molecules than those of invadopodia. Overall, our results indicate that EMT has a major effect on the transcription and synthesis of both intra- and extracellular proteins, including laminins and their receptors, and on the structure and dynamics of oral squamous carcinoma cells.

4 REVIEW OF THE LITERATURE

4.1. Progression of carcinomas

The development of cancer in humans is a complex event that may proceed over a period of decades. Through a process termed cancer progression, normal cells evolve into cells with increasingly neoplastic phenotypes (Greer 2006; Weinberg 2007). Cancer progression is driven by accumulation of multiple genetic mutations and epigenetic alterations of DNA that affect the genes controlling traits such as cell motility, proliferation, survival and angiogenesis. Genetic abnormalities in cancer typically have an effect on two general classes of genes. First, oncogenes are cancer-promoting genes that may be activated in cancer cells, resulting in novel properties, e.g., excess growth and division, sustained angiogenesis, protection against cell death, escape from normal tissue boundaries and acquisition of invasive and metastatic abilities (Hanahan and Weinberg 2000). Second, tumour suppressor genes may become inactivated in cancer cells, causing abnormal DNA replication, cell cycle control and cell orientation and adhesion within tissues. The order and mechanistic means to achieve these properties can vary between different tumours (Hanahan and Weinberg 2000).

Over 90% of tumours arise from epithelia and are called carcinomas (Weinberg 2007). Carcinomas are considered benign (carcinoma *in situ*) if they remain in the same tissue compartment, and malignant if individual carcinoma cells or groups of cells invade the surrounding stroma (Fidler 2003; Weinberg 2007). As a consequence of malignant transformation, invasive cancer cells penetrate through epithelial basement membranes (BM) and proliferate in the surrounding mesenchymal stroma. After local invasion, they penetrate lymph or blood vessel walls (intravasation), move via circulation and become lodged in microvessels of distant tissues. Then, they again pass through endothelial BMs (extravasation), invade the parenchyma and establish secondary colonies (Bosman et al. 1992; Liotta and Kohn 2001; Fidler 2003). Epithelial-mesenchymal transition (EMT) may represent one of the mechanisms by which carcinoma cells acquire migratory and cell survival abilities to escape from their primary locations (Section 4.3). Each step of tumourigenesis is essential and requires interactions between tumour cells and their microenvironment. In fact, the network of extracellular matrix (ECM) molecules

surrounding a tumour can facilitate or hinder tumour progression and is gaining a role as an important participant in tumourigenesis (Ingber 2002; Tlsty and Coussens 2006). Moreover, non-malignant mesenchymal stromal cells, such as fibroblasts, may alter the microenvironment of normal epithelial cells to predispose them to malignant transformation (Liotta 1984; Liotta and Kohn 2001; Kalluri and Neilson 2003). Furthermore, fibroblasts residing near tumours, called carcinoma-associated fibroblasts, seem to promote the growth of their parent tumours and have been suggested to originate from EMT (Petersen et al. 2003; Orimo et al. 2005).

4.2. Oral squamous cell carcinoma (SCC)

Head and neck squamous cell carcinoma (SCC) represents a major worldwide health problem. It includes cancers of the oral and nasal cavity, paranasal sinuses, pharynx and larynx. Oral cancer is the sixth most prevalent cancer in the world, ranking third in developing countries and eighth in developed countries. Over 80% of these lesions are SCCs. Approximately 500 new cases of oral cancer are diagnosed each year in Finland and 274 000 cases globally. The number of yearly deaths related to oral cancer is 150 in Finland and 127 000 worldwide (Parkin et al. 2005; Finnish Cancer Registry 2007).

Oral mucous membranes and the surrounding structures are composed of stratified squamous epithelium supported by a fibrous connective tissue lamina propria and a submucosa of fibroadipose tissue. Minor salivary glands, nerves and capillaries course throughout the submucosa (Greer 2006). Most oral SCCs arising from these mucous membranes show a very aggressive phenotype. They rapidly invade the surrounding tissues and metastasize early. Sometimes oral SCC lesions are preceded by mucosal alterations with dysplastic changes, but highly malignant tumours may also occur directly without any pre-existing clinically detectable mucosal change. The current management for oral SCC includes radiation therapy and surgery, either alone or in combination with chemotherapy. However, less than 50% of oral SCC patients survive for over five years, and this survival rate has not improved in the last 30 years. The most important causes of treatment failure are cancer recurrence and local invasion (Kramer et al. 2005; Greer 2006; Ziober et al. 2006; Pitiyage et al. 2009).

The main risk factors for oral cancer include tobacco smoking or chewing, alcohol consumption and viral infections such as human papilloma virus (Greer 2006; Mehrotra and Yadav 2006). Other predisposing agents are previous family history of oral cancer, poor nutrition and such immune deficiencies as human immunodeficiency virus (HIV). Genetic alterations related to malignant transformation of oral cancer include alterations in tumour suppressor genes, loss- or gain-of-function mutations and chromosomal amplifications. More specifically, changes in genes and proteins controlling the cell cycle, apoptosis, angiogenesis, cytoskeleton and cell adhesion have been revealed (Mehrotra and Yadav 2006; Ziober et al. 2006; Pitiyage et al. 2009). Because little is known about the molecular basis underlying the progression of oral SCC to an invasive phenotype, it is very difficult to predict individual tumour aggressiveness and to design effective treatment plans. Therefore, identification of molecular markers that help in the prediction of disease progression is needed to improve the management of oral cancer.

4.3. Epithelial-mesenchymal transition (EMT)

Epithelial cells are adherent cells that form continuous layers due to their cell-cell adhesion complexes, namely, tight junctions, adherens junctions and desmosomes. Epithelial cells display a polarized, apico-basal morphology and organize hemidesmosomal complexes at their basal sides, which enable tight and stable attachment to the BM. Mesenchymal cells, in contrast, are spindle-shaped, end-to-end polarized cells that lack most of the intercellular junctions. Mesenchymal cells, e.g., fibroblasts and smooth muscle cells, are able to migrate as individual cells through the ECM. Epithelial-mesenchymal transition (EMT) is considered a fundamental process in which epithelial cells acquire mesenchymal traits (Figure 1). EMT has its origins in development, occurring during implantation, gastrulation, neural crest formation and embryo- and organogenesis (Nieto 2002; Thiery 2002; Hay 2005). During implantation extravillous cytotrophoblast cells undergo EMT to infiltrate the endometrium (Vicovac and Aplin 1996). In gastrulation, epiblast cells migrate and produce three distinct germ layers, the ectoderm, mesoderm (primary mesenchyme) and endoderm. In nervous system development, the epithelial cells in the primary neural tube undergo EMT to become migratory neural crest cells. During further development the neural crest cells differentiate into, for instance, peripheral neural ganglia, bone and cartilage of the jaws, melanocytes

and glial cells. Tertiary EMT occurs, e.g., in the development of heart valves, in which three cycles of EMTs and METs (mesenchymal-epithelial transitions) take place (Savagner 2001; Pérez-Pomares and Muñoz-Chápuli 2002).

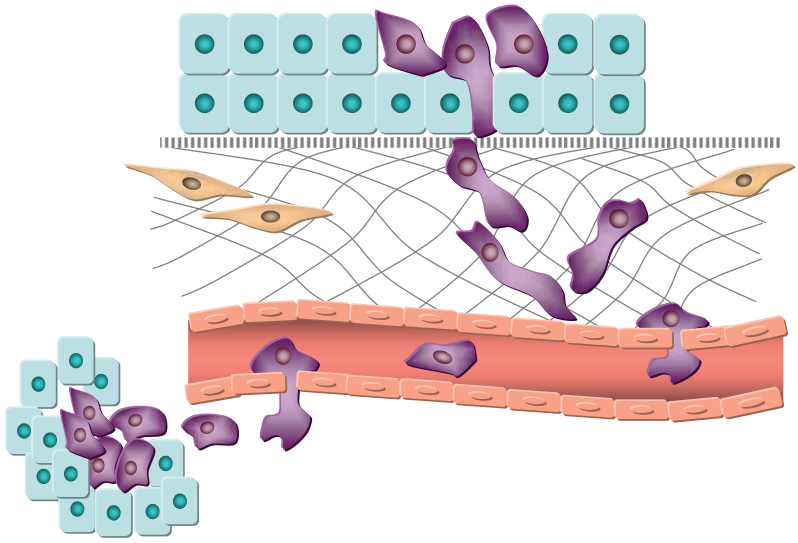


Figure 1. *A schematic illustration of epithelial-mesenchymal transition and mesenchymal-epithelial transition (modified from Peinado et al. 2007; Weinberg 2007).*

In the adult organism, EMT plays a role mainly in wound-healing, tissue regeneration and inflammation, but abnormal EMT activation leads to pathogenic situations such as fibrosis and carcinogenesis (Kalluri and Weinberg 2009). In renal fibrosis, renal tubular epithelial cells are turned into myofibroblasts by EMT, which consequently deposit high levels of ECM (Iwano et al. 2002; Zeisberg and Kalluri 2004). The end result is tubulointerstitial fibrosis, which obstructs filtering functions of the kidney glomeruli. In the lung, the myofibroblasts responsible for the fibrotic cascade may be derived from alveolar epithelium via EMT (Willis et al. 2006). A similar, TGF-β-mediated EMT has been recognized in lens epithelial cells, leading to cataract (de Iongh et al. 2005). In carcinogenesis, EMT has been suggested to initiate invasive and metastatic behaviour in carcinoma cells (Thiery 2002; Thiery 2003). Progression of solid tumours may involve spatial and temporal events of EMT, which enable cell migration and invasion (Figure 1). Subsequently, at the site of metastasis, the disseminated mesenchymal tumour cells must undergo a reverse transition, MET, resulting usually in the recapitulation of the phenotype

of their primary tumours. This suggests that cellular plasticity, the ability to undergo both EMT and MET, is a key feature of a malignant cell (Thiery 2002; Thiery 2003; Kalluri and Weinberg 2009).

4.3.1. Molecular definition of EMT

EMT is a culmination of transcriptional and protein modification events that leads to a long-term, although occasionally reversible, cellular change. In EMT, cell-cell adhesion junctions are reduced, usually via transcriptional repression and delocalization of proteins situated in the tight and adherens junctions as well as in the desmosomes (Nieto 2002; Thiery 2002; De Craene et al. 2005a). E-cadherin is downregulated and N-cadherin expression may emerge. β-catenin is frequently lost from the cell membrane and translocated to the nucleus, where it may participate in EMT signalling events. Apart from E-cadherin, other epithelial genes, including desmoplakin, Muc-1, cytokeratin-18, occludin, claudin-1 and claudin-7, are downregulated (Cano et al. 2000; Guaita et al. 2002; Ikenouchi et al. 2003; Ohkubo and Ozawa 2004; Vandewalle et al. 2005). On the other hand, mesenchymal markers, such as vimentin and fibronectin, are upregulated (Cano et al. 2000; Yokoyama et al. 2003). Also some controversies of the importance of EMT in carcinomas have risen (Tarin et al. 2005; Thompson et al. 2005; Christiansen and Rajasekaran 2006). As different carcinomas represent different patterns of EMT proteins, it may be difficult to predict whether the cells of a certain tumour have undergone EMT or not. In addition, many transcription factors controlling EMT are short-lived, their detection is complicated (Zhou et al. 2004) and EMT may continue without their constant presence. Moreover, EMT could be a transient state of the cell, which again sets challenges for its detection (Christiansen and Rajasekaran 2006; Weinberg 2007). Therefore, further investigations on the specific markers of EMT are required.

4.3.2. E- and N-cadherin

In the adherens junction, cadherins mediate cell-cell adhesion through their extracellular domains and connect to the actin cytoskeleton through their cytoplasmic domains by association with α-, β-, γ- and p120- catenins (Semb and Christofori 1998; Behrens 1999)

(Figure 2). Cadherin anchorage to the actin cytoskeleton stabilizes the junctional structure and contributes to maintenance of cell morphology and control of cell motility. Through homophilic interactions, cadherins contribute to sorting cells of different lineages during embryogenesis, establishing cell polarity, and maintaining tissue morphology and cell differentiation (Semb and Christofori 1998; Van Aken et al. 2001). Most epithelial cells express E-cadherin, whereas mesenchymal cells express various cadherins, including N-cadherin, R-cadherin and cadherin-11 (Cavallaro and Christofori 2004).

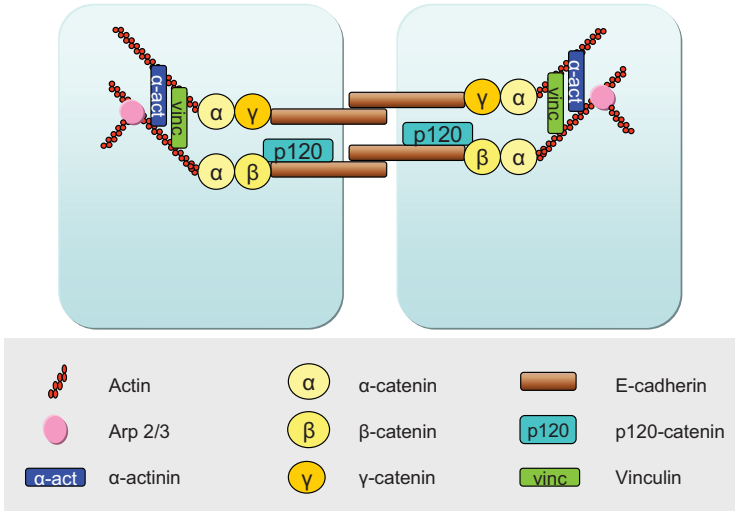


Figure 2. *The adherens junction (modified from Van Aken et al. 2001; Cavallaro and Christofori 2004).*

E-cadherin (also known as epithelial cadherin, cadherin-1, type 1 or uvomorulin) is considered the main gatekeeper of epithelial tissue integrity. It has been proposed that the loss of E-cadherin-mediated cell adhesion is a prerequisite for tumour cell invasion and formation of metastases (Christofori 2003). E-cadherin-deficient mice present with dissociated, unpolarized cells and defective formation of the trophectoderm, and die *in utero* before implantation (Larue et al. 1994; Riethmacher et al. 1995). Decreased expression of E-cadherin has been shown to correlate with increased cell migration and invasion *in vitro*, and *vice versa*, forced expression of E-cadherin in invasive mammary carcinoma cells results in a restoration of a non-invasive phenotype, suggesting that E-cadherin is a tumour- and invasion-suppressor gene (Vleminckx et al. 1991). Loss of E-

cadherin has been connected to cell dedifferentiation and metastasis in several carcinomas, e.g., breast, colorectal, gastric, and head and neck carcinomas, where it may predict an infiltrative growth pattern, lymph node metastasis and poor patient prognosis (Schipper et al. 1991; Gabbert et al. 1996; De Leeuw et al. 1997; Chow et al. 2001; Kanazawa et al. 2002; Lim et al. 2004). Fragments consisting of the E-cadherin extracellular domain have been detected in the circulation of carcinoma patients (Katayama et al. 1994) and were suggested to implicate dissociation of cell-cell adhesion leading to invasion. Importantly, in a mouse pancreatic β-cell tumour model, maintenance of E-cadherin caused arrest of tumour development at the adenoma stage, whereas expression of dominant-negative E-cadherin induced early invasion and metastasis, supporting the hypothesis that loss of E-cadherin is a rate-limiting step in progression from adenoma to carcinoma (Perl et al. 1998).

One of the first recognized signs of EMT is the downregulation of E-cadherin in the adherens junction. This phenomenon has been suggested to occur mainly through transcriptional downregulation of the E-cadherin gene CDH1, but may result from mutations or deletions of the gene, hypermethylation of the promoter, post-translational modifications of the protein or cleavage of E-cadherin by matrix metalloproteinases (MMPs) (Hirohashi 1998; Van Aken et al. 2001; Kanazawa et al. 2002). Downregulation of the CDH1 gene occurs through binding of transcription factors to a CANNTG sequence, called the E-box motif, within the promoter site of the E-cadherin gene (Bussemakers et al. 1994).

In carcinomas, e.g., oral SCC, E-cadherin may be replaced by N-cadherin (neuronal cadherin, cadherin 2, type 1) in a process called cadherin switching, resulting in a change from tight cell-cell adhesion to a more loosely connected and possibly more dynamic type of adhesion (Islam et al. 1996; Cavallaro et al. 2002; Cavallaro and Christofori 2004; Maeda et al. 2005b). Occasionally, the E-cadherin levels may persist, but additional neoexpression of N-cadherin, cadherin-11, P-cadherin or T-cadherin is found (Shimoyama and Hirohashi 1991; Nieman et al. 1999; Tomita et al. 2000; Riou et al. 2006; Vered et al. 2010). Overexpression of N-cadherin in oral SCC and breast carcinoma cells downregulates the levels of endogenous E-cadherin by accelerating its degradation (Islam et al. 1996; Nieman et al. 1999). Furthermore, cells that express significant amounts of E-

cadherin but only small amounts of N-cadherin still have increased motility, suggesting that N-cadherin participates in cell migration independently of E-cadherin (Nieman et al. 1999; Hazan et al. 2000; Hazan et al. 2004; Rosivatz et al. 2004). It is possible that loss of E-cadherin prevents adhesion to other epithelial cells, whereas upregulation of N-cadherin may enable interaction with stromal cells, and, subsequently, cell motility (Cavallaro and Christofori 2004). Taken together, loss of E-cadherin has been detected in several carcinomas and is considered a major hallmark of EMT. However, the presence of N-cadherin in carcinomas, as well as the role of cadherin switching in EMT, remains largely unsolved.

4.3.3. Transcription factors Snail and Slug

The first member of the Snail superfamily of zinc-finger transcription factors, Snail, was identified in *Drosophila melanogaster*, where it was shown to be indispensable for mesoderm formation (Simpson 1983; Grau et al. 1984; Boulay et al. 1987; Alberga et al. 1991). Subsequently, over 50 family members have been described in many species, including humans, other vertebrates and invertebrates. Vertebrates express three isoforms of Snail, namely Snail (also called Snail1), Slug (Snail2) and Smuc (Snail3), which seem to have developed through evolutionary gene duplications (Nieto et al. 1994; Barrallo-Gimeno and Nieto 2005). The Snail transcription factors share common structural features including a highly conserved DNA-binding carboxyterminal region with four to six C_2H_2-type zinc finger repeats, whereas the aminoterminal region is more divergent (Nieto 2002) (Figure 3). Snail family members act as transcriptional repressors through binding to CAGGTG E-box sequences, motifs targeted also by basic helix-loop-helix (bHLH) and ZEB transcription factors (Mauhin et al. 1993). Furthermore, a Snail/ Gfi-1 (SNAG) domain located in the aminoterminal region enhances the repressor activity (Grimes et al. 1996), and a nuclear export sequence (NES) regulates Snail's cytoplasmic location and activity (Domínguez et al. 2003).

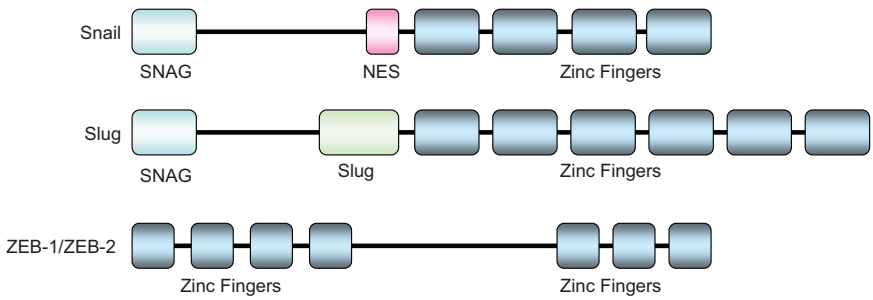


Figure 3. *Main structural domains of transcription factors Snail, Slug, ZEB-1 and ZEB-1 (modified from Domínguez et al. 2003; Peinado et al. 2007).*

The genes encoding for Snail and Slug are highly homologous and in certain stages of development have overlapping expression (Sefton et al. 1998). They seem, however, to have separate roles. Snail-deficient mouse embryos exhibit abnormal mesoderm morphology and fail to gastrulate, which leads to an accumulation of epithelial, E-cadherin-positive cells that are unable to migrate, and, eventually, to death of the embryo (Carver et al. 2001). By contrast, Slug-deficient mice are viable, despite slower growth, malformations of the craniofacial area and discoloration (Jiang et al. 1998). Snail mutations have not been described in humans. Patients with Slug mutations show similar phenotypes to mice, which are related to defective functions of the neural crest. In piebaldism, Slug deletion results in congenital white forelock and depigmented skin (Sánchez-Martín et al. 2003). In Waardenburg syndrome type 2, the patients suffer from deafness and impaired melanocyte function and migration (Sánchez-Martín et al. 2002).

During embryonic development Snail genes function in the EMTs of, for instance, formation of the neural crest (Nieto et al. 1992; Sefton et al. 1998). More generally, they seem to induce cell migration. They also act as survival factors, as they confer resistance to DNA damage and direct apoptotic stimuli (Vega et al. 2004). Snail may have an additional role in determination of left-right asymmetry (Sefton et al. 1998). Many signalling cascades, such as TGF-β, FGF, Wnt, MEK/ERK and Notch signalling, may control the levels of Snail or Slug (De Craene et al. 2005b; Peinado et al. 2007). Snail protein is also under post-transcriptional regulation. For instance, glycogen synthase kinase 3β (GSK3β) phosphorylates Snail, promoting its nuclear export and degradation in the proteasome (Zhou et al. 2004). Inhibition of GSK3β, in turn, increases the amount of

Snail and lengthens the time it can affect gene expression in the nucleus (Zhou et al. 2004). Importantly, Snail has been shown to be a repressor of E-cadherin transcription during both embryonic development and tumour progression (Thiery 2002; Thiery 2003). Snail overexpression is related to the acquisition of invasive properties in different human carcinoma cell lines (Yokoyama et al. 2001; Yokoyama et al. 2003). A reverse correlation between Snail and E-cadherin mRNAs has been reported in carcinoma cell lines (Batlle et al. 2000; Cano et al. 2000; Yokoyama et al. 2001). Snail mRNA is expressed in invasive cells of mouse skin tumours and in biopsies from patients with ductal breast, gastric and hepatocellular carcinomas (Cano et al. 2000; Blanco et al. 2002; Rosivatz et al. 2002; Sugimachi et al. 2003). It has been suggested to be an early marker of a malignant phenotype in breast cancer (Blanco et al. 2002). However, the studies of Snail in malignancies have been hindered by the lack of specific antibodies that could corroborate the presence of Snail protein in patient samples. Furthermore, the functions of Snail may extend beyond repression of E-cadherin, i.e., the array of Snail target genes is far from complete.

4.3.4. Transcription factors ZEB-1 and ZEB-2

Other transcription factors connected to EMT are ZEB-1 (zinc finger E-box binding protein 1, also known as delta E-box factor 1, δEF1, or TCF8) and ZEB-2 (also known as Smad interacting protein 1, SIP1), which belong to the ZEB family of transcription factors (Postigo and Dean 1997; Postigo et al. 1997; Grooteclaes and Frisch 2000; Postigo and Dean 2000; Comijn et al. 2001). ZEB-1 and ZEB-2 are characterized by two separate clusters of C_2H_2-type zinc finger domains and a centrally located, less conserved and non-DNA-binding homeodomain (Verschueren et al. 1999). They regulate TGF-β/ bone morphogenetic protein (BMP) signalling through differential recruitment of coactivators p300 and P/CAF and co-repressor CtBP to the Smad complex (Postigo 2003). Furthermore, ZEB-1 and ZEB-2 downregulate E-cadherin expression and may induce EMT in different cell lines *in vitro* (Verschueren et al. 1999; Grooteclaes and Frisch 2000; Comijn et al. 2001; Eger et al. 2005). For instance, ZEB-2 overexpression induces loss of cell aggregation, enhances invasion and downregulates certain tight junction and desmosomal proteins in colon carcinoma cell lines (Vandewalle et al. 2005).

Mice deficient for the gene encoding for ZEB-1, zfhx1a, develop to term, but die shortly after birth (Takagi et al. 1998). They have short limbs and trunk, craniofacial defects and T cell deficiency. Homozygous mutant embryos lacking the gene encoding for ZEB-2, zfhx1b, display early arrest in neural crest migration and fail to survive (Van de Putte et al. 2003). These embryos have elevated E-cadherin mRNA levels in their neural ectoderm and visceral endoderm. In humans, ZEB-1 mutations have been detected in posterior polymorphous corneal dystrophy, which includes abnormal corneal BMs and impaired endothelial cell migration (Krafchak et al. 2005). ZEB-2 mutations cause Mowat-Wilson syndrome, a form of Hirschsprung's disease associated with microcephaly, mental retardation and dysmorphic facial features (Zweier et al. 2002).

In cancer, ZEB-1 expression has been implicated as a poor prognostic factor in colorectal carcinoma, and ZEB-2 is correlated with lack of E-cadherin expression in oral SCC and intestinal type gastric carcinoma (Rosivatz et al. 2002; Maeda et al. 2005a; Peña et al. 2005; Spaderna et al. 2006). Similar to the Snail family, the specific roles of ZEB-1 and ZEB-2 in tumourigenesis are not fully understood.

4.4. Extracellular matrix (ECM)

The extracellular matrix (ECM) provides the physical environment in which the cells reside. It provides a substrate for cell anchorage, tissue form and function and guides cell migration. The ECM also transmits signals to cells that modify their functions such as growth, proliferation and differentiation. The cells, on the other hand, actively modulate the consistency of their surrounding ECM by degrading and secreting new molecules. The interactions between cells and ECM molecules are mediated through cell-specific receptors, for instance, integrins (Gustafsson and Fässler 2000; Geiger et al. 2001; Aszódi et al. 2006).

The ECM of connective tissues is predominantly composed of fibrillar polymers, including collagens and elastins, which are embedded within a mixture of non-fibrillar components, such as fibronectins and tenascins, and ground substance. The relative proportions and arrangements of fibrillar and non-fibrillar components dictate the overall physical properties of a particular ECM (Aszódi et al. 2006). In addition, specialized

sheets of the ECM called basement membranes contain molecules such as collagen type IV, laminins and nidogen (Miner and Yurchenco 2004).

Many ECM proteins are large multifunctional molecules containing multiple domains that may bind several other molecules simultaneously. The ground substance consists of glycosaminoglycans and proteoglycans. Glycosaminoglycans, such as hyaluronan and heparan sulphate, consist of repeated sulphated oligosaccharide units. Glycosaminoglycans bind to a proteoglycan core protein and form large macromolecules such as versican and aggrecan. The glycosaminoglycan side-chains contain negatively charged residues, attracting water molecules and forming a hydrated gel that resists compressive forces. Growth factors and signalling molecules are trapped into this gel (Gustafsson and Fässler 2000; Aszódi et al. 2006). Collagens, the most ubiquitous proteins in human tissues, are glycoproteins that share a structural homology of three α chains intertwined into a triple helix (Myllyharju and Kivirikko 2004). Collagen fibres provide mechanical strength, organize the matrix and enable cell adhesion and migration. Elastic fibres, consisting of elastin and microfibrils, are arranged into a branching pattern among the collagen fibres. They limit the distensibility of the tissues and prevent tearing from excessive stretching (Ramirez 2000). Fibronectins are large glycoproteins that function in blood in a soluble form, but in tissues as insoluble fibrils composed of fibronectin multimers. They mediate cell adhesion and are especially prominent in loose connective tissues, granulation tissue, embryonic BMs and stroma (Bosman et al. 1992). Matricellular proteins, including tenascins, thrombospondins, osteopontin and SPARC (secreted protein, acidic and rich in cysteine), are a structurally unrelated protein family that functions as adaptors and modulators of cell-matrix interactions. They have a strictly regulated expression, being especially abundant during embryogenesis, tissue repair and regeneration, and are suggested to confer anti-adhesive properties to cells (Murphy-Ullrich 2001; Bornstein and Sage 2002).

4.5. Basement membrane

Basement membranes (BMs), present in multicellular organisms, are the first extracellular matrices produced during embryogenesis. The BM is an amorphous, dense, sheet-like structure of 50-100 nm in thickness. BMs are usually found beneath epithelial and

endothelial cells and surrounding muscle, adipose and Schwann cells (Bosman et al. 1992; Kalluri 2003). The BM acts as a regulator of cell attachment, differentiation and growth, as well as a passive barrier that segregates tissue compartments. The BM provides structural support and regulates cell behaviour and polarization. It also mediates signals from the ECM to the cytoplasm and binds growth factors, hormones and ions. During embryogenesis, tissue repair and regeneration BMs guide cell migration (Merker 1994; Flug and Köpf-Maier 1995).

Ultrastructural analysis has indicated that BMs consist of three layers. Adjacent to the plasma membrane of the adherent cell is an electron-lucent layer, called the lamina rara or lamina lucida (Merker 1994). The lamina lucida, however, may be an artefact derived from tissue dehydration. The lamina densa, an electron-dense layer, consists of a large network of filaments and is considered the main BM zone. Lamina fibroreticularis, restricted to only certain epithelia, lies at the stromal side of the BM and consists of type VII collagen anchoring fibrils (Merker 1994). Epithelial BMs were long assumed to be produced exclusively by adjacent epithelial cells. However, it has become clear that the BM arises through an interaction between epithelial and stromal cells (Bosman et al. 1992).

The main components of BMs are laminins, type IV collagen, heparan sulphate proteoglycans and nidogen/ entactin. Minor components include agrin, SPARC, osteopontin, fibulins and type XV and XVIII collagens. Altogether, 50 different proteins have been identified in the BM. Currently, 15 laminins and three isoforms of type IV collagen have been recognized (Erickson and Couchman 2000; Borza et al. 2001; Yurchenco et al. 2004; Khoshnoodi et al. 2008). Each BM may contain highly variable components, and may perform significantly different functions in regulating organ-specific behaviour. Distinct from all other BM components, only laminin and type IV collagen molecules are able to initiate the self-assembly of BM into sheet-like structures. Previously, most models of BM organization assumed that type IV collagen would serve as the major scaffold upon which the laminin network would be deposited. However, it has been established that the laminin polymers function as the initial template (Timpl and Brown 1996; Yurchenco et al. 1997; Li et al. 2002). After the laminin molecules are formed and secreted, they concentrate at the plasma membrane via binding to cellular

receptors, e.g., integrins and α-dystroglycan. Adjacent laminin molecules bind each other via stable interactions between the short-arm globular LN domains. Type IV collagen polymers organize their own network, which is stabilized by covalent crosslinks and bridged to laminins through nidogen/ entactin. The covalent bonding of type IV collagen provides a great deal of the mechanical stability to the BM. Type IV collagen with the triple-helical chain composition α1α1α2(IV) is the most ubiquitous BM collagen, whereas collagens α3α4α5(IV) and α5α5α6(IV) have more restricted expressions (Borza et al. 2001; Myllyharju and Kivirikko 2004; Khoshnoodi et al. 2008). Nidogen provides binding sites for heparin sulphate proteoglycans, especially perlecan. Perlecan and other proteoglycans, such as collagens XV and XVIII and agrin, potentially confer selective filtration properties and serve as reservoirs for growth factors (Timpl and Brown 1996; Yurchenco et al. 2004). This multimolecular scaffold then provides specific interaction sites for yet other BM constituents.

Discontinuous or thin BMs have been found in many carcinomas, including oral SCC (Kannan et al. 1994; Flug and Köpf-Maier 1995; Hagedorn et al. 1998; Kosmehl et al. 1999; Määttä et al. 2001). In laryngeal SCC, loss of BM components, especially type IV collagen, is inversely correlated with the degree of tumour differentiation (Hagedorn et al. 1998). Cancer cells, which themselves present marked heterogeneity, appear to produce different patterns of BM components, resulting in imbalances in the composition and assembly of BMs (Flug and Köpf-Maier 1995; Ingber 2002; Tlsty and Coussens 2006). The loss of BM may also be due to increased matrix turnover caused by active degrading proteases or by remodelling by the tumour cells. Furthermore, the tumour BM may be significantly less crosslinked and therefore more susceptible to proteolysis, remodelling and turnover (Kalluri 2003).

4.6. Laminins

Laminins are a family of extracellular matrix proteins that are located primarily in BMs. The first laminin was isolated in intact form from the Engelbreth-Holm-Swarm (EHS) tumour (Timpl et al. 1979). Through interactions with specific cell surface receptors, laminins regulate various cellular functions such as adhesion, motility, proliferation, differentiation and apoptosis. The three subunits of laminins, designated α, β and γ chains,

assemble to form a cross- or T-shaped structure. Five α, four β and three γ chains have been identified. To date, 15 different laminin heterotrimers have been found, although many more combinations are theoretically possible (Miner and Yurchenco 2004). The laminin isoforms are expressed in a cell-, tissue- and developmental stage-specific manner. Laminins are present in all BMs, and reciprocal differences in their structure and receptor interactions enable variation in their functions (Patarroyo et al. 2002).

Laminins are large glycoproteins with a relative molecular mass (M_r) ranging from ca. 400 000 to 900 000. All laminins share some degree of structural homology. The laminin molecule consists of one long chain and two to three short chains linked together by disulphide bridges (Figure 4). The long chain is formed from intertwined α-γ chains, whereas the short chains consist of single α-γ chains (for a thorough review of laminin structure, see Colognato and Yurchenco 2000; Aumailley et al. 2005). The N-terminus of each chain has a LN domain, used in polymerization of laminins, followed by epidermal growth factor (EGF)-like (LE) domains, laminin four (L4 or LF) domain and laminin β knob (Lβ) domain. The C-terminus of the coiled-coil long arm harbours five globular domains LG1-LG5, which contain binding sites for, e.g., integrins, heparin, α-dystroglycan and Lutheran blood group glycoproteins. The short arms of laminin isoforms show the greatest variability in domain number and arm length. For instance, laminin-111 has full-length arms, whereas laminin-332 has truncations in every short arm and laminins-411/ -421 have truncations in the α4 chain short arm. By contrast, laminins-511/ -521 have additional domains that lengthen their α5 chains. Many laminins further undergo post-translational proteolytic cleavage, producing small laminin fragments that may themselves have some functionality (Yurchenco et al. 1997; Colognato and Yurchenco 2000; Aumailley et al. 2005). The assembly of BMs is dependent on the primary polymerization of laminins, which, in turn, is controlled by the secretion of the α chain (Matsui et al. 1995b; Yurchenco et al. 1997).

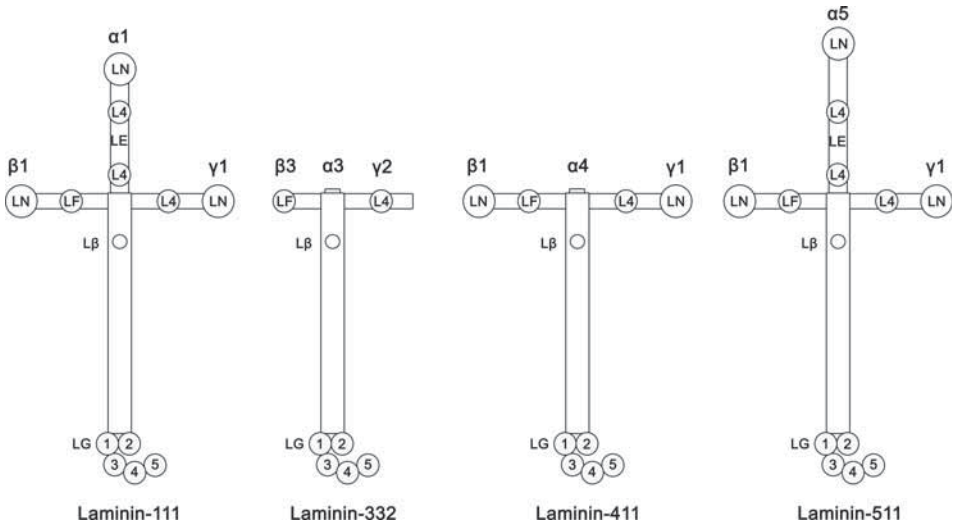


Figure 4. *Structure of laminins -111, -332, -411 and -511 (modified from Aumailley et al. 2003; Aumailley et al. 2005).*

Several different names have been given to laminin trimers since the first laminin, such as merosin, kalinin and nicein. To obtain a more consistent nomenclature, the laminin heterotrimers were named in the order of their discovery (laminins 1-15) (Burgeson et al. 1994). As it eventually became problematic to remember and recognize the different isoforms by these numbers only, a second nomenclature was adopted in 2005 (Aumailley et al. 2005). This nomenclature, which designates the chain composition of different laminins, is used in this thesis. For example, laminin-1, composed of α1, β1 and γ1 chains, is now called laminin-111, and laminin-5 (α3β3γ2) is called laminin-332 (Table 1). The corresponding genes for each chain are called LAMA, LAMB and LAMC, respectively (Aumailley et al. 2005).

Table 1. *Nomenclature of laminins.*

Chain composition	Current abbreviation	Previous abbreviation	Previous names
α1β1γ1	Laminin-111	Laminin-1	EHS-laminin
α2β1γ1	Laminin-211	Laminin-2	merosin
α1β2γ1	Laminin-121	Laminin-3	s-laminin
α2β2γ1	Laminin-221	Laminin-4	s-merosin
α3Aβ3γ2	Laminin-332 (-3A32)	Laminin-5 (-5A)	BM-600, epiligrin, kalinin, ladsin, nicein
α3Bβ3γ2	Laminin-3B32	Laminin-5B	
α3β1γ1	Laminin-311 (-3A11)	Laminin-6 (-6A)	k-laminin
α3β2γ1	Laminin-321 (-3A21)	Laminin-7 (-7A)	ks-laminin
α4β1γ1	Laminin-411	Laminin-8	
α4β2γ1	Laminin-421	Laminin-9	
α5β1γ1	Laminin-511	Laminin-10	
α5β2γ1	Laminin-521	Laminin-11	
α2β1γ3	Laminin-213	Laminin-12	
α4β2γ3	Laminin-423	Laminin-14	
α5β2γ3	Laminin-523	Laminin-15	

Laminin α1 and α3, together with β3 and γ2 chains, are mainly expressed in epithelial cells (Patarroyo et al. 2002). Laminin α1 chain has a limited distribution and is present, e.g., in the endometrium, kidney, mammary gland, ovary, placenta and prostate (Virtanen et al. 2000), and laminin α2 chain is expressed in skeletal and cardiac muscle, peripheral nerves and capillaries (Colognato and Yurchenco 2000). Laminin α2 and α4 chains are mainly expressed by mesenchymal cells. Typically, both epithelial and mesenchymal cells participate in the synthesis of laminin isoforms of a single BM. The BM of fetal oral squamous epithelium contains laminin chains α2, α3, α5, β1, β2, β3, γ1 and γ2, and the adult oral epithelium contains laminin chains α3, α5, β1, β2, β3, γ1 and γ2 (Kosmehl et al. 1999; Pakkala et al. 2002).

4.6.1. Laminin-332

The gene encoding for laminin α3 chain, LAMA3, consists of 76 exons on chromosome 18q11.2 and was first found in human foreskin keratinocytes (Ryan et al. 1994; McLean et al. 2003). Laminin α3 chain protein has since been identified as a constituent of laminins-

332 (α3β3γ2), -311 (α3β1γ1) and -321 (α3β2γ1). Laminin-332, formerly known as BM-600, epiligrin, kalinin, ladsin, nicein or laminin-5, was described as a cell adhesion and scattering factor and a component of the anchoring filaments in BMs (Verrando et al. 1987; Carter et al. 1991; Rousselle et al. 1991; Marinkovich et al. 1992; Watt and Hotchin 1992; Miyazaki et al. 1993). Rotary shadowing electron microscopy has demonstrated that it is a truncated, even, rod-like molecule (Rousselle et al. 1991). The α3 chain mRNA exists in two alternatively spliced transcript variants, producing a shorter M_r 200 000 α3A and a longer M_r 325 000 α3B chain. Laminin α3A chain is especially enriched in epithelia, being present in simple, squamous, compound and stratified epithelia, whereas α3B chain expression is weak in the epidermis, but readily found in the lung and central nervous system (Galliano et al. 1995). Also the laminin γ2 chain has two mRNA variants, of which the longer form is epithelium-specific and the shorter form is restricted to the cerebral cortex, lung and kidney tubules (Airenne et al. 1996). According to the new laminin nomenclature, laminin-332 is considered to include the α3A chain, and the term laminin-3B32 is used otherwise (Aumailley et al. 2005). Laminin-332 is initially synthesized in a M_r 460 000 precursor form and is composed of three polypeptides, the ca. M_r 200 000 α3 chain, M_r 145 000 β3 chain and M_r 155 000 γ2 chain (Marinkovich et al. 1992; Matsui et al. 1995b). The β3 and γ2 chains seem to be linked together in the cytoplasm first, after which the α chain is introduced to the dimer. Laminin-332 chains are further post-translationally N-glycosylated. Extracellularly, the chains are processed to gain the 165 000 α3' chain and 105 000 γ2' chain forms, which assemble into 440 000 (α3'β3γ2) and 400 000 (α3β3γ2') laminin trimers, respectively. Several proteases, such as BMP-1, MMP-2, MMP-3, MMP-20, membrane-type 1-MMP (MT1-MMP) and plasmin, may cleave the γ2 chain short arm and release the following fragment to the ECM (Aumailley et al. 2003; Pirilä et al. 2003; Katayama and Sekiguchi 2004; Miner and Yurchenco 2004; Ziober et al. 2006).

In the epidermal BM, laminin-332 is a component of the anchoring filaments and plays an essential role in the stable anchorage of basal keratinocytes to the underlying dermis. Laminin-332 is highly adhesive, as it binds integrin $\alpha_6\beta_4$ in hemidesmosomes. However, laminin-332 may also have a pro-migratory function, as it is expressed in epithelial wound margins and migrating keratinocytes in culture (Ryan et al. 1994; Goldfinger et al. 1999; Patarroyo et al. 2002). The switch in functional states may be caused by the different

processing of the α and γ chains, but this remains largely unsolved. It is possible that cleavage of the α3 chain induces a change towards a form that actively binds integrin $\alpha_6\beta_4$ and enables stable adhesion, whereas cleavage of the γ2 chain changes the static form to a motile one (Goldfinger et al. 1999; Miyazaki 2006).

Mice exhibiting laminin α3, β3 or γ2 chain knock-out die at the neonatal stage and suffer from blisters and erosions of the skin and oral cavity, indicating that laminin-332 is an important regulator of epidermal cell-BM interaction (Ryan et al. 1994; Meng et al. 2003; Mühle et al. 2006). This is consistent with the phenotype of patients with mutations in any of the laminin-332 chains. Junctional epidermolysis bullosa is a severe, often lethal, disease that causes generalized blistering of the skin and gastrointestinal mucosae (Pulkkinen and Uitto 1999). Similar symptoms arise in anti-laminin cicatrical pemphigoid, which is caused by autoantibodies against the laminin α3 chain (Kirtschig et al. 1995). An N-terminal deletion in the α3A chain leads to laryngo-onycho-cutaneous syndrome, characterized by defective healing of skin erosions, nail dystrophy and development of granulation tissue in the eye and larynx (McLean et al. 2003).

The amounts of laminins vary in different cancers. The presence of laminin-332 has been reported in several carcinomas, for instance, in colorectal, pancreatic and some renal cell carcinomas (Lohi et al. 1996; Tani et al. 1997; Lohi et al. 2000). On the other hand, reduced amounts of laminin-332 have been reported in, for example, breast, lung and prostate cancers *in vivo* and *in vitro* (Martin et al. 1998; Akashi et al. 2001; Brar et al. 2003; Katayama and Sekiguchi 2004). Laminin β3γ2 chains are synthesized as a dimer and retained in the cytoplasm in colorectal carcinoma (Sordat et al. 1998). The γ2 chain may have additional roles in tumour invasion, as cytoplasmic and extracellular overexpression of γ2 monomer has been detected in invasive fronts of, e.g., colorectal carcinoma and oral SCC (Koshikawa et al. 1999; Ono et al. 1999; Yamamoto et al. 2001). However, most of the studies have been conducted with monoclonal antibodies (MAbs) against only laminin γ2 chain and have been erroneously interpreted to report the expression of the whole laminin-332 trimer (Ziober et al. 2006). Therefore, the roles of laminin-332 in carcinomas and especially in EMT remain to be established.

4.6.2. Laminin-511

The laminin α5 chain gene, LAMA5, consists of 80 exons and is located in chromosome 20q13.2-q13.3. First identified in mice and then in humans, the laminin α5 chain is considered to be evolutionarily most related to the laminin α3 chain (Miner et al. 1995; Durkin et al. 1997; Miner et al. 1997; Doi et al. 2002). The laminin α5 chain is a component of laminins-511 (α5β1γ1), -521 (α5β2γ1) and -523 (α5β2γ3) heterotrimers (Miner et al. 1997; Libby et al. 2000). Rotary shadowing has shown that laminin-511 (formerly called laminin-10) is a cruciform molecule with an elongated N-terminal α5 chain (Doi et al. 2002). Similarly to the processing of the laminin α3 chain, the laminin α5 chain undergoes tissue-specific glycosylation and post-translational cleavage, resulting in the secretion of M_r 350 000-400 000 forms. Together with M_r 200 000 β1 and γ1 chains, it comprises a M_r 800 000 laminin-511 trimer (Champliaud et al. 2000; Doi et al. 2002).

Discrepancies regarding the distribution and functions of laminins have existed due to misinterpretations in the use of laminin preparations and antibodies. In cell adhesion and migration studies, many previous investigations have used commercial laminin preparations from human placenta, assumed to contain laminin-111. However, this placental laminin preparation has since been shown to include mainly laminins-511 and -521 (Ferletta and Ekblom 1999). Furthermore, MAb 4C7, widely used in laminin distribution studies, was initially thought to detect the laminin α1 chain (Engvall et al. 1986). Based on reports using different antibodies and *in situ* hybridization, MAb 4C7 was established to recognize the laminin α5 chain (Tiger et al. 1997). Currently, the laminin α5 chain is acknowledged to be widely expressed in embryonic and adult BMs (Miner et al. 1997). Laminin-511 is present in practically all BMs, including epithelia and endothelia. Laminin-521 (formerly called laminin-11), on the other hand, is limited to certain BMs, such as those of neuromuscular synapses in skeletal muscle, the perineurium of peripheral nerves, and BMs of smooth muscle arterioles and kidney glomeruli (Miner et al. 1995; Gullberg et al. 1999; Miner and Patton 1999). Laminin-523 has been detected in the retina (Libby et al. 2000). Laminin-511 is a potent cell adhesive agent, and it also has a role in cell migration and proliferation (Kikkawa et al. 2000; Doi et al. 2002). Laminin-511 may also have a barrier function, as it seems to hinder the migration of T lymphocytes through endothelia (Sixt et al. 2001).

The importance of the laminin α5 chain is highlighted by the phenotype of knock-out mice. The mice suffer from various developmental defects, including defects in neural tube closure, digit separation, placental labyrinth, kidney and lung development, and die by day E16.5 during late embryogenesis (Miner et al. 1998; Miner and Li 2000). The absence of the laminin α5 chain evokes accumulation of laminin α1, α2 and α4 chains, which can be detected at the weakened, discontinuous BMs (Miner et al. 1998). Furthermore, laminin α5 chain-deficient skin grafts transplanted into nude mice do not develop any hair, suggesting that laminin-511 is essential also in hair morphogenesis (Li et al. 2003). MET is impaired in the kidneys of laminin α5 chain-deficient mice, observed as a breakdown of BM, disorganized glomerular cells and defective vascularization, suggesting that the laminin α5 chain could participate in mediating the epithelial transformation (Miner and Li 2000).

As the laminin α5 chain and laminin-511 are widely distributed in BMs, their presence has also been detected in malignancies. For instance, expression of laminin-511 has been shown to be well-preserved in renal cell and prostate carcinoma (Lohi et al. 1996; Brar et al. 2003). However, the laminin α5 chain or laminin-511 expression is reduced in invasive, budding areas of oral SCC, colorectal carcinoma and lung adenocarcinoma, in which it is associated with lymph node metastasis (Kosmehl et al. 1999; Lohi et al. 2000; Akashi et al. 2001). The role of laminin-511 in progression of carcinomas is incompletely understood.

4.6.3. Laminin-411

The gene encoding for the laminin α4 chain, LAMA4, contains 39 exons spanning over 122 kb and is located in chromosome 6q21 (Richards et al. 1994; Iivanainen et al. 1995; Richards et al. 1996; Iivanainen et al. 1997; Richards et al. 1997). The laminin α4 chain has been identified in laminins-411 (α4β1γ1), -421 (α4β2γ1) and -423 (α4β2γ3) (Frieser et al. 1997; Miner et al. 1997; Libby et al. 2000). In rotary shadowing microscopy, laminins-411 and -421 have a truncated, T-shaped ultrastructure (Frieser et al. 1997; Kortesmaa et al. 2000). The laminin α4 chain resembles the laminin α3A chain, as the short arm mainly consists of LE domains, but also shares similarity with the laminin α2 chain, which is located in close proximity, on chromosome 6q22-23 (Richards et al. 1996; Richards et al.

1997). The N- or C-terminal parts of the laminin α4 chain may be post-translationally modified by glycosylation, addition of glycosaminoglycans or chondroitin sulphate, or by proteolytic cleavage, resulting in size variations of M_r ca. 180 000-230 000 (Kortesmaa et al. 2000; Talts et al. 2000; Fujiwara et al. 2001; Sasaki et al. 2001; Kortesmaa et al. 2002). The laminin α4 chain has two identified transcript variants, which differ by 21 nucleotides (Hayashi et al. 2002).

Laminin-411, a M_r 570 000-650 000 trimer, operates in cell migration, invasion and endothelial transmigration (Sixt et al. 2001; Khazenzon et al. 2003). It seems to participate also in wound-healing and angiogenesis (Fujiwara et al. 2001). Laminin-411 containing the longer α4B transcript may be more potent in promoting cell spreading than the one containing the α4A transcript (Hayashi et al. 2002). Many blood cells, such as monocytes, B and T lymphocytes, NK cells and thrombocytes, synthesize, secrete, adhere and migrate on laminin-411 (Geberhiwot et al. 1999; Pedraza et al. 2000; Geberhiwot et al. 2001). It is, however, considered a relatively poor adhesion substrate (Fujiwara et al. 2001; Sixt et al. 2001). The laminin α4 chain is widely distributed in tissues of mesenchymal origin, such as smooth, cardiac and skeletal muscle, adipose tissue and peripheral nerves. It is also found in stroma, salivary glands, epidermis and the gastrointestinal tract and is especially detected in vascular BMs (Iivanainen et al. 1995; Richards et al. 1996; Frieser et al. 1997; Miner et al. 1997; Lefebvre et al. 1999; Petäjäniemi et al. 2002). Laminin-411 is the most ubiquitous form, secreted by, e.g., adipocytes and endothelial cells (Niimi et al. 1997; Kortesmaa et al. 2000). Other α4 chain laminins have more restricted distributions; laminin-421 localizes to arterial BMs and the neuromuscular junction, whereas laminin-423 has been detected in the retina (Libby et al. 2000; Patton et al. 2001; Ljubimova et al. 2004).

Laminin α4 chain-deficient mice are viable and fertile. However, they show haemorrhages and anaemia from E11.5 to the neonatal period, reflecting impaired microvessel maturation (Thyboll et al. 2002). In addition, the adult mice represent abnormal development of neuromuscular synapses, defective Schwann cell myelinization, mild ataxia and features of cardiomyopathy (Patton et al. 2001; Wallquist et al. 2005; Wang et al. 2006). Neutrophils, activated by an inflammatory response, fail to extravasate

(Wondimu et al. 2004). In humans, laminin α4 chain mutations may have a role in the development of dilated cardiomyopathy (Knöll et al. 2007).

The laminin α4 chain has been detected in several mesenchymal cancer cell lines, including leiomyosarcoma, glioma, neuroblastoma and fibrosarcoma cells (Iivanainen et al. 1997; Fujiwara et al. 2001; Hayashi et al. 2002). Laminin-411 may promote glioma cell invasiveness *in vitro* (Khazenzon et al. 2003). In glioma, upregulation of the laminin α4 chain and laminin-411 in the endothelial BMs is correlated with higher tumour grade and poor prognosis (Ljubimova et al. 2001; Ljubimova et al. 2004). However, the role of the laminin α4 chain and laminin-411 in malignancies, especially carcinomas, remains elusive.

4.7. Laminin receptors

4.7.1. Integrins

Integrins are cell surface receptors that are considered to be the prime mediators of cell-matrix adhesions (Hynes 2002). Integrins modulate a variety of cell functions, including cell survival, proliferation, morphogenesis, differentiation, migration, invasion and metastasis. The first integrins, later named integrins $\alpha_5\beta_1$ and $\alpha_v\beta_3$, were found to bind the minimal recognition sequence consisting of arginine, glycine and aspartic acid (RGD) that was present in fibronectin and vitronectin (Pytela et al. 1985a; Pytela et al. 1985b). Integrins are non-covalently linked heterodimeric transmembrane proteins, which act as receptors for ECM components, e.g., laminins, collagens, fibronectin and vitronectin. Also other ECM molecules, such as nidogen/ entactin, perlecan and SPARC, possess integrin binding sites. Some integrins bind counter-receptors of other cells. Several pathogens, such as HIV and papilloma viruses, use integrins to gain access into cells (van der Flier and Sonnenberg 2001a). Currently, 18 α and 8 β integrin subunits have been characterized in mammals. Different combinations of single α and β subunits dimerize to form at least 24 receptors with distinct but also often overlapping specificities for ECM proteins. Different integrin isoforms arise through alternative mRNA splicing and post-translational modifications (van der Flier and Sonnenberg 2001a; Watt 2002). Furthermore, genes

encoding for six novel α subunits and one β subunit have been detected in genome-wide surveys, although their existence remains to be confirmed. Expression of integrins is dependent on cell and tissue type, as well as on the stage of cell differentiation. Many integrin heterodimers recognize more than one ligand, and some ligands are recognized by more than one integrin (van der Flier and Sonnenberg 2001a). The α and β subunits that together dictate the ligand-binding specificity have large extracellular domains and are connected to the cytoplasm by single membrane-spanning domains. The non-catalytic cytoplasmic portions are generally small, ca. 30-50 amino acids, except for the 1000 amino-acid-long tail of the integrin β_4 subunit. Perhaps due to the unique characteristic of the integrin β_4 tail, it mediates linkage to cytokeratins (Cks) instead of actin filaments. The cytoplasmic tails of several β subunits contain NPxY domains, which are used for interaction with adaptor proteins like talin and tensin (Hynes 2002; Legate and Fässler 2009). Recruitment of adaptor proteins to the cytoplasmic domains leads to conformational changes and cytoskeletal reorganization (inside-out signalling). The binding of a ligand to the integrin heterodimer changes the conformation and activates the integrin and the subsequent signalling cascades (outside-in signalling). The strength of ligand binding is modulated by integrin clustering, mechanical tension, association with accessory molecules and cations such as Mn^{2+}, Mg^{2+} and Ca^{2+} (Watt 2002; Mould and Humphries 2004). Mn^{2+} stabilizes a high-affinity conformation, whereas Ca^{2+} is inhibitory and promotes a low-affinity conformation. Phosphorylation of the cytoplasmic domains or proteolytic cleavage may also have a role in ligand binding.

A multitude of integrin-binding proteins reside at the cytoplasmic side of cell membrane. These include such proteins as α-actinin, talin, tensin and filamins, which mediate the link to the cytoskeleton and may serve as additional docking sites for other molecules (Otey and Carpén 2004; Le Clainche and Carlier 2008). Signalling molecules, e.g., focal adhesion kinase (FAK) and integrin-linked kinase (ILK), may operate in integrin activation (Giancotti and Ruoslahti 1999; van der Flier and Sonnenberg 2001a). Integrin binding to ECM ligands activates FAK and mediates ERK signalling to promote cell survival and migration (Hood and Cheresh 2002). ILK, on the other hand, binds the cytoplasmic tails of integrin β_1, β_2 and β_3 subunits, stabilizes integrin-actin interactions, mediates integrin signalling and regulates actin polymerization (Hannigan et al. 1996; Li et al. 1999; Mulrooney et al. 2000). Furthermore, growth factors, such as EGF, interact

with integrins and potentially enhance integrin signalling through clustering of growth factor receptors. Integrins seem to influence the expression of other integrin complexes as well as other cell-cell adhesion molecules (Giancotti and Ruoslahti 1999; van der Flier and Sonnenberg 2001a; Guo and Giancotti 2004).

Many integrins, including $\alpha_1\beta_1$, $\alpha_2\beta_1$, $\alpha_3\beta_1$, $\alpha_6\beta_1$, $\alpha_6\beta_4$, $\alpha_7\beta_1$, $\alpha_9\beta_1$, $\alpha_v\beta_3$, $\alpha_v\beta_5$ and $\alpha_v\beta_8$ heterodimers, may serve as laminin receptors (Belkin and Stepp 2000; Hynes 2002). Integrins $\alpha_3\beta_1$ and $\alpha_6\beta_4$, among others, bind to the LG domains of laminin α chains, whereas $\alpha_2\beta_1$ can interact with LN domains of laminin α-γ chains (Belkin and Stepp 2000). Integrins $\alpha_1\beta_1$ and $\alpha_2\beta_1$ are considered mainly collagen receptors, whereas $\alpha_3\beta_1$ and $\alpha_6\beta_1$ recognize primarily laminins. Integrins $\alpha_{IIb}\beta_3$, $\alpha_3\beta_1$, $\alpha_4\beta_1$, $\alpha_4\beta_7$, $\alpha_5\beta_1$, $\alpha_8\beta_1$, $\alpha_v\beta_1$, $\alpha_v\beta_3$, $\alpha_v\beta_6$ and $\alpha_v\beta_8$ bind fibronectin (van der Flier and Sonnenberg 2001; Hynes 2002). Stratified squamous epithelia express a range of integrins, including $\alpha_2\beta_1$, $\alpha_3\beta_1$ and $\alpha_6\beta_4$. In the epidermis, integrin expression is largely confined to the basal layer, whereas the oral epithelium expresses integrins also in suprabasal layers (Jones et al. 1993).

The main receptors for laminin-332 are integrins $\alpha_3\beta_1$, $\alpha_6\beta_1$ and $\alpha_6\beta_4$. Also integrin $\alpha_2\beta_1$ may have some cell-specific binding capacity (Carter et al. 1991; Rousselle and Aumailley 1994; Orian-Rousseau et al. 1998). In addition to integrins, the LG4-5 domains potentially bind α-dystroglycan and syndecan, and the γ2 chain interacts with type VII collagen, fibulins and nidogens (Aumailley et al. 2003). Integrins $\alpha_3\beta_1$ and $\alpha_6\beta_1$ are regarded as the principal mediators of adhesion to laminin-411 (Kortesmaa et al. 2000; Pedraza et al. 2000; Fujiwara et al. 2001; Geberhiwot et al. 2001). Depending on the cell type, integrins $\alpha_2\beta_1$, $\alpha_6\beta_4$, $\alpha_7\beta_1$, $\alpha_M\beta_2$, $\alpha_v\beta_3$, α-dystroglycan, fibulins, heparin and sulphatides may also have adhesive interactions with laminin α4 chain or its LG domain fragments (Geberhiwot et al. 1999; Kortesmaa et al. 2000; Pedraza et al. 2000; Talts et al. 2000; Gonzalez et al. 2002; Patarroyo et al. 2002; Wondimu et al. 2004). The interactions between laminin-511 and the ECM are mainly mediated through integrins $\alpha_3\beta_1$ and $\alpha_6\beta_1$. Laminin-511 is also bound by several other receptors, including integrins $\alpha_2\beta_1$, $\alpha_6\beta_4$, $\alpha_v\beta_3$, α-dystroglycan and Lutheran (Tani et al. 1999; Kikkawa et al. 2000; Pouliot et al. 2000; Pouliot et al. 2001; Sasaki and Timpl 2001; Kikkawa et al. 2002). The receptors utilized depend on the cell type, the functional state of the cell, e.g., migration or adhesion, and the presence of cytokines or growth factors.

In humans, several genetic diseases stem from mutations in integrin subunits. For instance, the severe skin blistering disease junctional epidermolysis bullosa is due to mutations in genes encoding either the α_6 or β_4 subunit (van der Flier and Sonnenberg 2001a). Integrins are also gaining a role as important mediators of malignant conversion (Guo and Giancotti 2004). Cells that have become neoplastic are much less dependent on ECM adhesion for survival and proliferation (Ruoslahti and Giancotti 1989; Giancotti and Ruoslahti 1999). Cancer cells enhance the expression of those integrins that favour their proliferation, survival and migration, whereas they downregulate the expression of integrins that mediate their adhesion to the ECM (Hood and Cheresh 2002; Guo and Giancotti 2004). The switches in integrin expression are complex and depend on the origin of tissue, histological type of tumour and stage of progression. The major integrin receptors of oral epithelial cells as well as oral SCC include $\alpha_2\beta_1$ $\alpha_3\beta_1$, $\alpha_6\beta_1$ and $\alpha_6\beta_4$ (Kramer et al. 2005; Ziober et al. 2006).

4.7.2. Lutheran

Cells can bind laminins and other ECM components also via non-integrin receptors, such as α- and β-dystroglycans, lectins, syndecans and Lutheran blood group glycoproteins (Belkin and Stepp 2000; Patarroyo et al. 2002; Kikkawa and Miner 2005). Lutheran is a transmembrane glycoprotein that belongs to the immunoglobulin family (Kikkawa and Miner 2005). Two different isoforms arise from the Lutheran gene, M_r 85 000 Lutheran and M_r 78 000 basal cell adhesion molecule, B-CAM. The B-CAM molecule lacks a 40 amino-acid-long cytoplasmic tail, including the SH3 domain required for intracellular signalling (Rahuel et al. 1996). Lutheran mediates binding of erythrocytes to endothelia and is overexpressed in erythrocytes of sickle-cell anaemia patients (El Nemer et al. 1998; Udani et al. 1998). These erythrocytes adhere to laminin more strongly than normal erythrocytes. Lutheran reacts specifically with the LG3 domain of α5 chain laminins (Parsons et al. 2001; Kikkawa et al. 2002). The binding site of Lutheran resides close to that of integrins, implying that they may compete for the binding to laminin the α5 chain. Lutheran expression has been found in various tissues, including the lung, liver, prostate, kidney and arterial walls (Parsons et al. 1995; Rahuel et al. 1996). It occurs on the basal surfaces of many epithelial cells and on muscle cells adjacent to laminin α5 chain-

containing BMs (Moulson et al. 2001). Only limited information is available on the role of Lutheran in cancer. B-CAM has been detected in colon and ovarian carcinoma cell lines and is overexpressed in ovarian carcinomas (Campbell et al. 1994; Määttä et al. 2005). In ovarian cancer progression, Lutheran/ B-CAM expression is non-polarized, which was suggested to indicate loss of stabilizing interactions with the BM (Määttä et al. 2005).

4.8. Cell adhesions

Adhesion of cells to each other and to the surrounding ECM is fundamental for the maintenance of tissue architecture, function, cell migration and induction of cell adhesion-mediated signalling. Epithelial cells are connected through several intercellular junctions (Figure 5).

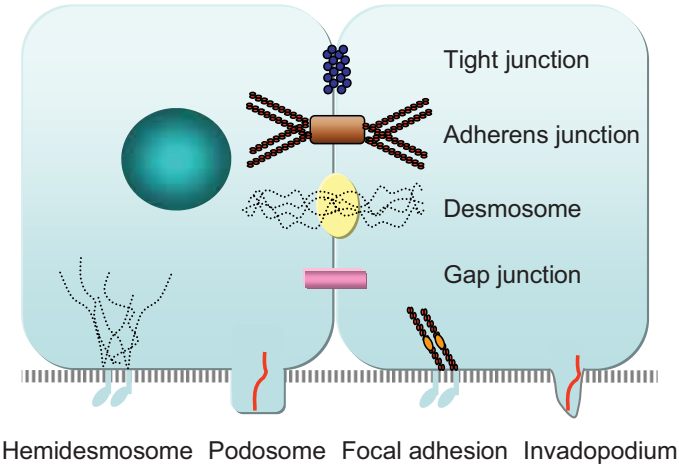


Figure 5. *Different types of cell adhesions.*

Epithelial cell adhesion to the underlying BM is mediated by, e.g., focal complexes, focal adhesions, hemidesmosomes and podosomes (see Section 4.10.1 for podosomes). In some epithelial cells, the early stages of cell attachment to BM or ECM are mediated by hyaluronan molecules residing at the pericellular coat. After attachment, the cells spread out and form narrow cell extensions, called filopodia, or broad lamellipodia (Faix and Rottner 2006; Yamaguchi and Condeelis 2007). Punctate focal complexes appear next under the protrusive lamellipodia. They contain, for instance, integrin $\alpha_v\beta_3$, talin,

phosphotyrosine and paxillin, which gather to the immediate cell membrane and are involved in binding of the actin cytoskeleton to the cell membrane. Next, vinculin, α-actinin, FAK and Arp 2/3 sequentially enter the maturing focal complex (Zaidel-Bar et al. 2004). Focal complexes assemble and disassemble quickly in response to Rho GTPase signalling. Through recruitment of zyxin and integrin $\alpha_5\beta_1$, a subset of these adhesions may grow and transform into larger, streak- or spearhead-shaped focal adhesions. The transition depends on actomyosin contractility, which applies force at cell-ECM adhesions (Geiger et al. 2001; Zamir and Geiger 2001; Zaidel-Bar et al. 2004). The hitherto unorganized actin mesh is arranged into densely packed straight bundles of filaments, i.e., actin stress fibres. Focal adhesions are multimolecular structures that consist of over 50 adaptor proteins, e.g., cytoskeletal proteins, serine/ threonine kinases, GTPase modulators, several actin-binding, -capping or -bundling molecules and proteoglycans (Figure 6). Focal adhesions are considered to enable stable and firm adhesion, and they operate as mechanosensors transmitting tensile signals from the ECM to the actin cytoskeleton (Geiger et al. 2001; Zamir and Geiger 2001; Geiger and Bershadsky 2002; Wehrle-Haller and Imhof 2002). In addition, they seem to act as signalling centres from which various intracellular pathways emanate to regulate cell growth, survival and gene expression. Focal adhesions may further evolve into fibrillar adhesions that consist of elongated, tensin-rich fibrils. Mechanical tension appears to be involved also in this turnover. Characteristics of fibrillar adhesions are the substitution of integrin $\alpha_v\beta_3$ by integrin $\alpha_5\beta_1$, low levels of phosphotyrosine and their more central location near the nucleus. These molecules participate in the formation of fibronectin fibrils (Zaidel-Bar et al. 2004).

Hemidesmosomes are cell-ECM adhesion sites that directly connect the epithelial intermediate filaments, Cks, to the underlying BM (Figure 6). Hemidesmosomes are specific structures of different epithelia, including stratified squamous, transitional and pseudostratified epithelia (Nievers et al. 1999). They mediate firm adhesion and provide resistance to mechanical stress. In skin, hemidesmosomes reside between the epidermis and dermis, where they maintain skin integrity. The assembly of hemidesmosomes begins by the gathering of integrin $\alpha_6\beta_4$ to the cell membrane. The binding of integrin $\alpha_6\beta_4$ to hemidesmosomal protein-1 (HD1)/ plectin is considered to be central in the assembly of a hemidesmosome. In some simple epithelia, e.g., in the intestine, type II hemidesmosomes comprise only these molecules attached to Ck filaments (Hieda et al. 1992; Litjens et al.

2006). In type I hemidesmosomes, bullous pemphigoid (BP) antigens BP180 (collagen XVII) and BP230 are further recruited to the complex. Through its extracellular domain, integrin $\alpha_6\beta_4$ binds to laminin-332 in the BM and transducts signals to the cytoplasm (Owaribe et al. 1991; Niessen et al. 1997; Nievers et al. 1999).

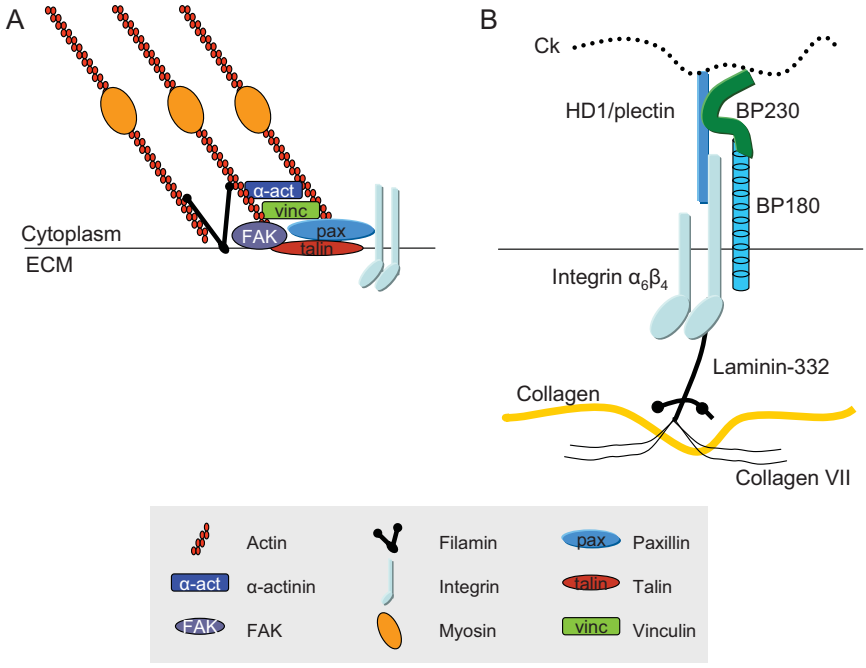


Figure 6. *Focal adhesion (A) and the hemidesmosome (B) (modified from Zamir and Geiger 2002; Littjens et al. 2006).*

4.9. Cell migration and invasion

Cell migration is essential in physiological tissue development and homeostasis, including embryonic morphogenesis, immune surveillance, inflammation and wound-healing. Furthermore, it is a key event in neoplastic dissemination and metastasis. Extracellular stimuli, including growth factors, chemoattractants or structural proteins provided by the ECM induce changes in intracellular signalling cascades and in cell polarization (Lauffenburger and Horwitz 1996). The migratory cells produce a pericellular matrix on which they migrate. For instance, during wound-healing, keratinocytes secrete a provisional matrix containing, e.g., fibronectin and laminin-332. The ECM receptor

pattern of the migrating cells also changes (Gailit et al. 1994; Larjava et al. 1996). During cell migration on planar surfaces the forward cell protrusion of the filopodia or lamellipodia is driven by actin polymerization (Lauffenburger and Horwitz 1996; Pollard et al. 2000; Ridley et al. 2003). In lamellipodia, actin filaments form a branched network mediated by Arp 2/3, whereas in filopodia they are organized into parallel bundles (Faix and Rottner 2006). New globular actin monomers (G-actin) are added to the barbed end of the growing filamentous actin (F-actin). At the pointed end of these filaments, monomeric actin is liberated by depolymerization. This process is referred to as actin treadmilling (Wehrle-Haller and Imhof 2002; Wehrle-Haller and Imhof 2003). Several GTPases, for instance, Rac, Cdc42 and RhoA, activate WASP proteins, which induce the formation of actin branches mediated by the Arp 2/3 complex. Actin polymerization, in turn, is regulated by numerous proteins that control the availability of actin monomers (profilin), branching (α-actinin, cortactin, filamins), debranching and depolymerizing proteins (cofilin), as well as capping and severing proteins (gelsolin) (Pollard et al. 2000; Pollard and Borisy 2003; Ridley et al. 2003; Otey and Carpén 2004; Kramer et al. 2005). In order to transform the treadmilling to cell movement, the growing actin filaments that push the cell membrane are anchored in place through focal complexes and focal adhesions. In some cells, such as macrophages, cell migration is mediated through another type of actin-based adhesion structure, namely, the podosome (Section 4.10.1). The maturing focal adhesions, enriched in integrins and other adhesion proteins, pull the cell forward against the resistance of focal adhesions at the rear of the cell. Myosin II motor proteins provide the force of traction. In addition, the microtubule system may be involved, as the orientation of the microtubule-organizing centre changes in migrating cells, and microtubules are frequently found to target the focal adhesion sites (Ridley et al. 2003; Wehrle-Haller and Imhof 2003). At the retractive side of the cell, the focal contacts disassemble. The integrin affinity for the ECM is reduced, the integrin complexes are internalized and recycled to the cell front, addition of new cytoskeletal linker proteins is inhibited and the actin filaments are depolymerized (Bretscher and Aguado-Velasco 1998; Hood and Cheresh 2002; Wehrle-Haller and Imhof 2002; Friedl and Wolf 2003).

Cell invasion through the BM has been described to constitute three steps, namely, cell attachment to BM, focal BM proteolysis and cell migration through the BM (Liotta 1984; Liotta and Kohn 2001). Cell invasion occurs in several physiological events, such as

embryonic implantation, inflammation and wound-healing, and in various diseases, including atherosclerosis and cancer. The invasion of individual cells in 3D substrata corresponds to the migration of single cells after loss of cell adhesion. After detachment, individual cells invade the adjacent stroma and maintain the cell-ECM contacts rather than the cell-cell contacts (Friedl and Bröcker 2000). The cells may follow an adhesive, fibroblast-like type of migration described above or a more rapid amoeboid crawling. In the former type, used by single carcinoma cells or cells of mesenchymal cancers, such as fibrosarcoma, the cells assemble focal adhesion-like contacts. The formation of pseudopodia, a 3D equivalent of lamellipodia, or invadopodia in malignant cells (Section 4.10.2) is followed by secretion of proteolytic enzymes. This is gained through integrin-mediated recruitment of surface proteases, such as seprase, cathepsins and MMPs, to ECM contacts. Some MMPs activate each other, and thus, regulate the onset and extent of pericellular proteolysis (Condeelis and Segall 2003; Friedl and Wolf 2003; Wolf et al. 2003; Yamaguchi et al. 2005b; Carragher et al. 2006).

In the amoeboid type of migration, detected in lymphoma, and some carcinoma cells, such as small-cell lung carcinoma, the tumour cell undergoes a marked cytoskeletal reorganization and seems to pass the ECM filament networks without the need for substantial proteolysis (Wolf et al. 2003; Carragher et al. 2006). Furthermore, carcinoma cells, such as breast carcinomas, may migrate in tissues as chains of tumour cells, indicating preserved contact and communication. This type of invasion confers high metastatic capacity and poor prognosis. Some carcinoma cells migrate as coherent sheets that also maintain their cell-cell and cell-ECM contacts. These cells tend to invade through the paths of least resistance, e.g., along lymphatic and blood vessels or nerves. The cancer cells in migrating clusters may express different characteristics, for instance, the cells at the front may secrete increased amounts of MMPs, and the cells at the rear may express more adhesion receptors or deposit ECM proteins (Friedl and Bröcker 2000; Friedl and Wolf 2003).

4.10. Cell-ECM adhesion and invasion complexes

4.10.1. Podosomes

Podosomes are vertical accumulations of the actin cytoskeleton, first described at the ventral cell membranes of macrophages, osteoclasts and Rous sarcoma virus-transformed fibroblasts (Lehto et al. 1982; Marchisio et al. 1984; Tarone et al. 1985). Since then, podosomes have been reported in epithelial, endothelial and vascular smooth muscle cells and by recent definition, they appear in non-malignant cells (Hai et al. 2002; Moreau et al. 2003; Spinardi et al. 2004; Linder 2007). However, the majority of studies thus far have addressed the podosomes of macrophages or osteoclasts, in which podosomes have a role in cell adhesion, migration and matrix degradation. For instance, prior to bone resorption, osteoclasts assemble podosomes to form a broad ring fused around an area targeted for resorption. Podosome formation enables close contacts and stabilizes the bone matrix-osteoclast interface, producing an isolated compartment between the ruffled border and the bone surface (Marchisio et al. 1984; Lakkakorpi and Väänänen 1991). During monocyte maturation into macrophages the assembly of podosomes mediates extravasation through vessel walls into tissues (Lehto et al. 1982).

Podosomes consist of an F-actin core and several cytoskeletal proteins, such as cortactin, N-WASP and Arp 2/3 complex, which are involved in actin network organization (Schuuring et al. 1993; Linder et al. 2000a; Pfaff and Jurdic 2001; Mizutani et al. 2002) (Figure 7). The core is surrounded by a ring of scaffolding and adhesion molecules, including paxillin, talin and vinculin (Lehto et al. 1982; Marchisio et al. 1988; Pfaff and Jurdic 2001). The core and ring are connected through linker proteins such as α-actinin (Lehto et al. 1982; Marchisio et al. 1984). A cloud of F-actin and G-actin has been reported to surround the podosome structure (Destaing et al. 2003). Actin has been suggested to be continuously polymerized and depolymerized at podosomes, based on actin polymerization complex containing Cdc42, N-WASP and Arp 2/3 (Linder et al. 1999; Linder et al. 2000b) and actin-severing protein gelsolin localizing to podosomes (Gavazzi et al. 1989). Furthermore, photobleaching experiments show rapid turnover of actin molecules in osteoclast podosomes (Destaing et al. 2003). Degradation of ECM, considered one of the functions defining podosomes, is suggested to occur through

regulated expression of MMPs such as MT1-MMP and MMP-9 (Sato et al. 1997; Delaissé et al. 2000). However, the depth and extent of degradation, depicting whether or not podosomes are invasive structures, remain undetermined.

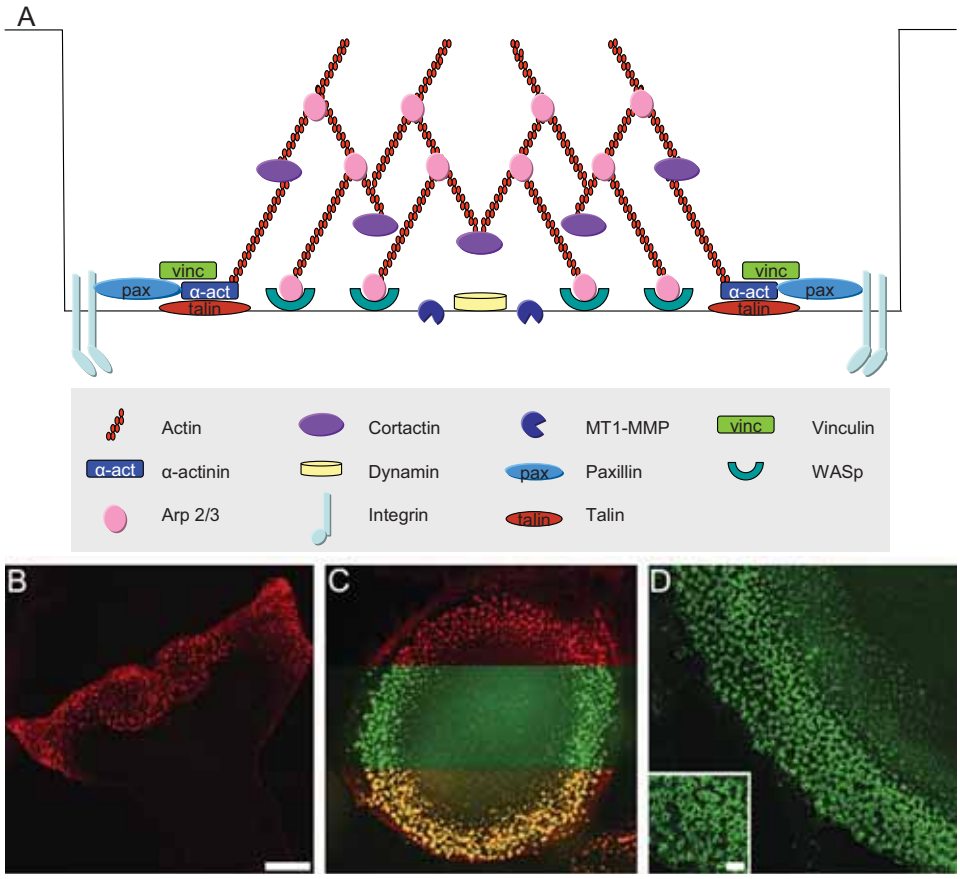


Figure 7. *A: Podosome structure (scheme modified from Linder and Aepfelbacher 2003). B-D: Podosomes of human osteoclasts assemble into clusters or belts. B: F-actin localizes to podosome cores. C: Red, F-actin; green, cortactin; yellow, overlay of figures. D: α-actinin in podosome rings. Scale bars, 10 and 5 µm, respectively. Osteoclasts were obtained by inducing human blood monocyte/ macrophages to differentiate for 7 days with 25 ng/ml macrophage-colony stimulating factor and 40 ng/ml soluble Receptor activator of the nuclear factor κ B ligand (RANKL).*

Interference reflection microscopy has shown that podosomes lie in close proximity to the ECM, suggesting that they mediate adhesion (Lehto et al. 1982; Marchisio et al. 1984). In agreement with this observation, several integrins are enriched at podosomes. Depending on the cell type, integrin β_1 subunit localizes at the podosome core, and integrin α_3, α_v, α_X,

β_2 and β_3 subunits localize at the ring structure (Marchisio et al. 1988; Zambonin-Zallone et al. 1989; Gaidano et al. 1990; Pfaff and Jurdic 2001; Spinardi et al. 2004). Furthermore, transmission electron microscopy studies have early suggested that podosomes form cylindrical protrusions to the ECM, from which their name, depicting cellular feet, originates (Tarone et al. 1985).

In microscopic images, individual podosomes are dot-like accumulations, but they can assemble, e.g., in endothelial cells or transformed fibroblasts into circular or crescent-shaped arrangements called rosettes (Tarone et al. 1985). In osteoclasts, podosomes form several superstructures, i.e., clusters, rings or belts, depending on the state of differentiation, ECM composition and resorption cycle (Akisaka et al. 2001; Destaing et al. 2003). The podosome cores of osteoclasts have a height of ca. 0.5 μm and a diameter of 0.3-0.5 μm (Gavazzi et al. 1989; Destaing et al. 2003). The average life-span of osteoclast podosomes is approximately 2-12 minutes, thus implying a dynamic structure (Kanehisa et al. 1990; Akisaka et al. 2001; Destaing et al. 2003). Furthermore, osteoclasts may use cyclic assembly and disassembly of the actin core in podosomes to generate high rates of cell motility (Kanehisa et al. 1990).

Podosomes have previously been interpreted as modified focal adhesions, as they share some morphological similarities as well as similar protein composition, including paxillin, talin and vinculin. Focal adhesions, however, are elongated structures that have a tangential orientation with respect to the ECM (Geiger et al. 2001). They do not protrude the plasma membrane, nor do they possess significant ECM degradation ability (Chen et al. 1984; Tarone et al. 1985; Gavazzi et al. 1989; Linder et al. 2000a; Pfaff and Jurdic 2001). Furthermore, it has been suggested that an intact microtubule system is needed in podosome formation in macrophages and osteoclasts, although the situation is unclear in epithelial cell podosomes (Linder et al. 2000b; Destaing et al. 2003; Spinardi et al. 2004). Microtubules target focal adhesions, providing crosstalk to the actin cytoskeleton (Palazzo and Gundersen 2002). However, they may not be essential in focal adhesion assembly; in fact, disruption of the microtubules by nocodazole in fibroblasts leads to enhanced focal adhesion formation (Bershadsky et al. 1996; Linder et al. 2000b; Destaing et al. 2003). As for focal adhesions, the *in vivo* existence of podosomes is still controversial. However, when osteoclasts are cultured on digestible bone or dentine matrices, podosomes develop,

which supports a role for podosomes also in living organisms (Teti et al. 1999; Chellaiah et al. 2000; Destaing et al. 2003).

Absence of podosomes have been reported in osteopetrosis, in which osteoclasts are unable to resorb bone properly, resulting in calcified, brittle bone structure and recurrent fractures (Teti et al. 1999). In Wiskott-Aldrich syndrome (WAS), WAS protein mutations prevent podosome organization in macrophages and dendritic cells, causing defective cell orientation and impaired movement towards the antigen and subsequently to the lymphatic organs (Linder et al. 1999). These may be the culprits for WAS patients' feeble inflammatory cell chemotaxis, leading to immune defects and even increased susceptibility to lymphomas (Stewart et al. 2001). In atherosclerosis, vascular smooth muscle cells respond to vascular injury or inflammation by proliferating and migrating from the tunica media to the tunica intima. The surplus of smooth muscle cells results in constriction of the vessel walls, impairing blood circulation, for instance, to the heart muscle (Newby and Zaltsman 2000). In this process, activated smooth muscle cells are suggested to acquire podosomes that may accumulate MMPs, for instance MMP-9, to surpass the BMs and to enable cell migration (Raines 2000; Gimona and Buccione 2006). Also macrophages and T lymphocytes that cluster to the region harbour podosomes and may gather MMPs to produce tissue destruction and further inflammation (Newby and Zaltsman 2000; Raines 2000). Apart from cell trafficking and immune surveillance, podosomes may have a role in malignancies arising from the haematopoietic cell lineage. Podosomes have been detected in B lymphocytes of patients suffering from chronic lymphocytic and hairy cell leukaemia, whereas they are not found in normal B lymphocytes (Caligaris-Cappio et al. 1986). On the other hand, in chronic myeloid leukaemia, characterized by erroneously constitutive tyrosine kinase signalling, dendritic cells are devoid of podosomes, which impairs their adhesion, spreading and migration (Dong et al. 2003).

Taken together, podosomes have been detected in cells that reside at tissue interfaces. These cells can adhere firmly when needed, for instance, in the turbulence of the blood stream, and can degrade ECM to cross anatomical boundaries, to gain information about the surrounding environment or to generate passages for other cells such as osteoblasts in

bone. Podosomes may also operate in cancer, although reports of podosomes in carcinoma cells are largely missing.

4.10.2. Invadopodia

Invadopodia are actin-rich membrane protrusions in invasive cancer cells such as melanoma, breast adenocarcinoma and fibrosarcoma (Chen et al. 1994; Mueller et al. 1999). Resembling podosomes, they contain a well-established actin-regulatory machinery, containing cortactin, N-WASP, Arp 2/3 complex, paxillin, gelsolin and phosphotyrosine (Bowden et al. 1999; Yamaguchi and Condeelis 2007) (Figure 8). In contrast to podosomes, the structure of invadopodia is less organized around the F-actin core, and no ring structure is detected (Weaver 2006). Other reported and largely cell type-dependent differences between podosomes and invadopodia are in their size, number, persistence and localization. Invadopodia have a more diverse diameter of 1-8 μm, and may appear in fewer numbers than podosomes (1-10/ cell vs. 20-100/ cell) (Linder 2007). Whereas osteoclast podosomes have short, minute-scale lifetimes, those of invadopodia in mammary carcinoma cells may vary from minutes to several hours (Yamaguchi et al. 2005a). Furthermore, invadopodia have been reported to reside close to the Golgi apparatus, and thus, near the protein synthesis and secretion systems (Baldassarre et al. 2003). Especially, localization of actin and cortactin and a direct association with ECM degradation sites have been used to define the presence of invadopodia (Bowden et al. 1999; Gimona and Buccione 2006; Weaver 2006).

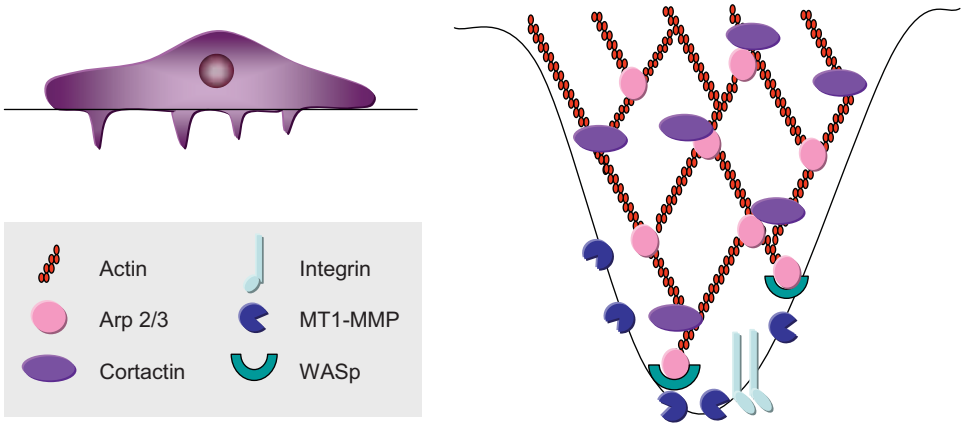


Figure 8. *The invadopodium (modified from Stylli et al. 2008; Yilmaz and Christofori 2009).*

Some integrin subunits, i.e., α_3, α_5, α_v, β_1 and β_3, have been found in invadopodia of melanoma or breast carcinoma cells (Mueller et al. 1999; Deryugina et al. 2001; Artym et al. 2002). It is not certain that the integrins *per se* elicit adhesive strength; they may instead have a more vital role in signalling or cytoskeletal organization, for instance, in gathering other proteins to the cell membrane (Weaver 2006). In fact, integrin $\alpha_3\beta_1$ recruits proteolytic enzyme seprase to invadopodia, and integrin $\alpha_5\beta_1$ is needed for the initial contact between the cell membrane and ECM preceding invadopodia formation in melanoma cells (Mueller et al. 1999; Deryugina et al. 2001).

Functions of invadopodia in matrix degradation and cell invasion are emphasized by the finding that invasion potential of breast carcinoma cells is directly correlated with ECM degradation activity and ECM phagocytosis occurring through their invadopodia (Coopman et al. 1998; Kelly et al. 1998). In line with the assumption that invasive cells encounter and degrade various ECM components, a wide array of proteolytic enzymes have been detected in invadopodia. MMP-2 and MMP-9 localize to invadopodia of melanoma, breast carcinoma or head and neck SCC cells, and docking of MT1-MMP to invadopodia is required for invasion of melanoma cells (Chen et al. 1994; Nakahara et al. 1997; Sato et al. 1997; Deryugina et al. 2001; Clark et al. 2007). In general, MT1-MMP has been shown to activate MMP-2 and MMP-9 in a complex including also a tissue inhibitor of MMPs, TIMP-2 (Hernandez-Barrantes et al. 2000; Toth et al. 2003). Apart from MMPs, different membrane-bound serine proteases, such as seprase and dipeptidyl

peptidase IV, accumulate in invadopodia of melanoma cells (Monsky et al. 1994; Artym et al. 2002; Ghersi et al. 2002). In contrast to MMPs, which are activated from proenzymes by cleavage of inhibitory fragments, serine proteases must oligomerize before they are active (Chen and Kelly 2003). In this event, integrins may operate in invadopodia (Mueller et al. 1999; Deryugina et al. 2001).

In conclusion, invadopodia are found in invasive carcinoma cells and potentially have large proteolytic capacities, but may also have possible roles in traits such as cell migration, invasion and metastasis. The majority of studies thus far are limited to a narrow selection of breast carcinoma and melanoma cell lines. These previous reports need to be interpreted with caution since they may describe functions of podosomes, invadopodia, or even other actin-based structures such as filopodia, lamellipodia or microspikes. Recently, the denomination of podosomes and invadopodia has been under additional debate, and it has been proposed that the definition for podosomes should be restricted to include podosomes only in non-cancerous cells and invadopodia in malignant cells (Linder 2007). The molecular and functional mechanisms underlying podosomes and invadopodia are still largely unsolved.

5 AIMS OF THE STUDY

EMT is suggested to enable neoplastic cells to become migratory and invasive and break through epithelial BMs. However, a molecular signature and specific markers to identify EMT in different carcinomas are lacking. Furthermore, the ECM deposited via epithelial-mesenchymal interactions may itself participate in carcinogenesis.

Specific aims of this study were:

1. To characterize the changes related to spontaneous EMT detected in recurrent, invasive oral SCC cells compared with primary oral tumour cells. The effects of transcription factor Snail overexpression in primary SCC cells were also assessed.
2. To produce a MAb against Snail.
3. To analyse the expression of Snail protein in normal and malignant cell lines and tissues.
4. To investigate the effects of EMT on the synthesis and secretion of laminins-332, -511 and -411 and on their ECM receptors such as integrins and Lutheran. To determine whether Snail can bind to promoter sites of laminin α5 and α4 chain genes.
5. To examine the differences between the structure and dynamics of cell adhesion and invasion complexes, podosomes and invadopodia in primary tumour and EMT-experienced oral SCC cells.

6 MATERIALS AND METHODS

The study protocols were approved by the Animal Experimentation Committee of the University of Helsinki (Helsinki, Finland) and the Ethics Committee or the Animal Experimentation Ethics Committee of Institut Municipal d'Investigació Mèdica (Barcelona, Spain). The Joint Ethics Committee of University of Turku and Turku University Central Hospital (Turku, Finland) approved the use of patient samples to produce cell lines. All patients signed an informed consent.

6.1. Cell lines and cell culture (I-IV)

Oral squamous cell carcinoma cell line UT-SCC-43A (43A) is derived from a primary gingival tumour of a 75-year-old Finnish female. The tumour was staged as $T_4N_1M_0$, and was histologically a moderately to well-differentiated grade 2 SCC (Haikonen et al. 2003). UT-SCC-43B (43B) is derived from a recurrent tumour from the same patient after radiation therapy and surgery. The cell lines were established by methods described earlier (Takebayashi et al. 2000). To obtain cell line 43A-SNA, 43A cells were stably transfected with full-length, haemagglutinin-tagged cDNA of murine Snail (Batlle et al. 2000), manually cloned and selected with 200 μg/ml G418 (Sigma-Aldrich, St. Louis, MO, USA).

Pancreatic carcinoma cells AsPC-1, BxPC-3, HPAC, PANC-1 and RWP-1, colon carcinoma cells HT-29 and SW-620, and murine fibroblasts NIH-3T3 were obtained from the American Type Culture Collection (Manassas, VA, USA). HT-29 M6 cells contained a tetracycline-controlled transactivator, which induced expression of haemagglutinin-tagged murine Snail when tetracycline (4 μg/ml) was withdrawn from the culture medium as described (Batlle et al. 2000). Human embryonal fibroblasts and human gingival fibroblasts were obtained from a local source.

The cells were cultured in Roswell Park Memorial Institute (RPMI) 1640 medium (Sigma-Aldrich; St. Louis, MO, USA) supplemented with 10% fetal calf serum (FCS) and antibiotics, or in a subset of studies, in defined serum-free keratinocyte growth medium (KGM-1; PromoCell, Heidelberg, Germany). CO_2-Independent Medium (Gibco/

Invitrogen, Paisley, UK), supplemented with 10% FCS, was used in live-cell imaging. In some experiments, the cells were exposed to proteasome inhibitor MG132 (10 μM; Sigma-Aldrich) for 1-5 hours to inhibit destruction of labile transcription factor proteins, or monensin (5 μM; Sigma-Aldrich) overnight, to inhibit secretion of newly synthesized proteins (Tartakoff 1983). Additionally, cycloheximide (10 μg/ml; Sigma-Aldrich) was used to inhibit protein synthesis (Clark et al. 1986), cytochalasin B (10 μg/ml; Sigma-Aldrich) to disrupt the actin cytoskeleton, demecolcine (10 μg/ml; Sigma-Aldrich) to disrupt the microtubule network and EGF (100 ng/ml; Sigma-Aldrich) to induce cell migration.

6.2. Animals (I, II)

Female Balb/c mice and nude, athymic Balb/c$^{nu/nu}$ mice were obtained from Harlan (Horst, the Netherlands) and housed at the Meilahti Experimental Animal Centre, University of Helsinki. Tissues from CD-1 mice and CD-1 mouse embryos (Harlan) were obtained from the Institut Municipal d'Investigació Mèdica (Barcelona, Spain). The animals had *ad libitum* access to standard diet and water and were housed at an ambient temperature of 20-22°C throughout the studies.

6.3. Tissues (II)

Paraffin-embedded biopsies from colon adenocarcinoma, cervical SCC, laryngeal SCC, sarcoma, fibrosarcoma and fibromatosis were retrieved from the files of Servei d'Anatomia Patològica, Hospital del Mar (Barcelona, Spain), or the Departament de Patología, Hospital Virgen de la Salud (Toledo, Spain). Tissues from CD-1 mice and mouse embryos (Harlan) were formalin-fixed and embedded in paraffin. The 4-μm sections were dewaxed, rehydrated and subjected to immunohistochemistry.

6.4. Immunocytochemistry, immunohistochemistry and microscopy (I-IV)

The cells were grown on glass coverslips and fixed by immersion in prechilled methanol at -20°C or freshly prepared 4% paraformaldehyde at room temperature (RT) for 15 minutes. Primary mouse MAbs (Table 2) were applied for 1 hour, followed by Alexa Fluor 488, 568 or 594 goat anti-mouse IgG conjugates (Molecular Probes/ Invitrogen, Eugene, OR, USA) for 30 minutes. For double-labelling, the specimens were exposed to secondary rat MAbs or polyclonal rabbit or goat antisera, followed by Alexa Fluor 488, 568 or 594 goat anti-rat, goat anti-rabbit or donkey anti-goat IgG conjugates (Molecular Probes/ Invitrogen), respectively. The specimens were embedded in sodium veronal-glycerol buffer (1:1, pH 8.4) or in Vectastain mounting medium (Vector Laboratories, Burlingame, CA, USA) and covered with cover slips. For negative controls, the primary antibody was omitted.

Immunohistochemical labellings of human tissues were performed with the CSA II system (Dako, Glostrup, Denmark) based on the detection of horseradish peroxidase (HRP) – conjugated anti-mouse immunoglobulins, fluorescyl-tyramide amplification, HRP-conjugated anti-fluorescein detection and diaminobenzidine enhancement following the manufacturer's instructions. Antigen retrieval was accomplished by boiling the samples in 10 mM citrate buffer (pH 6.0) for 5 minutes. After blocking of non-specific binding with phosphate-buffered saline (PBS) supplemented with 1% skim milk, the sections were treated with the primary antibody at RT for 2 hours. In immunohistochemistry of mouse tissues, antigen retrieval was accomplished by boiling the samples in Tris-EDTA (pH 9.0) for 15 minutes. Endogenous peroxidase activity was quenched with 4% hydrogen peroxide in PBS, supplemented with 0.1 sodium azide, at RT for 15 minutes. After washing with PBS containing 1% bovine serum albumin (BSA) to block non-specific binding, the antibody was applied and the samples were incubated at 4°C overnight. After washing, the bound antibody was detected with the Envision system (Dako) based on the detection of HRP activity, and finally, the sections were counterstained with haematoxylin.

The specimens were studied with a Leica Aristoplan microscope (Leica Microsystems, Wetzlar, Germany) or an Olympus AX70 Provis microscope (Olympus Corporation,

Hamburg, Germany) equipped with appropriate filters, UplanFl 10x/ 0.30 NA, 20x/ 0.50 NA, 40x/ 0.75 NA, PlanAPO 60x/ 1.40 NA oil or 100x/ 1.30 oil objectives and AnalySiS Pro 3.0 software (Olympus Corporation). Laser scanning confocal microscopy was performed with a Leica TCS SP2 AOBS system (Leica Microsystems) with argon excitation line 488 nm, DPSS 561 nm or helium-neon 633 nm, HCX PL APO CS 40x/ 1.25 NA or 63x/ 1.40 NA oil immersion objectives and Leica Confocal software. Image stacks were acquired through the specimen using a standardized 120 nm z-sampling density. Selected image stacks were deconvolved and restored using theoretical point spread function and iterative maximum likelihood estimation algorithm (Huygens Professional software, Scientific Volume Imaging BV, Hilversum, the Netherlands). In double-labelled specimens, each channel was imaged sequentially to prevent cross-contamination between fluorochromes.

Table 2. *Antibodies, antisera, fluoroprobes and gene constructs used in this study.*

Specificity	Monoclonal antibody	Reference
Laminin α2 chain	5H2	Leivo and Engvall 1988
Laminin α3 chain	BM2	Marinkovich et al. 1992
Laminin α3 chain, unprocessed	12C4	Goldfinger et al. 1999
Laminin α4 chain	168FC10	Petäjäniemi et al. 2002
Laminin α4 chain	3H2	Wondimu et al. 2004
Laminin α5 chain	4C7	Engvall et al. 1986
Laminin β2 chain	S5F11	Wewer et al. 1997b
Laminin β3 chain	6F12	Marinkovich et al. 1992
Laminin γ1 chain	113BC7	Määttä et al. 2001
Laminin γ2 chain	D4B5	Mizushima et al. 1998
Laminin γ2 chain when complexed in Lm-332	GB3	Matsui et al. 1995a
Bullous pemphigoid protein BP180	233	Owaribe et al. 1991
Cortactin	4F11	Upstate/ Millipore, Charlottesville, VA, USA
Cytokeratins 5, 14	KA1	Nagle et al. 1986
Cytokeratins 8, 18, 19	2A4	Virtanen et al. 1985
E-cadherin	Clone 36	BD Biosciences, San Jose, CA, USA
E-cadherin	HECD-1	Shimoyama et al. 1989

Filamin A	PM6/317	Chemicon/ Millipore, Temecula, CA, USA
Focal adhesion kinase	2A7	Upstate/ Millipore
Hemidesmosomal protein 1/ plectin	HD-121	Hieda et al. 1992
Haemagglutinin	Clone 3F10	Roche, Mannheim, Germany
Integrin α_1 subunit	TS2/7	Hemler et al. 1984
Integrin α_3 subunit	J143	Fradet et al. 1984
Integrin α_6 subunit	GoH3	Sonnenberg et al. 1987; Chemicon, Temecula, CA, USA
Integrin α_v subunit	LM142.69	Cheresh and Spiro 1987
Integrin β_1 subunit	102DF5	Ylänne and Virtanen 1989
Integrin β_4 subunit	AA3	Tamura et al. 1990
Integrin β_5 subunit	1A9	Pasqualini et al. 1993
Integrin-linked kinase	ILK	Upstate/ Millipore
Lutheran	BRIC221	Parsons et al. 1997; AbD Serotec/ Morphosys, Oxford, UK
MT1-MMP	LEM-2/15	Gálvez et al. 2001
N-cadherin	13A9	Johnson et al. 1993
Phosphotyrosine	PY20	Molecular Probes/ Invitrogen, Eugene, OR, USA
Snail	173EC3, 173CE2	Studies I-II
αII-spectrin	101AA6	Ylikoski et al. 1990
Talin	MCA725S	AbD Serotec/ MorphoSys
Tensin	Clone 5	BD Biosciences
β-tubulin	DM3B3	Blose et al. 1984
Vimentin	65EE3	Virtanen et al. 1985

Antiserum	**Species**	**Reference**
Laminin α4 chain	rabbit	Iivanainen et al. 1997
Laminin γ2 chain	rabbit	Sugiyama et al. 1995
Laminin-332	rabbit	Filenius et al. 2001
Annexin 2	rabbit	P.Navarro, IMIM, Barcelona, Spain
Arp 2/3	rabbit	Upstate/Millipore
Fibronectin	rabbit	Dako
Lutheran	rabbit	Moulson et al. 2001
MMP-2	goat	R&D Systems, Wiesbaden, Germany
MMP-9	goat	R&D Systems
Pacsin 2	rabbit	Abgent, San Diego, CA, USA
Vinculin	rabbit	Lehto et al. 1982

Specificity	Fluoroprobe	Reference
Cytoplasm (thiol compounds)	CellTracker Orange	Molecular Probes/ Invitrogen
F-actin	Rhodamine phalloidin	Molecular Probes/ Invitrogen
Nucleus (DNA)	Hoechst 33258 (DAPI)	Riedel-de Haën AG, Seelze-Hanover, Germany
Nucleus (DNA)	TO-PRO-3	Molecular Probes/ Invitrogen

Gene construct	Accession number	Reference
EGFP-actin	AY582799	BD Biosciences
EGFP-cortactin	NM_007803	Zhu et al. 2007
EGFP-filamin A	NM_001110556	Nakamura et al. 2006
GFP-Slug	NM_011415	Domínguez et al. 2003
GST-Snail, haemagglutinin-Snail	NM_011427	Batlle et al. 2000

6.5. Stable and transient transfections (I-IV)

43A cells were manually cloned by picking single cells with suction from sparse cell cultures under microscopic control. The cells were transfected with a pIRES vector (Clontech, Mountain View, CA, USA) containing haemagglutinin epitope-tagged, full-length cDNA of murine Snail (Batlle et al. 2000) or with empty plasmids as controls using JetPei reagent (Qbiogene, Carlsbad, CA, USA), based on polyethylenimine cationic transfection (Boussif et al. 1995). Efficiency of Snail transfections was monitored using immunofluorescence labellings with MAb to haemagglutinin (Roche). Individual 43A-SNA cell clones were manually isolated after selection with 400 μg/ml G418 (Sigma), and they were maintained in 200 μg/ml G418. The experiments in Study I were performed with at least five different stable Snail-transfected clones in addition to uncloned 43A-SNA cells. Furthermore, GFP-Slug (Domínguez et al. 2003) -transfected RWP-1 cells were used in Study II to verify that MAb to Snail did not crossreact with Slug. In Study IV, 43A and 43B cells were transiently transfected with EGFP-actin (BD Biosciences), EGFP-cortactin (Zhu et al. 2007) or EGFP-filamin A (Nakamura et al. 2006), using Fugene HD reagent (Roche) based on lipofection (Jacobsen et al. 2004). To gain maximal transfection efficiency and to ensure reorganization of the cytoskeletal structures, second passage cells after transfections were used in Study IV.

6.6. Production of monoclonal antibodies against Snail (I, II)

Nine-week-old female Balb/c mice (Harlan) were immunized subcutaneously with 1-2 µg of murine GST-Snail fusion protein (Batlle et al. 2000) in ImmunEasy adjuvant (Qiagen, Hilden, Germany). The adjuvant, containing bacterial cytosine-guanine dinucleotides that the mammalian immune system considers as a sign of infection, was used to enhance the immune reaction. Immunizations were repeated twice, after which the final, fourth immunizations were performed by injecting the tail veins with the antigen mixed in PBS. The spleens were harvested and minced, and polyethylene glycol was used in the fusion with P3X63Ag8.653 murine myeloma cells (American Type Culture Collection) by standard methods (Köhler and Milstein 1975). The cells were seeded on 96-well plates in Hypoxanthine Aminopterin Thymidine selection medium (HAT medium; Biological Industries, Kibbutz Beit Haemek, Israel) with 10% Ab-Max medium (ABCELL, Tampere, Finland) and 20% FCS in RPMI, which allowed only B cell-myeloma cell fusions to survive. Immunofluorescence labellings, Western blots and enzyme-linked immunosorbent assay (ELISA) were used in the characterization of the MAbs (Section 7.2). In ELISA, 96-well plates were coated with GST-Snail fusion protein or GST alone overnight at 4°C. After blocking with 1% BSA in PBS, undiluted supernatant from hybridoma cell cultures was applied for 2 hours at 37°C. After five washes with 0.05% Tween 20 in PBS, the bound MAbs were incubated with alkaline phosphatase-coupled goat anti-mouse immunoglobulins (AbD Serotec/ Morphosys) for 2 hours at 37°C, and with 2 mg/ml phosphatase substrate (Sigma) in carbonate buffer, pH 9.5, for 1 h at 37°C. The enzyme activity was measured with a spectrophotometer at 405 nm. Two of the hybridomas, producing MAbs 173CE2 (IgG_{2a}) and 173EC3 (IgG_1), were manually cloned and subsequently cultured in RPMI medium supplemented with 10% or 20% FCS and antibiotics. The immunoglobulin isotype and light chain composition of the MAbs were determined with Mouse Isotyping Kit MMT1 (AbD Serotec/ Morphosys), and the MAbs were purified with GammaBind Plus Sepharose beads (Amersham Biosciences, Uppsala, Sweden).

6.7. Immunoprecipitation (I, III, IV)

For immunoprecipitations, 43A, 43B and 43A-SNA cells were deprived of methionine for 30 minutes to 1 hour, after which they were radioactively labelled with [^{35}S]methionine (50 μCi/ml; Amersham Biosciences) at 37°C overnight. To detect the chains of laminin-332 (Study I), laminins-411/ -421 and laminins-511/ -521 (Study III), the culture medium was collected, cleared by centrifugation and supplemented with normal mouse or rabbit serum and 0.5% Triton X-100. To detect laminin-332 from cell-free ECM material (Study I), the cells were treated thrice with 0.5% sodium deoxycholate (DOC; Sigma) in 10 mM Tris-HCl, 150 mM NaCl, 1 mM phenylmethylsulfonyl fluoride (PMSF), pH 8.0, on ice for 10 minutes, and washed thrice in 2 mM Tris-HCl, 150 mM NaCl, 1 mM PMSF, pH 8.0, on ice. The ECM material was scraped off from culture plates with rubber policeman and solubilized in ice-cold radioimmunoprecipitation assay buffer (10 mM Tris-HCl, pH 7.2, 150 mM NaCl, 0.1% sodium dodecyl sulphate [SDS], 1.0% Triton X-100, 1.0% DOC, 5 mM EDTA, 1 mM PMSF). For immunoprecipitations of integrins and Lutheran (Study III), [^{35}S]methionine-labelled cells were scraped off from culture plates and similarly solubilized in radioimmunoprecipitation assay buffer. For immunoprecipitations of laminin γ1 chain (Study III), the cells were left unlabelled. For immunoprecipitations of integrins (Study IV), the cells were surface-labelled with 0.2 mg/ml NHS-SS-biotin (Pierce, Rockford, IL, USA) and solubilized in 100 mM Tris, 150 mM NaCl, 1 mM $CaCl_2$, 1 mM $MgCl_2$, 1% Triton X-100, 0.1% SDS and 0.1% Nonidet P-40, pH 7.4. For immunoprecipitations of FAK (Study IV), the cells were treated with 60 mM KCl, 1 mM EDTA, 2 mM EGTA, 1 mM cysteine, 40 mM imidazole, pH 7.0, supplied with 0.5% Triton X-100, 1 mM PMSF and 1 mM Na_3VO_4, on ice for 30 minutes. The supernatant was collected and the treatment repeated.

The samples were then preabsorbed with uncoupled GammaBind Plus Sepharose beads (Amersham Biosciences), followed by application to GammaBind Plus Sepharose beads prebound with antibodies (Table 1), and incubated in a rolling shaker at 4°C overnight. For negative controls, the primary antibody was omitted. The precipitated proteins were separated with SDS polyacrylamide gel electrophoresis (SDS-PAGE) following Laemmli's procedure with reducing or non-reducing 5% to 10% gels. [^{14}C]Methylated Molecular Weight Marker (Amersham Biosciences) was used as a size marker.

Radioactively labelled proteins were detected from dried gels using Hyperfilm MP (Amersham Biosciences). Other immunoreactive proteins were then subjected to Western blotting.

6.8. Western blot analysis (I-IV)

For Western blots, cells scraped from culture plates or previously immunoprecipitated samples were diluted in reducing Laemmli's sample buffer. In Study I, laminin-332 was recovered from overnight cultures of serum-free RPMI medium with ammonium sulphate precipitation by treatment with 0.53 g/ml ammonium sulphate, 0.5 mg/ml gelatin, 0.02% sodium azide and 1 mM PMSF. The proteins were then separated with SDS-PAGE and transferred onto nitrocellulose filters, which were blocked with 5% skim milk (BD Biosciences) in PBS. After addition of the MAbs or antisera, the immunoreactive bands were detected either with Vectastain Elite ABC kit (Vector Laboratories), based on avidin-biotin peroxidase complex, using goat anti-mouse or goat anti-rabbit immunoglobulins, nickel intensification and diaminobenzidine (Sigma) as a substrate, or with SuperSignal West Pico Chemiluminescent Substrate (Pierce, Rockford, IL, USA), using HRP-coupled anti-mouse or anti-rabbit immunoglobulins (Dako), or HRP-coupled MAb to phosphotyrosine (Table 2). Equal loading of proteins was verified with Amido Black (Sigma) labellings or with MAb to β-tubulin (Table 2). Molecular Weight Marker (M.W. 30 000-200 000; Sigma) was used as a size marker.

For detection of Snail in Study II, cell extracts were incubated in a buffer containing 50 mM Tris-HCl, pH 8.0, 150 mM NaCl, 1 mM EGTA, 1% DOC, 1% Triton X-100, 0.2% SDS and protease and phosphatase inhibitors (5 mM NaF, 1 mM Na_3VO_4, 2 mM β-glycerolphosphate, 10 mg/ml leupeptin, 10 mg/ml aprotinin, 10 mg/ml pepstatin, 2 mM Pefablock [Boehringer Mannheim, Germany]) on ice for 30 minutes. Cell lysates were centrifuged and the supernatant was used for Western blot analysis. The proteins were separated with SDS-PAGE using 15% gels, transferred onto nitrocellulose filters, and analysed as above. Equal loading of proteins was verified with rabbit antiserum to annexin 2 (Table 2).

6.9. Northern blot analysis (I, III)

Total RNA of 10 000 000 43A, 43B and 43A-SNA cells was extracted with Eurozol (EuroClone, Milan, Italy), or by acid phenol-guanidium thiocyanate-chloroform extraction method as described by Chomczynski and Sacchi (1987), and the mRNAs were enriched by capturing the poly-A-tails with Dynabeads Oligo $(dT)_{25}$-beads (Dynal Biotech, Oslo, Norway). The mRNAs were separated in denaturing 1.2% agarose gels and transferred by upward capillary transfer onto Hybond membranes (Amersham Biosciences). The membranes were washed with 6 x SSC (0.9 M NaCl, 0.09 M sodium acetate, pH 7.0), air-dried for 30 minutes, UV-crosslinked and hybridized with non-radioactive, digoxigenin-labelled (DIG) probes (Roche).

In Study I, the cDNA probes were produced with DIG High Prime DNA Labelling and Detection Starter Kit II by excising inserts with restriction enzymes and labelling them with DIG. The nucleotide sequences and restrictions sites were verified by DNA sequencing. The following cDNA probes were generated: 702 bp EcoRI fragment of laminin α3 chain (in pCRII plasmid, Invitrogen; Ryan et al. 1994), 534 bp EcoRI/ HindIII fragment of laminin γ2 chain (in pGEM 3Z plasmid, Promega; Airenne et al. 1996), full-length, 800 bp EcoRV/ BamHI cDNA of human Slug (in pcDNA3 plasmid; Domínguez et al. 2003) and 500 bp NcoI/ NotI fragment of human Snail (in pGEM-T plasmid, Promega; Batlle et al. 2000). Full-length, 3.5 kb EcoRI cDNA of murine ZEB-1 (in pcDNA3 plasmid; Invitrogen) was received from Tom Genetta (Children's Hospital, Philadelphia, PA, USA), and full-length, 3.6 kb NcoI/ XbaI cDNA of human ZEB-2 (in pCs2Mt plasmid; Turner and Weintraub 1994) was from Antonio Postigo (Washington University School of Medicine, St. Louis, MO, USA; Postigo 2003). A PstI fragment of GAPDH was used as a control (in pBluescript plasmid, Stratagene; Fort et al. 1985). Prehybridization and hybridization in high SDS hybridization buffer (7% SDS, 50% deionized formamide, 5 x SSC, 0.1% N-lauroylsarcosine, 2% Blocking Solution [Roche], 50 mM sodium phosphate, pH 7.0) were carried out at 50°C for 30 minutes and for 18 hours, respectively. The probes were detected with alkaline phosphatase-conjugated anti-DIG antibody and CSPD, and the blots were exposed to Hyperfilm MP (Amersham Biosciences). For re-use of the blots, the previously detected probes were erased with boiling in 0.1% SDS for 10 minutes, after which the blots were rinsed in 0.1 M maleic acid, 0.15 M NaCl, pH 7.5,

0.2% Tween 20, and stored in 2 x SCC. A 0.24-9.5 kb RNA ladder was used as a size marker (Life Technologies, Gaithersburg, MD, USA).

In Study III, the cRNA probes for the laminin α5 chain and the laminin α4 chain were generated from plasmid cDNA templates as follows: antisense cRNA probe for the laminin α5 chain was generated by linearizing pBluescript SK+ plasmid (Stratagene, La Jolla, CA, USA) covering nucleotides 9805-11 332 (Durkin et al. 1997), with NotI, and incorporating DIG label by *in vitro* transcription using DIG RNA Labelling kit (SP6/T7) and T7 RNA polymerase (Roche). Antisense cRNA probe for the laminin α4 chain was generated by linearizing pBluescript plasmid covering nucleotides 94-2808 (Kortesmaa et al. 2000), with EcoRI, using T7 RNA polymerase. Prehybridization and hybridization with DIG Easy Hyb (Roche) were carried out at 68°C for 30 minutes and for 18 hours, respectively. The probes were thereafter detected as above. For re-use of the blots, the membranes were washed twice in stripping solution (50% formamide, 5% SDS, 50 mM Tris-HCl, pH 7.2) at 80°C for 60 minutes and re-probed. Hybridizations with antisense GAPDH probes were used to confirm the equal loading of mRNA, and hybridizations with sense cRNA probes were used as negative controls. Digoxigenin-labelled RNA molecular weight marker I (Roche) was used as a size marker.

6.10. Preparation of crude nuclear extracts (I)

For evaluation of endogenous Snail in pancreatic adenocarcinoma cell line PANC-1, the cells were grown to confluency, trypsinized and treated with trypsin-neutralizing solution (PromoCell). The cells were collected by centrifugation, allowed to swell in ice-cold, hypotonic cell homogenization buffer (10 mM HEPES-KOH, pH 7.9, 1.5 mM $MgCl_2$, 10 mM KCl, 0.5 mM dithiothreitol, 0.5 mM PMSF) for 10 minutes on ice and centrifuged. To disrupt the cell membranes and release the nuclei, the pellet was resuspended in ice-cold buffer (0.5% Triton X-100, 50 mM Tris-HCl, pH 7.9) and homogenized on ice with a Dounce homogenizer. Lysis of cells was followed under a microscope, after which the cells were washed in cell homogenization buffer, centrifuged and used in Western blotting (Sambrook and Russell 2001).

6.11. Quantitative reverse transcription polymerase chain reaction (II)

To analyse whether expression of Snail was dependent on serum, NIH-3T3 cells were starved of serum for 24 hours, after which they were exposed to 10% FCS for 0-24 hours. Total RNA was extracted with GenElute Mammalian total RNA kit (Sigma). Analysis of Snail RNA levels was performed with QuantiTect SYBR Green RT–PCR (Qiagen). All quantifications were performed in triplicate and normalized to the endogenous control cyclophilin or hypoxanthine-guanine phosphoribosyltransferase. Relative quantification values for each target gene, compared with the calibrator for that target, were expressed as $2^{-(Ct-Cc)}$, in which Ct and Cc are mean threshold cycle differences after normalizing to controls. The following oligonucleotides were used to detect Snail: 5'-TTCCAGCAGCCCTACGACCAG-3' (forward) and 5'-CTTTCCCACTGTCCTCATC-3' (reverse).

6.12. Wound-healing assay *in vivo* (II)

After induction of anaesthesia with isoflurane (Abbot Laboratories, Abbot Park, IL, USA), the dorsums of CD-1 mice (Harlan) were shaved free from hair, and the skins were cleaned with 70% ethanol. Four full-thickness wounds were aseptically made with a 2-mm biopsy punch lateral to the spine of each animal. Wound closure was monitored daily. The mice were sacrificed at 2, 3, 5 or 7 days post-wounding, and the wounded tissues were collected and subjected to immunohistochemistry.

6.13. Cell morphology and cell invasion assays (III, IV)

Cell morphology, cytoskeletal structures and cell invasion abilities were studied with modified Boyden chambers. Matrigel (5 mg/ml; BD Biosciences) was coated on Falcon FluoroBlok Individual Cell Culture Inserts (BD Biosciences) with 8 μm pores at 37°C for 1 hour. Altogether 50 000 cells in 350 μl of cell culture medium were added to the upper chamber, and 900 μl of culture medium was added to the lower chamber. The cells were grown at 37°C overnight, after which the filters were fixed in 4% paraformaldehyde and labelled with rhodamine phalloidin (Molecular Probes/ Invitrogen). The filters were

detached from the inserts with a scalpel, mounted in Vectashield mounting medium on objective slides and covered with cover slips. The cells on both sides of the filter were examined. The cells that had invaded through the ECM and the filter pores to the lower sides of the filters were photographed using an Olympus AX70 microscope with UPlanFl 10x/ 0.30 NA, 20x/ 0.50 NA, or 40x/ 0.75 NA objectives or a Leica TCS SP2 AOBS confocal microscope with an HCX PL APO CS 63x/ 1.40 NA oil immersion objective. The experiments were performed at least in triplicate.

6.14. Chromatin immunoprecipitation and polymerase chain reaction (III)

Chromatin immunoprecipitations (ChIP) were performed on 43A-SNA cells with a ChIP-IT Express Assay Kit (Active Motif, Carlsbad, CA, USA) to analyse whether Snail binds to gene promoter sites of laminin α5 and α4 chains. 43A-SNA cells were fixed with 1% formaldehyde at RT for 15 minutes to crosslink the DNA-binding proteins to DNA. After cell lysis on ice for 30 minutes, the DNA was sheared into fragments with a Dounce homogenizator and enzymatically digested at 37°C for 15 minutes. A portion of chromatin lysate was stored as an Input control. DNA-protein complexes were immunoprecipitated at 4°C overnight using Protein G beads with 2-6 µg of negative control mouse IgG antibody (Dako), positive control RNA polymerase II antibody provided by the kit, or MAb 173EC3 against Snail (Studies I and II). The DNA was eluted, the crosslinks were reversed at 94°C for 15 minutes, the proteins were removed with Proteinase K at 37°C for 1 hour and the DNA was used as a template for PCR.

Promoter sequences for laminin α5 (NM_005560) and α4 (NM_002290) chain genes were extracted from human genome sequence with Genomatix Gene2Promoter software (Genomatix Software, Munich, Germany). Overlapping primers (Tables 2 and 3 in Study III) covering the genomic region 3000 bp upstream of laminin α5 and α4 transcription start sites were designed with Primer3 software (Rozen and Skaletsky 2000) and were produced by Oligomer (Helsinki, Finland). Primers were ca. 20 nucleotides long, and were designed to minimize primer dimers, to have a 45-55% GC concentration and to have a melting temperature (Tm) of ca. 60°C. Primers for GAPDH, used to detect the control Input DNA, were provided in the kit. PCR amplification was performed with AmpliTaq Gold DNA

polymerase (Applied Biosystems, Foster City, CA, USA) in a thermal cycler (RoboCycler Gradient 40; Stratagene) as follows: initial denaturation at 95°C for 10 minutes, 40 cycles with denaturation at 95°C for 1 minute, annealing at 60-64°C for 1 minute, extension at 72°C for 1 minute and a final extension for 20 minutes. The samples were fractionated through 1% agarose gels with a 100 bp DNA ladder (Invitrogen). MatInspector software (Genomatix Software) was used to screen the laminin α5 and laminin α4 chain promoter sites for the E-box (5′-CA(C/G)(C/G)TG-3′) and Z-box (5′-CAGGT(G/A)-3′) motifs.

6.15. Quantitative cell adhesion assay (III)

Quantitative cell adhesion experiments were based on a method detecting intracellular acid phosphatase activity (Prater et al. 1991). The wells of 96-well cell culture plates were coated with 4 μg/ml recombinant human laminin-411, 4 μg/ml native human laminin -511 or 5 μg/ml human plasma fibronectin at RT for 1 hour. Recombinant laminin-411, comprising human laminin α4 and γ1 chains and murine laminin β1 chain, was produced in a mammalian expression system (Kortesmaa et al. 2002). Native laminin-511 was purified from the culture medium of PANC-1 cells with immunoaffinity chromatography (Tani et al. 1999). Fibronectin was purified from outdated human plasma (Finnish Red Cross Blood Transfusion Service, Helsinki, Finland) with gelatin-Sepharose affinity chromatography (Amersham Biosciences) (Engvall and Ruoslahti 1977). After three washes with PBS, the wells were post-coated with 3% BSA (Sigma) at RT for 1 hour to inhibit unspecific binding of proteins. To prevent the synthesis of endogenous proteins during the adhesion experiment (Clark et al. 1986), the cells were preincubated with cycloheximide (10 μg/ml; Sigma) at 37°C for 1 hour, after which the cells were trypsinized, treated with trypsin-neutralizing solution (Promocell) and collected by centrifugation. Altogether 20 000 43A, 43B and 43A-SNA cells in serum-free cell culture medium supplied with 10 μg/ml cycloheximide were placed into each well, and the plates were incubated at 37°C for 1 hour. After careful washing in PBS to remove non-adherent cells, phosphatase substrate solution (6 mg/ml phosphatase substrate in 50 mM sodium acetate buffer, pH 5.0; Sigma, 1% Triton X-100) was added, and the plates were incubated at 37°C for 1 hour. The reaction was stopped with 1 M NaOH, and the absorbances were measured with a spectrophotometer at 405 nm. Wells that were coated with only BSA

were used as controls. The experiments were performed at least in triplicate, and absorbances were expressed as ±SD of three wells.

6.16. Wound-healing assay *in vitro* (IV)

The cells were grown to confluency on coverslips and wounded with a rubber policeman. After washing with PBS, non-viable cells were removed with careful suction and fresh cell culture medium was applied. The cells were allowed to grow and migrate at 37°C for 2-24 hours, after which they were fixed in 4% paraformaldehyde at RT and labelled with appropriate antibodies. EGF (100 ng/ml, Sigma-Aldrich) was used in some experiments to induce cell migration in 43A cells. The images were acquired with a Leica TCS SP2 AOBS confocal microscope with an HCX PL APO CS 40x/ 1.25 NA oil immersion objective as above.

6.17. Random cell migration assay (IV)

For random cell migration (Entschladen et al. 2005), the cells were labelled with 20 μM CellTracker Orange (Molecular Probes/ Invitrogen) in serum-free RPMI culture medium at 37°C for 30 minutes. After trypsinization and treatment with trypsin-neutralizing solution, 100 000 43A and 43B cells were seeded on coverglass bottom dishes (coverglass thickness 1.5; MatTek, Ashland, MA, USA) in pre-warmed CO_2-Independent Medium (Gibco/ Invitrogen) supplemented with 10% FCS and allowed to attach for 20 minutes. Cell migration was analysed using epifluorescence imaging at 37°C with an Olympus IX71 inverted microscope and a TILL Photonics imaging system (TILL Photonics/ Agilent Technologies, Munich, Germany) with UPlanFl 10x/ 0.30 NA dry objective, polychrome IV monochromator, and TILLvisION software v. 4.01. Cells were exposed to 540 nm monochromatic light for 20 ms with 5-minute intervals for 10 hours, and emission was collected using a 605/55 nm bandpass filter. The trajectory length, distance between the start and end points and directionality of the trajectories were analysed with ImageJ version 1.41e software (Rasband WS: ImageJ, National Institutes of Health, Bethesda, MD, USA, http://rsb.info.nih.gov/ij/, 1997-2008) using an MTrackJ plugin (by Erik Meijering). The experiments were repeated at least three times.

6.18. Analysis of podosomes and invadopodia on different ECM substrata (IV)

To analyse the effects of different ECM components on the number and morphology of podosomes and invadopodia, 43A and 43B cells were seeded on glass coverslips that were coated with 4 μg/ml type I collagen, 4 μg/ml plasma fibronectin, 2 μg/ml laminin-332 or 2 μg/ml laminin-511. Type I collagen was obtained from rat tails (Sigma-Aldrich), and fibronectin was purified as above. For these experiments, purified human laminin-332 was obtained from Patricia Rousselle (Institut de Biologie et Chimie des Protéines, Unité Mixte de Recherche, Université Lyon, France), and purified human laminin-511 was from Kiyotoshi Sekiguchi (Institute for Protein Research, Osaka University, Japan). The cells were allowed to adhere and assemble podosomes or invadopodia for 48 hours at 37^{o}C. The cells were fixed in 4% paraformaldehyde and labelled with rhodamine phalloidin. The percentage of cells that had organized at least two podosomes or invadopodia per cell were counted in 10 microscope fields (ca. 20-40 cells/ field) using an Olympus AX70 Provis microscope with a 40x/ 0.75 NA objective. The experiments were repeated at least three times.

6.19. *In situ* zymography for ECM degradation (IV)

To analyse the presence of podosomes and invadopodia and the ECM degradation capacities of 43A and 43B cells, we performed *in situ* zymography assays. Glass coverslips were coated with fluorescein-conjugated gelatin (0.2 mg/ml in 2% sucrose buffer; Molecular Probes/ Invitrogen) for 2 hours, crosslinked with 0.5% glutaraldehyde for 15 minutes and treated with $NaBH_4$ (5 mg/ml) at RT for 3 minutes. Fluorescein-conjugated gelatin was quenched with two washes of RPMI medium at 37^{o}C for 30 minutes and coated with 1 μg/ml fibronectin at RT for 1 hour. Fibronectin was purified as above. 43A and 43B cells were seeded on coverslips, incubated at 37^{o}C for 2-15 h, fixed with 4% paraformaldehyde and labelled with rhodamine phalloidin and TO-PRO-3. The degraded areas of the matrix were visible as dark foci devoid of fluorescence. Images were acquired with a Leica TCS SP2 AOBS confocal microscope with an HCX PL APO CS 63x/ 1.40 NA oil immersion objective using sequential scanning and were deconvolved with Huygens Professional software as above. 3D reconstructions and relative volume

calculations (μm^3) of actin fluorescence intensity (n=5-9 cells per time point) were performed with Imaris software (Bitplane, Zurich, Switzerland). The results were normalized against a standard curve generated using 0.5, 1.0 and 2.0 μm diameter carboxylate-modified polystyrene microspheres (FluoSpheres Size Kit, Molecular Probes/ Invitrogen). Degradation cavities produced by cells (n=33 for 43A; n=32 for 43B cells) were photographed with an Olympus AX70 Provis microscope with a 60x/ 1.40 NA oil objective, counted and analysed with ImageJ software. The resorption areas per cell (μm^2) were measured by thresholding (maximum entropy thresholding plugin by Jarek Sacha) after background subtraction (rolling ball background subtraction plugin by Michael Castle and Janice Keller).

6.20. Field emission scanning electron microscopy (IV)

43A and 43B cells were cultured on glass coverslips and fixed in 2.5% glutaraldehyde in 0.1 M sodium cacodylate buffer (pH 7.2) at RT for 30 minutes. The samples were washed thrice with cacodylate buffer, dehydrated through a graded series of ethanol, and treated with hexamethyldisilazane. The samples were then coated with 20 μM chromium with Emitech K575X sputter coater (Emitech, Kent, UK) and studied under a field emission scanning electron microscope (FESEM, JEOL JSM-6335F; JEOL, Tokyo, Japan) at 5–15 kV operating voltage and 0-45° inclination.

6.21. Live-cell imaging and total internal reflection fluorescence microscopy (IV)

To analyse the functions of podosomes and invadopodia in live cells, 43A and 43B cells were transfected with EGFP-actin or EGFP-cortactin and seeded on coverglass bottom dishes in pre-warmed CO_2-Independent Medium supplemented with 10% FCS. Epifluorescence images were acquired using an Olympus IX71 inverted microscope with a PlanAPO 60x/ 1.20 NA water immersion objective at 37°C and a TILL Photonics imaging system. Cells were exposed to 480 nm monochromatic light for 20-100 ms with 10-s intervals for 30 minutes or with 5-minute intervals for 15 hours, and emission was collected using a 520 nm longpass filter. The exposure times and acquisition intervals

were chosen to avoid phototoxicity caused by the excitation wavelength. 2D deconvolution was performed with Huygens Professional software, and the images were further analysed and movies compiled with ImageJ followed by QuickTime Pro version 7.4 and H.264 codec (Apple Inc., Cupertino, CA, USA) softwares. In some experiments, the cells were treated with cycloheximide, cytochalasin B, demecolcine (10 µg/ml; Sigma-Aldrich) or their combination.

Total internal reflection fluorescence (TIRF) microscopy was used to assess the events at the narrow cell-ECM surface interface. TIRF images were acquired with an Olympus IX71 inverted microscope equipped with a CellR imaging system, a 476 nm solid state 20 mW laser, a PLAPON 60x/ 1.45 NA TIRF objective and a Hamamatsu Orca ER CCD camera. To ensure evanescent field detection, a mixture of carboxylate-modified fluorescent 20 nm and 200 nm polystyrene beads (Molecular Probes/ Invitrogen) was immobilized onto the surface of coverglass bottom dishes, and the laser angle was optimized for TIRF detection of the 20 nm particles. For prolonged TIRF imaging, a motorized Nikon Eclipse Ti-E TIRF system was used with a TI-ND6-Perfect Focus Unit, NIS-Elements AR software, a Coherent Sapphire 488 nm solid state 20 mW laser, a CFI APO 100x/ 1.49 NA TIRF objective and a Nikon DS-Qi1MC camera (Nikon Instruments, Melville, NY, USA). Images were acquired at 37^{o}C with 10-s intervals for 30-60 minutes or with 30-s intervals for 6-12 hours.

6.22. Fluorescence recovery after photobleaching (IV)

The exchange and kinetics of fluorescent molecules in live cells were studied with fluorescence recovery after photobleaching (FRAP) experiments. 43A and 43B cells were transfected with EGFP-actin, EGFP-cortactin or EGFP-filamin A and seeded on coverglass bottom dishes in CO_2-Independent Medium. FRAP was performed at 37^{o}C with a Leica TCS SP2 AOBS confocal microscope with an argon excitation line of 488 nm and an HCX PL APO LU-V-I 63x/ 0.9 NA water immersion objective, using a 200 µm pinhole (1.12 Airy) and a zoom factor of 4. With 512x512 pixel image format and 1000 Hz scanning speed, prebleaching was carried out with 10 pulses at low-intensity illumination and bleaching with 5 high intensity short pulses (3.3 s total). Zoom-in function for the region of interest was used to increase the bleaching power. Fluorescence

recovery was monitored by time-lapse imaging for a total duration of 135 s under low intensity illumination. After raw data measurement, the background was subtracted, and the data was corrected and normalized taking into account laser intensity fluctuations and loss of fluorescence during recording (Rabut and Ellenberg 2005). Half-time of recovery, plateau of recovery and mobile and immobile fractions were calculated with Prism 4.0 software using non-linear regression (GraphPad Software, La Jolla, CA, USA). For each FRAP experiment, an area of 10 μm^2 was bleached and the fluorescence recovery was measured from a 1.35 μm^2 region of interest surrounding podosomes (n=25), invadopodia (n=25) or cell extensions (n=9). When cell extensions were imaged, the average distance between the extension and cell surface was ca. 3 μm.

6.23. Statistical analysis (II-IV)

Statistical analyses were performed using a two-tailed, unpaired *t*-test, or the analysis of one-way variance (ANOVA) followed by Bonferroni´s post hoc test, and non-linear regression analysis (Prism 4.0 software). $P<0.05$ was regarded as statistically significant. The results are expressed as ± SD or SEM.

7 RESULTS

7.1. Characterization of EMT in oral SCC cells (I)

7.1.1. Endogenous EMT in oral SCC cells (I)

43A cells were obtained from a primary squamous cell carcinoma of the oral cavity and 43B cells from its recurrent tumour after irradiation therapy and surgery. Our first aim was to study how these two cell lines differ from each other *in vitro*. In cell culture, 43A cells grew as islands and showed a typical epithelial, cobblestone morphology, whereas 43B cells showed a more fibroblastoid morphology and retained only a few cell-cell contacts. When the cells were grown in KGM-1 cell culture medium, which is used to promote the growth of epithelial cells over non-epithelial cells, 43A cells thrived and proliferated, whereas 43B cells were unable to survive. Immunolabelling with rhodamine phalloidin revealed that actin filament bundles encircled 43A cells, while 43B cells harboured actin stress fibres. Concerning intermediate filaments, immunolabelling and Western blots with MAbs KA1 and 2A4 detected Cks typical for simple epithelia (Cks 8, 18 and 19) and for stratified epithelia (Cks 5 and 14) (Bragulla and Homberger 2009) in 43A cells. In 43B cells, only focal immunoreactivity for Cks 8, 18 and 19 was found, and no immunoreactivity for Cks 5 or 14. Western blots showed minor amounts of Cks 8 18, and 19 in 43B cells. In addition, 43A cells showed only irregular accumulations of vimentin with MAb 65EE3 near the cell nuclei, in contrast to 43B cells, which showed strong, fibrillar vimentin arrays that appeared to be concentrated in one or two polar clusters at the cell periphery. These observations were supported by Western blots, revealing a strong M_r 54 000 band corresponding to vimentin.

As these results suggested several mesenchymal characteristics in 43B cells, we further analysed the expression of adherens junction proteins E-cadherin and N-cadherin. Loss of E-cadherin and emergence of N-cadherin have been reported *in vivo* and *in vitro* in progression of oral SCC (Islam et al. 1996; Chen et al. 2004), and their reciprocal expression may be linked to EMT (Tran et al. 1999; Vandewalle et al. 2005). MAb HECD-1 showed reactivity for E-cadherin at the cell-cell junctions of 43A cells, whereas 43B cells were negative. In contrast, 43A cells did not react with MAb 13A9 against N-

cadherin, but 43B cells showed strong, serrated immunoreactivity at the cell-cell junctions. In Western blots, 43A cells revealed a M_r 120 000 band of E-cadherin and a faint M_r 127 000 band of N-cadherin, whereas 43B cells showed no reaction against E-cadherin, but strong bands corresponding to N-cadherin. These results, including the E-cadherin to N-cadherin switch, indicated that 43B cells had undergone an endogenous EMT.

7.1.2. Induction of EMT by overexpression of Snail in oral SCC cells (I)

To further investigate the events of EMT in oral SCC cells, we transfected 43A cells with haemagglutinin-tagged cDNA of Snail, a transcription factor that has gained increasing evidence as a major inducer of EMT (Batlle et al. 2000; Cano et al. 2000). Stable Snail transfectants were rather difficult to establish, as the transfected cells seemed to engage apoptosis. This may be due to the finding that downregulation of E-cadherin via the Akt pathway can lead to apoptosis (Kurrey et al. 2005). Transfection efficiency was controlled with immunolabellings and Western blots with MAb to haemagglutinin as well as with newly established MAbs to Snail (Section 7.2). Stable 43A-SNA transfectants were manually subcloned to gain cell lines with homogeneous and high ectopic expression of Snail. Subcloning was supported by the finding that in uncloned cultures the cells that do not express the Snail transgene overpopulate the stable transfectants (Ohkubo and Ozawa 2004). The morphology of 43A-SNA cells resembled that of 43B cells; the cells failed to organize compact colonies in culture and represented an elongated, fibroblastoid phenotype with sparse cell-cell contacts. 43A-SNA cells showed similar actin stress fibres as 43B cells, and immunolabellings and Western blots revealed no evidence of Cks 5 or 14, and only traces of Cks 8, 18 and 19. Instead, 43A-SNA cells synthesized prominent vimentin filaments, and production of mesenchymal N-cadherin substituted that of E-cadherin. These findings suggested that 43A-SNA cells had undergone a full EMT as a result of expression of Snail.

7.1.3. Expression of E-cadherin repressors in oral SCC cells (I)

In order to characterize which of the several possible E-cadherin repressors were present in 43A, 43B and 43A-SNA cells, we performed Northern blots with cDNA probes. 43A cells expressed a faint 5.7 kb transcript of ZEB-1 and a prominent 2.1 kb transcript of

Slug, but not ZEB-2 or Snail. 43B cells showed a stronger band for ZEB-1, prominent double bands of ca. 5.6 kb corresponding to ZEB-2, and a weaker band for Slug compared with 43A cells. 43B cells showed no expression of Snail. 43A-SNA cells, however, showed a potent 1.0 kb transcript of Snail as expected, but also bands corresponding to ZEB-1, ZEB-2 and Slug. These studies suggested that 43A cells expressed only a minor amount of ZEB-1 and a high amount of Slug mRNA, but Snail transfection in 43A-SNA cells augmented the expression of ZEB-1 and induced expression of ZEB-2 mRNA. Expression of Slug was diminished in 43B and 43A-SNA cells relative to 43A cells. As both ZEB-1 and ZEB-2 mRNAs were present in 43B and 43A-SNA cells, they may be important in EMT of oral SCC cells.

7.2. Production and specificity of monoclonal antibodies against Snail (I, II)

Next, we aimed to generate a MAb that would detect Snail protein in human cell lines and tissues. The hybridomas producing MAbs were created by immunizing mice with GST-Snail fusion protein (Batlle et al. 2000) (Section 6.6). The initial screening of the hybridomas was performed with immunofluorescence labellings using 43A-SNA cells, and the hybridomas potentially producing MAbs specific to Snail were cloned. The specificity of the MAbs was further analysed with immunofluorescence labellings, ELISA and Western blots. In immunolabellings with 43A-SNA cells, MAbs 173CE2 (IgG_{2a}) and 173EC3 (IgG_1) as well as their subclones showed strong Snail immunoreactivity in the nuclei, excluding the nucleoli. Only occasionally was immunoreactivity detected in the cytoplasm. This finding is in accordance with the previous findings of GFP-Snail transfected HEK293 cells (Zhou et al. 2004). No immunoreaction occurred when the purified MAbs were preabsorbed with GST-tagged Snail protein. Furthermore, the MAbs did not crossreact with Slug in immunolabellings with GFP-Slug-transfected RWP-1 pancreatic carcinoma cells. In ELISA, the MAbs reacted only with Snail protein, and not with GST protein or negative controls. ELISA showed high affinity for both human and murine Snail proteins, and mapping of the epitope indicated that MAb 173EC3 reacted strongest to the 1-82 amino acid sequence of murine Snail. In Western blots of 43A, 43B and 43A-SNA whole-cell lysates, MAbs to Snail detected a M_r 32 000 polypeptide corresponding to Snail (Batlle et al. 2000) only in 43A-SNA cells. These results indicated

that MAbs 173CE2 and 173EC3 specifically recognize Snail protein in immunofluorescence labellings and Western blots of Snail-overexpressing cells.

7.3. Localization of Snail in human and mouse cell lines and tissues (I, II)

7.3.1. Localization and kinetics of Snail in cell lines (I, II)

To determine whether Snail antibody can detect endogenous Snail in human cell lines and the localization of endogenous Snail in cells, we labelled several pancreatic carcinoma cells, i.e., AsPC-1, BxPC-3, HPAC and PANC-1, with MAb 173CE2. Among these cell lines, previous studies have shown that apart from PANC-1 cells, all cells synthesize and secrete chains of laminin-332 and express hemidesmosomal proteins (Tani et al. 1997; Katayama et al. 2003). On the other hand, PANC-1 cells showed only low levels of integrin β_4 subunit and were strongly immunoreactive for N-cadherin, suggesting for an EMT profile (Section 7.4.1). PANC-1 cells showed heterogeneous immunoreactivity for Snail, whereas other pancreatic carcinoma cell lines were not reactive. The reactivity was strictly nuclear and excluded the nucleoli. For Western blots, we used nuclear extraction or pre-exposure of the cells to 10 μM proteasome inhibitor MG132, which represses the proteasomal degradation of, e.g., transcription factors (Zhou et al. 2004). Western blots of PANC-1 nuclear extracts showed a M_r 32 000 polypeptide, corresponding to Snail, and proteasome inhibitor treatment of cell lysates for 0-5 hours revealed increased levels of the polypeptide. Snail protein was found also in immunolabellings and Western blots of proteasome inhibitor-treated human embryonal, gingival and murine NIH-3T3 fibroblasts, as well as in SW-620 and HT-29 M6 colon carcinoma cell lines, the latter of which contained an inducible Snail cDNA. These results indicated that MAbs 173EC2 and 173CE3 are able to detect endogenous Snail in immunolabelling studies and Western blots.

As addition of serum has been shown to induce EMT in some cell lines, e.g., in rat bladder carcinoma cells NBR-II (Boyer et al. 1989), we were also interested in the effect of serum on the levels of Snail. When gingival fibroblasts were grown in serum-depleted cell culture medium for 24 hours, Snail immunoreactivity was lost. Next, the levels of Snail in

NIH-3T3 cells were analysed with a kinetic study. After 24 hours of starvation, serum was re-introduced to the cells, and the amounts of Snail mRNA and protein were analysed by Western blots and quantitative RT-PCR at different time points (0-24 hours). At three hours, the levels of both Snail mRNA and protein peaked. At 24 hours, the levels of Snail mRNA had declined back to the initial stage, but the protein levels exceeded the control. These results indicated that expression of Snail is not constitutive in fibroblasts, but is dependent on the presence of serum.

7.3.2. Localization of Snail in normal and malignant tissues (II)

Because the localization of Snail protein in human and mouse tissues has remained obscure due to the lack of specific antibodies, MAb 173EC3 was used to analyse the expression of Snail by immunohistochemistry, first in mouse embryonal tissues. At E7.5, Snail immunoreactivity was confined mainly to the mesoderm, but also to extraembryonic tissues, namely, the parietal endoderm, which is derived from the primitive endoderm, and the ectoplacental cone, derived from the trophectoderm. At E9.5, reactivity for Snail was detected in the branchial arches. At E15.5, Snail immunoreactivity was strong in the cells of developing cartilage, as well as in the lung mesenchyme. Snail reactivity was less intense in the lungs of two-day-old mice. In skin, Snail reactivity was detected only in the mesenchymal cells of the upper layers of the dermis at E15.5, and in two-day-old mice, it was found around the mesenchymal cells near the hair follicle at the dermal condensate.

As Snail has been suggested to induce EMT and a migratory phenotype in epithelial cells (Cano et al. 2000; Nieto 2002; Peinado et al. 2007), the expression of Snail was analysed in wound-healing of mouse skin. The wounded areas were collected from the mice 2, 3, 5 or 7 days after wounding, and MAb 173EC3 and haematoxylin were used in immunohistochemical labellings of the paraffin sections. Snail immunoreactivity was found especially in the migrating fibroblasts infiltrating the granulation tissue. These activated fibroblasts (Martin 1997) showed strong nuclear immunoreactivity for Snail already at day 2 post-wounding, but the levels of Snail fell on day 7, when the epidermis had recovered. To further investigate the role of Snail in activated fibroblasts, samples from fibromatotic patients were studied. Fibromatosis is a condition characterized by lesions of proliferating and locally-infiltrating fibroblastoid cells. Heterogeneous

immunoreactivity for Snail was found in fibroblastoid cells throughout the lesions. Fibrosarcoma and sarcoma, malignant tumours of mesenchymal origin, showed strong nuclear Snail immunoreactivity localizing to cells with the fibroblastoid phenotype.

Next, the expression of Snail was analysed in carcinoma samples, taking into account the results of Snail reactivity in fibroblastoid cells. In colon adenocarcinoma, Snail protein reactivity was detected mainly in the stroma and the bordering cells of tumour islets. Although the majority of Snail-positive cells showed an elongated phenotype, some cells located in the invasive fronts had epithelial characteristics. Samples from cervical SCC showed a similar finding; i.e., cells at the periphery of the tumour islands were reactive for Snail. Finally, colon carcinoma and laryngeal SCC sections were labelled with MAb 173EC3 against Snail and MAb clone 36 against E-cadherin. Snail reactivity was most commonly found at the edges of tumour cell islands and adjacent to the stroma in both carcinomas. Furthermore, E-cadherin was absent from these cells, although in some single cells, both proteins were expressed. In these carcinomas, Snail-positive elongated cells were also detected in the centre of the tumours. These results indicated that MAbs 173CE2 and 17EC3 are able to detect Snail in paraffin sections, and that Snail immunoreactivity is frequent in elongated, fibroblastoid cells, e.g., at the edges of skin wound, in cancers of mesenchymal origin and at the tumour-stroma interface of carcinomas.

7.4. Effect of EMT on expression and production of laminins (I, III)

7.4.1. Laminin-332 (I)

Laminin-332 is synthesized by most epithelial cells and is present in BMs of many carcinomas (Galliano et al. 1995; Aumailley et al. 2003; Miyazaki 2006). Laminin-332 or its chains have been suggested to contribute to invasion of carcinoma cells; however, the presence of laminin-332 has usually been studied only with antibodies against laminin γ2 chain (Ziober et al. 2006). We set out to investigate the effects of EMT on the synthesis and secretion of laminin-332 and laminin α3, β3 and γ2 chains in oral SCC 43A, 43B and 43A-SNA cells. Synthesis of laminin-332 was first studied with polyclonal antiserum to laminin-332. 43A cells showed prominent cell substratum-confined immunoreactivity to

laminin-332, whereas early passages (p3-6) of 43B cells revealed only cytoplasmic reactivity. Next, we analysed more thoroughly the synthesis and deposition of laminin-332 chains. MAb D4B5 against laminin γ2 chain showed a strong cell substratum-confined reactivity in 43A cells and a cytoplasmic reactivity in 43B cells. When we used MAb GB3, which recognizes laminin γ2 chain only when it is associated with laminin-332, a similar result was obtained in 43A cells. However, in 43B cells, no reactivity was detected with this MAb, suggesting that the cytoplasmic laminin γ2 chain was not affiliated with laminin α3 and β3 chains. Next, the synthesis and secretion of laminin-332 chains were studied with immunoprecipitations of 43A and 43B culture media and cell lysates. Polyclonal antiserum against laminin-332, as well as MAbs BM2 and D4B5 against laminin α3 and γ2 chains, all detected M_r 165 000 processed form of α3 chain, M_r 145 000 β3 chain, and M_r 155 000 unprocessed form as well as M_r 105 000 processed forms of γ2 chain in the 43A cell culture medium. MAb 12C4, which detects the unprocessed form of laminin α3 chain, precipitated the corresponding, unprocessed M_r 190 000 form of laminin α3 chain together with β3 chain, and the processed and unprocessed forms of γ2 chain only in the ECM-enriched material, but not in the cell culture medium of 43A cells. In immunoprecipitations of the culture medium obtained from early passages of 43B cells, polyclonal laminin-332 antiserum precipitated only β3 chain and the unprocessed form of γ2 chain. MAb against laminin α3 chain did not precipitate any polypeptides in the 43B cell culture medium. MAb against laminin γ2 chain showed β3 chain and the processed and unprocessed forms of γ2 chain. When we immunoprecipitated the cell culture medium from late passages of 43B cells with polyclonal antiserum to laminin-332, and MAbs to laminin α3 or γ2 chains, as well as with polyclonal antiserum to γ2 chain, no proteins were found. However, polyclonal γ2 chain antiserum precipitated the unprocessed form of γ2 chain in 43B cell lysates. Next, we evaluated the production of mRNA in 43A and late-passage 43B cells. Northern blots with cDNA probes showed 5.5 kb and 5.0 kb transcripts of laminin α3 and γ2 chains only in 43A cells. After prolonged exposure, a faint transcript of laminin γ2 chain was detected in late passages of 43B cells.

These results suggested that 43A cells synthesize and secrete processed and unprocessed forms of laminin α3 chain, β3 chain and processed and unprocessed forms of γ2 chain. The unprocessed α3 chain is deposited only to the ECM. Early passages of 43B cells do not synthesize or secrete α3 chain, but secrete β3γ2 chain dimer. Late passages of 43B

cells synthesize only the unprocessed form of laminin γ2 chain, which is retained in the cytoplasm. We also studied the synthesis of laminin-332 in 43A-SNA cells. Western blots detected no chains of laminin-332 in 43A-SNA cell lysates, and no immunoreactivity for laminin γ2 chain was seen. Taken together, EMT in oral SCC cells attenuates or ceases the synthesis and deposition of laminin-332.

7.4.2. Laminin-511 (III)

As we had found that EMT had an effect on the synthesis and secretion of laminin-332, we hypothesized that EMT could affect the expression of other laminin chains as well. Next, we studied the synthesis of laminin-511, which is ubiquitously expressed in epithelial BMs as well as by many carcinoma cells (Miner et al. 1997; Patarroyo et al. 2002). In Northern blots with cRNA probe, 43A cells expressed a strong 12.0 kb transcript of laminin α5 chain mRNA, and 43B cells expressed a slightly weaker transcript. In 43A-SNA cells, laminin α5 chain mRNA was absent. To investigate the synthesis of α5 chain protein, we exposed the cells to monensin, which inhibits the intracellular protein transport and thus their secretion outside the cell. MAb 4C7 against laminin α5 chain showed a strong vesicular cytoplasmic reactivity for laminin α5 chain in 43A cells, and a highly reduced reactivity in 43B cells. 43A-SNA cells were negative for laminin α5 chain. Immunoprecipitations of cell culture media obtained from radioactively labelled cells with MAb against laminin α5 chain showed prominent M_r 380 000 and 390 000 bands, corresponding to the sizes of laminin α5 chain (Champliaud et al. 2000), together with M_r ca. 220 000 β1 and γ1 chains in 43A cells. Similar, although distinctly weaker bands of laminin α5, β1 and γ1 chains were precipitated from 43B cell culture medium. In 43A-SNA cells, no polypeptides were found. Secretion of laminin β2 chain was studied with MAb SF11 against laminin β2 chain. No laminin β2 chain was observed in 43A, 43B or 43A-SNA cell culture media, suggesting that neither laminin-521 nor laminin-421 was produced. These results showed that 43A cells express laminin α5 mRNA and synthesize and secrete laminin-511, 43B cells secrete markedly reduced amounts of laminin-511 and 43A-SNA cells do not synthesize or secrete laminin-511. EMT appears to downregulate the synthesis and secretion of laminin-511.

7.4.3. Laminin-411 (III)

Next, we turned to laminin-411, which is produced mainly by cells of mesenchymal origin (Lefebvre et al. 1999; Petäjäniemi et al. 2002). Northern blots with cRNA probe against laminin α4 chain showed a 6.5 kb transcript of laminin α4 chain mRNA in 43B and 43A-SNA cells, but not in 43A cells. Immunolabellings with MAb 168FC10 against laminin-411 preceded by monensin treatment revealed vesicular accumulation of laminin-411 only in 43B and 43A-SNA cells. Immunoprecipitations of cell culture media with MAb 3H2 against laminin-411 did not detect any polypeptides in 43A cells, but found strong M_r 180 000 and 220 000 bands, corresponding to the sizes of β1 and γ1 chains (Champliaud et al. 2000), in 43B and 43A-SNA cells. As the precipitates of β1 and γ1 chains are of similar size to laminin α4 chain, we performed further studies to corroborate the presence of α4 chain. In immunoprecipitation of cell culture medium with MAb 113BC7 to laminin γ1 chain, followed by Western blot of the precipitated samples with polyclonal antiserum against laminin α4 chain, 43A cells were again negative for laminin α4 chain. However, prominent bands of M_r 180 000-220 000 laminin α4 chain were found in 43B and 43A-SNA cells. The slight size variation between the bands in 43B and 43A-SNA cells was possibly due to different glycosylation or glycosaminoglycan modification of the α4 chain, as previously detected, for instance, in human endothelial, rat Schwannoma and human embryonal kidney cells (Talts et al. 2000; Kortesmaa et al. 2002). Thus, laminin-411 transcription, synthesis and secretion are induced in EMT.

To extend our findings of laminin α5 chain downregulation and laminin α4 chain upregulation by EMT, we used chromatin immunoprecipitations to evaluate whether Snail binds directly to the gene promoter sites of laminin α5 and α4 chains in 43A-SNA cells. However, because the promoter sites of laminin α5 and α4 chains are unknown (Aberdam et al. 2000), we first designed primers to cover areas 3000 bp upstream of their gene transcription start sites. Immunoprecipitation of 43A-SNA cells with MAb 173EC3 to Snail and PCR amplification of the precipitated chromatin showed two regions (-1890/-1535; -1016/-572) upstream of laminin α5 chain gene and three regions (-2059/-1732; -1339/-1007; -873/-533) upstream of laminin α4 chain gene transcription start sites that could potentially function as binding sites for Snail. Lastly, we screened these regions for E-box motifs (5′-CANNTG-3′), which are the recognized binding sequences for Snail (Mauhin et al. 1993). Laminin α5 chain promoter region precipitate -1890/-1535 contained

one CAGGTG E-box, and the -1016/-572 precipitate contained two CAGGTG and two CAGCTG E-boxes. Laminin α4 chain promoter region precipitate -1339/-1007 contained one CAGGTG E-box, and the -873/-533 precipitate contained one CAGCTG E-box. The -2059/-1732 precipitate contained one CAGGTA Z-box, but no E-boxes; however, this sequence with only a single nucleotide deviation from E-box, CAGGTG→CAGGTA, has been shown to bind other Snail- and EMT-related transcription factors (Spaderna et al. 2006). Taken together, these results suggested that Snail binds to specific regions upstream of both laminin α5 and α4 chain genes and may directly control their expression.

7.5. Expression and distribution of cell surface receptors in EMT (I, III)

7.5.1. Integrin $\alpha_6\beta_4$ (I, III)

Integrin $\alpha_6\beta_4$ is an important part of the hemidesmosomal complex and connects the intermediate filaments to the BM and laminin-332 (Nievers et al. 1999; Kikkawa et al. 2000). It has also been reported to bind laminin-511 outside hemidesmosomes (Kikkawa et al. 2000; Pouliot et al. 2001). Owing to these qualities, integrin $\alpha_6\beta_4$ is considered a hallmark of the epithelial phenotype. 43A cells showed strong cell surface-confined immunoreactivity for both integrin α_6 and β_4 subunits. However, the reactivity was excluded from certain spot-like areas, a hemidesmosomal pattern described as "Swiss cheese" immunoreactivity (Spinardi et al. 1995). In 43B and 43A-SNA cells, cell surface reactivity for integrin α_6 subunit was irregular and did not organize in a hemidesmosome-like pattern. MAb AA3 to integrin β_4 subunit showed scattered reactivity in 43B cells, which was absent in 43A-SNA cells. Concerning other hemidesmosomal proteins (Litjens et al. 2006), MAb HD-121 against HD1/ plectin showed hemidesmosomal reactivity in 43A cells, whereas the protein had redistributed adjacent to cytoplasmic fibrils in 43B cells. In addition, MAb 233 against BP180 showed reactivity for hemidesmosomes only in 43A cells. These results suggested that 43A cells synthesize laminin-332 and laminin-511 and produce their receptor integrin $\alpha_6\beta_4$. In EMT-experienced 43B cells, the production of laminin-332 and -511 is diminished, and in 43A-SNA cells, the production has ceased together with their corresponding integrin receptors.

7.5.2. Integrin $\alpha_6\beta_1$ (III)

As our immunolocalization studies suggested that hemidesmosomal complexes were disintegrated in EMT-experienced 43B and 43A-SNA cells, and that immunoreactivity for integrin β_4 subunit was decreased, we searched for the integrin subunit that could bind the still present integrin α_6 subunit. Immunoprecipitation studies with MAb GoH3 against α_6 showed M_r 140 000 and 210 000 bands in 43A cells, which corresponded to integrin α_6 and β_4 subunits. 43B cells showed similar, although fainter bands, suggesting that some integrin α_6 subunit was still dimerized with integrin β_4 subunit in these cells. In 43A-SNA cells, however, MAb against α_6 precipitated a M_r 110 000 band, corresponding to integrin β_1 subunit, suggesting a switch from $\alpha_6\beta_4$ to $\alpha_6\beta_1$ in EMT. In line with their laminin synthesis profile, 43A-SNA cells hence produce integrin $\alpha_6\beta_1$, which is one of the few established receptors for laminin-411 (Kortesmaa et al. 2000; Fujiwara et al. 2001).

7.5.3. Integrin $\alpha_1\beta_1$ (III)

As the results showed that one mesenchymal integrin, $\alpha_6\beta_1$, was present in 43A-SNA cells, we also searched for other candidates, namely integrin $\alpha_1\beta_1$. This integrin is considered mainly a collagen-binding integrin detected primarily in mesenchymal cells and tissues such as smooth muscle cells, kidney mesangial cells and fibroblasts (Hemler et al. 1984). Immunoprecipitations with MAb 102DF5 against integrin β_1 subunit revealed a strong M_r 110 000 band, corresponding to integrin β_1 subunit, in 43A, 43B, and 43A-SNA cells. Several α subunits were precipitated with the β_1 subunit in all cells. Immunoprecipitation of 43A, 43B and 43A-SNA cells with MAb TS2/7 against integrin α_1 subunit showed M_r 200 000 and 110 000 bands, corresponding to integrin α_1 and β_1 subunits, only in 43A-SNA cells.

7.5.4. Integrin-linked kinase (III)

ILK functions as an adaptor between β_1, β_2 and β_3 integrin subunits and the actin cytoskeleton (Hannigan et al. 1996; Li et al. 1999; Guo and Giancotti 2004). ILK is a component of focal adhesion plaques and its activity is modulated by cell-ECM interactions (Hannigan et al. 1996; Li et al. 1999; Mulrooney et al. 2000). MAb against ILK showed no immunoreactivity in 43A cells. In 43B and 43A-SNA cells, strong ILK

reactivity was found at streak-like structures resembling focal adhesions. In Western blots, ILK was absent in 43A cells, but prominent M_r 59 000 bands, corresponding to ILK (Somasiri et al. 2001), were detected in 43B and 43A-SNA cell lysates.

7.5.5. Lutheran glycoprotein (III)

To further study the EMT-induced downregulation of laminin-511, we examined the presence of Lutheran, which is a specific receptor for laminin α5 chain (Kikkawa and Miner 2005). MAb BRIC221 to Lutheran showed strong immunoreactivity in 43A cells at the cell surface. However, 43B cells showed a markedly weaker and irregular immunoreactivity for Lutheran. 43A-SNA cells were completely devoid of Lutheran reactivity. These results were confirmed with immunoprecipitations using polyclonal antiserum against Lutheran. Strong levels of M_r 85 000 isoform of Lutheran (Parsons et al. 2001) were present in 43A cells, whereas low levels were found in 43B cell lysates, and no Lutheran was present in 43A-SNA cells. These results suggested that in conjunction with the decreasing levels of laminin-511, its receptor Lutheran is also lost in EMT.

7.6. Adhesion of oral SCC cells to different ECM substrata (III)

To address the potential functional role of laminins in the adhesion of oral SCC cells, we measured the adhesion efficiencies of 43A, 43B and 43A-SNA cells to fibronectin, laminin-511 and laminin-411. Wells of 96-well plates were coated with these proteins and the cells were allowed to adhere in the presence of cycloheximide, which prevents synthesis of endogenous proteins. In quantitative cell adhesion assays, 43A, 43B and 43A-SNA cells adhered strongly to 5 μg/ml fibronectin and 4 μg/ml laminin-511, as expected. However, adhesion of the cells to 4 μg/ml laminin-411 was minimal and significantly lower than to fibronectin or laminin-511 ($P<0.001$). As the cells encounter laminin-411 in combination with other ECM molecules *in vivo*, we investigated whether laminin-411 would be anti-adhesive when the cells are allowed to attach to an otherwise adhesive ECM component. We coated the wells with increasing amounts of laminin-411 (1-20 μg/ml) together with 5 μg/ml fibronectin or 4 μg/ml laminin-511. Laminin-411 significantly decreased the adhesion efficiency of 43A, 43B and 43A-SNA cells to fibronectin already at the concentration of 5 μg/ml ($P<0.001$). Laminin-411 concentration of 20 μg/ml

inhibited the adhesion of 43A and 43B cells to fibronectin totally and the adhesion of 43A-SNA cells by 60%. Laminin-411 concentration of 20 μg/ml inhibited the adhesion of 43A cells to laminin-511 slightly (P=0.06) and the adhesion of 43B and 43A-SNA cells significantly (P<0.001 for both). To address the possibility that laminin-411 would interfere with the adhesion to other proteins by binding to them, we performed immunoprecipitations. Immunoprecipitation of cell culture medium of 43B cells with MAb to laminin-411, followed by Western blot with polyclonal antiserum against fibronectin precipitated a M_r 220 000 band, corresponding to the size of fibronectin. These findings suggested that laminin-411 may interact with fibronectin by direct binding, thus compromising cell adhesion to it.

7.7. Effect of EMT on cell invasion, migration and wound-healing (III, IV)

To assess the changes induced by EMT in cell invasion, we seeded the cells on Matrigel-coated Boyden chambers and let the cells grow and invade for 24 hours. 43A cells grew in Matrigel as epithelioid cell islands with close cell-cell contacts, whereas 43B cells and especially 43A-SNA cells showed only small amounts of cell-cell contacts. Invasion of 43B and 43A-SNA cells was significantly increased relative to 43A cells (P<0.001 for both). 43B cells invaded to the lower Boyden chamber in amounts that were fivefold greater than those of 43A cells, whereas 43A cells were practically non-invasive. The invasion ability of 43A-SNA cells, on the other hand, was fiftyfold greater than that of 43A cells. When we examined the cytoskeletal structures of the cells with rhodamine phalloidin labelling, 43A and 43B cells, but not 43A-SNA cells, showed dot- or string-like actin-based accumulations on their ventral cell membranes that resembled podosomes and invadopodia, respectively (Lehto et al. 1982; Chen et al. 1994).

Next, we focused our interest on the actin-based structures in 43A and 43B cells. We then studied the migration of 43A and 43B cells and the presence of actin-based accumulations, first with *in vitro* wound-healing experiments. At two hours after wounding, stationary 43A cells were tightly attached to each other and showed a purse-string morphology, with actin filament cables extending from cell to cell at the wound margin, a situation detected previously in closure of corneal wounds (Danjo and Gipson 1998). After 24 hours, 43A

cells migrated as a common sheet of cells, maintaining close contacts at the leading edge and showing lamellipodial extensions. Rhodamine phalloidin labelling showed actin as podosome-like structures in 43A cells both at the wound border and in adjacent cells in the following cell rows. In 43B cells, ventral actin accumulations were present at all time points, although their appearance differed from those in 43A cells. 43B cells showed cell protrusions already after two hours of wounding. After 24 hours, 43B cells migrated as individual, elongated cells and showed actin-rich cell extensions with clubbed tips at their leading and trailing edges. When 100 ng/ml EGF was applied to induce cell migration, 43A cells again assembled similar actin-based accumulations. Only a few cells escaped the cell front and migrated as single cells. Migration ability of 43A cells did not transform the actin structures to resemble those in 43B cells.

To study the effects of EMT and the actin-based structures on random cell migration, the cells were followed with fluorescence time-lapse imaging for 10 hours. The mean trajectory length of 43A cells was 66±9.0 μm, whereas in 43B cells it was 339±23.7 μm. Thus, the trajectories of 43B cells were significantly longer than those of 43A cells ($P<0.0001$). The migration distance of both cells increased linearly with time. However, when we calculated the ratio of the total trajectory length and the distance between the end and start points of the trajectory, we found that the mean ratio of 43A cells was 54±14.7, whereas in 43B cells it was 12±1.8. This result indicated that the trajectories of 43A cells were highly convoluted relative to 43B cells ($P=0.0050$), revealing a rotatory movement in which 43A cells remained virtually stationary. On the other hand, the small ratio of 43B cells suggested that the cells migrated in a more directed fashion (Figure 9).

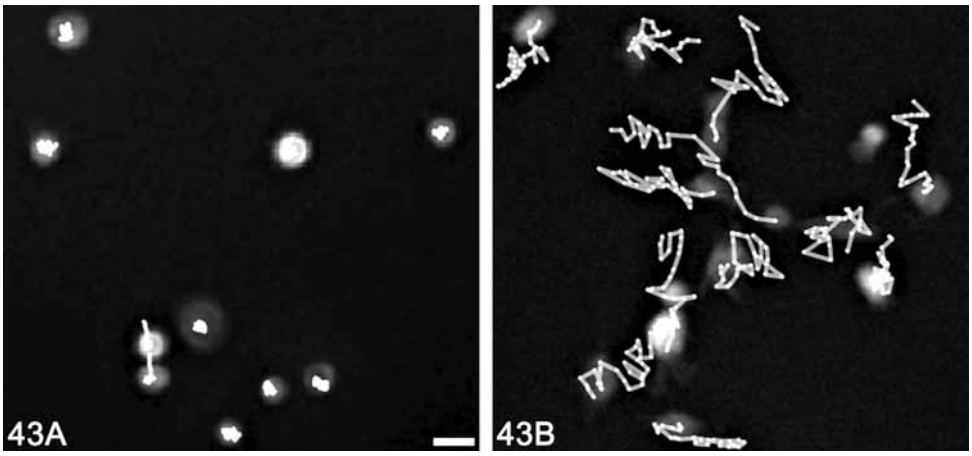


Figure 9. *The trajectories of 43A and 43B cells in a 10-hour follow-up. Random cell migration of 43A and 43B cells was examined with epifluorescence wide-field time-lapse microscopy. The trajectories of 43A cells were short and the cells remained immobile. The trajectories of 43B cells were fivefold longer than those of 43A cells. The mean velocity of 43A cells was 5.5±1.2 µm/h and of 43B cells 19.5±2.7 µm/h. Scale bar, 20 µm.*

We then analysed the number of actin-based structures in 43A and 43B cells. In a 48-hour assay, the majority of both cells (43A 86±1.9% and 43B 98±1.8%, $P<0.001$) formed actin accumulations on a glass matrix. To address the question of whether the ECM substrate has an effect on the formation of actin structures (Moreau et al. 2006), the cells were seeded on glass coverslips coated with type I collagen, fibronectin, laminin-332 or laminin-511. We detected no significant change in the morphology of actin accumulations in 43A or 43B cells as a function of ECM substrates. However, 43B cells formed less actin accumulations on fibronectin than on a plain glass matrix (90.2±2.5% vs. 97.9±1.8%, $P<0.05$).

7.8. Effect of EMT on structural proteins of podosomes and invadopodia (IV)

As cytoskeletal F-actin had a diverse distribution in 43A and 43B cells, we next studied whether the cytoplasmic actin accumulations were indeed podosomes and/or invadopodia. Podosomes and invadopodia are columnar actin-based cell adhesion structures that also elicit ECM degradation (Tarone et al. 1985; Chen et al. 1994). We seeded the cells on fluorescently labelled gelatin and studied the spatial and temporal organization of actin

and proteolysis of gelatin. After two hours of seeding, 43A cells showed actin in rhodamine phalloidin labellings as dot-like accumulations at the ventral cell membrane. The accumulations colocalized with proteolytic areas in the fluorescently labelled gelatin. In contrast, 43B cells showed actin in a more irregular manner, and the accumulations were more numerous and seemed smaller. 43B cells also showed membrane extensions that colocalized with the degradation cavities in gelatin. After five hours of seeding, the actin-based cell extensions in 43B cells had changed in shape. Now, the membrane extensions had gained club-like endings, which also localized at the gelatin cavities. In EGFP-actin-transfected 43B cells, we detected multiple narrow, tail-like projections of actin both inside and outside the cell. These structures could be seen in phase-contrast microscopy as dark dots and filaments near the basal cell surface. The morphology of 43A and 43B cells was further studied with FESEM. Broad lamellipodia and membrane-bulging nuclei were characteristic of epithelioid 43A cells. 43B cells, on the other hand, were covered with small round membrane buds and slender cell extensions that showed enlargement at the tips.

Taken together, the actin accumulations showed colocalization with degradation cavities in both cells, although their mutual morphology was diverse. The actin structures in 43A cells were similar to dot-like podosomes detected in, e.g., rat bladder carcinoma cells (Spinardi et al. 2004; Spinardi and Marchisio 2006), whereas the cytoplasmic organization of actin in EMT-experienced 43B cells showed twisted, tail-like structures that resembled those of invadopodia in melanoma cells (Baldassarre et al. 2006). The club-ended cell extensions in 43B cells differed from filopodia or other previously described cell structures.

Next, we studied which structural proteins would localize to podosomes, invadopodia and cell extensions in 43A and 43B cells. Podosomes usually consist of an inner actin core surrounded by a peripheral ring with adhesion and linker proteins, although the molecular interrelationship between the core and ring is controversial (Linder and Aepfelbacher 2003). Invadopodia do not have such a well-defined organization, and there is no clear division of core and ring (Weaver 2006). We used EGFP-actin-transfected cells or double-labellings with previously characterized podosome-related proteins (Arp 2/3, cortactin) to assure the localization to podosomes or invadopodia. HD1/ plectin immunoreactivity,

detected with MAb HD-121, was confined to hemidesmosomes as well as to podosome rings of EGFP-actin-transfected 43A cells. In 43B cells, reactivity was not found at the invadopodia, but localized to cytoplasmic fibrils. αII-spectrin localized to podosome rings in 43A cells, whereas in 43B cells only a diffuse, cytoplasmic reactivity was detected with MAb 101AA6 that did not localize to invadopodia. Arp 2/3 localized to podosome cores and covered the heads and tails of invadopodia. In double-labellings with polyclonal Arp 2/3 antiserum, talin was found only in the podosome rings of 43A cells. MAb MCA725S showed talin in focal adhesions in both cell types. Cortactin immunoreactivity was confined to podosome cores in 43A cells, the heads and tails of invadopodia and to the club-ended cell extensions in 43B cells. In double-labellings with MAb 4F11 to cortactin, vinculin was found at the podosome rings in 43A cells as well as in the invadopodia and cell extensions in 43B cells. Furthermore, polyclonal vinculin antiserum showed immunoreactivity in focal adhesions in 43B cells. As talin is considered a major intracellular adaptor mediating adhesion between the cell membrane and the cytoskeleton (Critchley 2004; Le Clainche and Carlier 2008), we next studied which other proteins could take its place in 43B cells. We turned to tensin, which has been implicated in capping the barbed ends of actin filaments (Le Clainche and Carlier 2008; Legate and Fässler 2009). Tensin immunoreactivity, detected with MAb Clone 5, was distributed diffusely in the cytoplasm of 43A cells, but did not localize to podosomes. In 43B cells, however, tensin was detected in invadopodia and cell extensions. MAb 2A7 to focal adhesion kinase (FAK) showed immunoreactivity in focal adhesions and podosome rings in 43A cells, whereas it was found only in focal adhesions in 43B cells. In Western blots of 43A and 43B cells, equal amounts of M_r 500 000 plectin, M_r 240 000 αII-spectrin, M_r 225 000 talin and M_r 117 000 vinculin were detected. Double bands of M_r 80 000 and 85 000, corresponding to cortactin, and M_r 200 000 band of tensin were found in both 43A and 43B cell lysates. Immunoprecipitation of FAK, followed by Western blot with MAb PY20 to phosphotyrosine, detected a strong M_r 125 000 band in 43A cells and a lighter band in 43B cells.

As podosomes and invadopodia have been reported to contain integrins that may have a role in adhesion or in gathering other proteins to the cell membrane (Marchisio et al. 1988; Mueller et al. 1999; Deryugina et al. 2001; Pfaff and Jurdic 2001; Weaver 2006), we set out to study which integrin subunits localize to these structures in 43A and 43B cells. To

ensure the localization to podosomes or invadopodia, the cells were transfected with EGFP-actin and labelled with appropriate antibodies. Integrin α_3 subunit immunoreactivity was enriched in 43A cells around the actin cores of podosomes. In 43B cells, integrin α_3 subunit localized at the cell membrane surrounding the invadopodia as well as at the cell extensions. A highly similar reactivity was found when the cells were labelled with MAb 102DF5 against integrin β_1 subunit. Immunoprecipitation experiments with MAb J143 against integrin α_3 subunit detected strong bands of M_r 150 000 and 110 000, corresponding to the sizes of integrin α_3 and β_1 subunits, in both cells. The same result was obtained with immunoprecipitations with MAb against β_1 subunit, suggesting the presence of integrin $\alpha_3\beta_1$ heterodimer in 43A and 43B cells. Integrin $\alpha_v\beta_5$ is linked to cell migration, for instance, in wound-healing (Gailit et al. 1994). Integrin α_v subunit immunoreactivity localized only to focal adhesions in 43A cells. In 43B cells transfected with EGFP-actin, integrin α_v subunit was found at the focal adhesions, but also at the heads of actin-based invadopodia. Integrin β_5 subunit immunoreactivity was faint in 43A cells and was not detected in podosomes. In contrast, integrin β_5 subunit localized to the heads of invadopodia in 43B cells, as well as to point and focal adhesions. Immunoprecipitation of surface-labelled cells with MAb LM 142.69 against integrin α_v subunit showed a faint, M_r 150 000 band in 43A cells, corresponding to integrin α_v subunit, and MAb 1A9 against integrin β_5 subunit showed again a faint M_r 100 000 band, corresponding to integrin β_5 subunit. In contrast, both MAbs against integrin α_v and β_5 subunits precipitated two strong bands in 43B cells, being congruent with the immunolocalization studies, and suggesting that α_v and β_5 are binding partners.

Cell adhesion, migration and invasion mediated by podosomes and invadopodia are suggested to occur through formation of membrane protrusions (Chen et al. 1994; Linder and Aepfelbacher 2003). Therefore, we studied the localization of pacsin 2, which through its F-BAR domain has been implicated in inducing tubulation of cell membranes (Qualmann and Kelly 2000; Heath and Insall 2008). Pacsin 2 was detected at the peripheral rings surrounding 43A cell podosomes. It was not detected in 43B cells. Furthermore, we studied the expression of filamin A, which is a potential binding partner for pacsin 2 in focal adhesions (Nikki et al. 2002). Strong immunoreactivity for filamin A was found at the podosome cores in 43A cells. In 43B cells, we found a temporal shift in filamin A protein expression. 43B cells organize invadopodia and produce ECM

degradation on fluorescently labelled gelatin matrix in two hours. During this time filamin A did not accumulate in invadopodia. Only after 15 hours could filamin A be detected in some cells harbouring invadopodia. Next, we transfected the cells with EGFP-filamin A in order to study whether or not the overexpression of filamin A had an effect on the localization of pacsin 2. EGFP-filamin A did not induce accumulation of pacsin 2 in invadopodia. In Western blots, the protein levels of M_r 56 000 pacsin 2 and M_r 280 000 filamin A, detected with polyclonal pacsin 2 antiserum and MAb PM6/317 to filamin A, were equal in both cell lines.

As one of the major functions of podosomes and invadopodia is suggested to be ECM degradation (Weaver 2006; Clark et al. 2007; Linder 2007; Weaver 2008), we studied which proteases would localize to podosomes and invadopodia. When the cells were seeded on fluorescently labelled gelatin, MT1-MMP expression was found in podosomes, invadopodia and cell extensions. MT1-MMP also localized to the degradation cavities in gelatin. Western blots with MAb LEM-2/15 confirmed the expression of M_r 50 000 MT1-MMP in both cell lines. MMP-2 and MMP-9 antisera showed vesicular immunoreactivity in both cells, but no specific localization to podosomes or invadopodia. The results of immunolocalization studies are summarized in Study IV, Table 2.

7.8.1. Morphologic and proteolytic differences between podosomes and invadopodia (IV)

To characterize the differences between podosomes and invadopodia further, we used 3D confocal imaging combined with *in situ* zymography assays. The cells were seeded on fluorescently labelled gelatin and allowed to adhere and organize podosomes and invadopodia for 2-6 hours. These time points were chosen to ensure that the cells had properly adhered and to prevent excess cell migration and cell division. Actin filaments were visualized with rhodamine phalloidin and the nuclei with TO-PRO-3. At four hours, 43A cells formed significantly less ($P<0.001$) podosomes per cell than 43B cells formed invadopodia (12.3±0.7 vs. 32.4±1.6). The vertical actin columns were wide in 43A cells, whereas they were narrow and tail-like in 43B cells. The columns in both cells protruded into the gelatin matrix. The relative volumes of podosomes, measured from 3D rendered confocal images, increased significantly in 2-6 hours (from 0.37±0.09 μm^3 to 1.05±0.14

μm^3, $P<0.05$), whereas the sizes of invadopodia increased only slightly (from 0.17±0.03 μm^3 to 0.40±0.03 μm^3, $P>0.05$). The volumes of podosomes were significantly larger than the volumes of invadopodia at 4-6 hours ($P<0.01$ for both). We also analysed in more depth the amount of gelatin degradation produced by the cells. 43A cells produced resorption areas that corresponded to the shapes of the round actin cores of podosomes. 43B cells, however, produced cavities of various shapes and sizes. 43B cells produced a significantly greater number of cavities per cell than 43A cells (126±13.6 vs. 70±12.1, $P<0.01$). Furthermore, the degradation area per cell was significantly larger under 43B cells than under 43A cells (231±36.1 μm^2 vs. 118±18.1 μm^2, $P<0.01$).

7.8.2. Dynamic differences between podosomes and invadopodia (IV)

The dynamics of podosomes and invadopodia in EGFP-actin-transfected cells was first studied with wide-field epifluorescence microscopy. In 30-minute time-lapse imaging, 43A cells showed dot-like podosomes that were immobile and highly stabile structures. 43B cells, on the other hand, showed numerous tail-like actin arrays that moved in a circular manner around their attachment sites at the basal cell membrane. Although vigorous rotation was detected at these invadopodia tails, the life-span of the whole invadopodia complex seemed long. Similar findings were obtained with EGFP-cortactin transfections. “Externalized invadopodia” could be detected in the retracting sides of cells as well as at the boundaries between two cells. Furthermore, we observed events in which the heads of invadopodia were released from their attachment to the basal cell membrane and the tails moved across the cytoplasm and eventually disappeared. When the migration of 43A cells was induced with EGF treatment, the podosomes were quickly assembled and disassembled as the cells moved. However, their morphology remained the same, indicating that the transformation from podosomes to invadopodia was not due to augmented migration activity. Next, we used TIRF microscopy to more accurately follow the events at the narrow, 100-200 nm evanescent field of the basal cell membrane. In 12-hour time-lapse TIRF imaging, 43A cell podosomes were again long-lived. A halo of EGFP-actin was found around podosomes, possibly consisting of actin monomers. When podosomes were left outside the cell membrane as a result of cell migration, they were quickly disassembled. In 43B cells, TIRF microscopy showed that the heads of invadopodia were attached to the basal cell membrane. The tails, however, were only

partially visible due to the narrow imaging plane. The cell extensions showed constant movement of EGFP-actin molecules. The invadopodia in 43B cells were not surrounded by actin halos similar to those seen in 43A cells.

The assembly of podosomes has been suggested to rely on an intact actin network, but also microtubules are required in some cells (Linder et al. 2000b; Evans et al. 2003). We treated the cells with cytochalasin B, which inhibits actin polymerization, and followed the events with wide-field time-lapse imaging for 30 minutes. The actin cytoskeleton of both cells disrupted rapidly and resulted in cytoplasmic aggregates. The podosomes, invadopodia, or cell extensions remained in place (Lehto et al. 1982; Akisaka et al. 2001; Spinardi et al. 2004), and no new podosomes or invadopodia developed during this time. When we treated the cells with demecolcine to depolymerize the microtubule system, the effects were even less pronounced, and podosomes, invadopodia, and cell extensions remained. A combination treatment with cytochalasin B and demecolcine resulted in the same outcome as cytochalasin B treatment alone. As organization of podosomes and invadopodia has been suggested to occur without new protein synthesis (Tarone et al. 1985; Linder and Aepfelbacher 2003), we applied cycloheximide to block the synthesis of new proteins. No new podosomes or invadopodia emerged in the 60-minute follow-up. These results suggested that microtubules, actin filaments and *de novo* synthesis of proteins are needed in these cells for successful podosome assembly.

Finally, to obtain information about the turnover of structural proteins in podosomes, invadopodia and cell extensions, we used FRAP experiments and transfections with EGFP-actin, EGFP-cortactin or EGFP-filamin A. After photobleaching (n=25), the plateau of fluorescence recovery for EGFP-actin was reached in podosomes in 64.4±5.2 s and in invadopodia after a significantly longer time (80.6±5.5 s; $P<0.05$). Half-time of recovery for EGFP-actin was 8.0±0.6 s in 43A podosomes, whereas it was significantly longer in 43B invadopodia (10.5±1.0 s; $P<0.05$). The mobile fraction of EGFP-actin in invadopodia was significantly smaller (92%, $P<0.001$) than the total recovery in podosomes. We also analysed the turnover of EGFP-actin in 43B club-ended cell extensions (n=9). After photobleaching, the recovery was slower in the cell extensions than in the cytoplasmic invadopodia; the plateau of recovery was reached in 74.4±16.5 s, the half-time of recovery was 11.9±3.2 s and the mobile fraction was 63%. Next, we measured the turnover of

EGFP-cortactin (n=25). The plateau of recovery was reached in 22.0±4.7 s in 43A cells and significantly slower in 43B cells (103.1±6.2 s; $P<0.0001$). The half-time of recovery for cortactin was 2.4±0.5 s in 43A podosomes, whereas it was 8.4-fold slower in 43B invadopodia (20.1±2.3 s; $P<0.0001$). The mobile fractions were 100% and 95%, respectively. After photobleaching of EGFP-filamin A (n=25), the plateau of recovery was reached rapidly in both cells (43A 35.2±3.0 s vs. 43B 44.2±4.1 s). The half-time of recovery was again significantly faster in podosomes than in invadopodia (3.8±0.2 s vs. 5.1±0.5 s; $P<0.05$), and the mobile fractions were 100% and 98%, respectively. Taken together, photobleaching experiments showed faster reorganization of EGFP-actin, EGFP-cortactin and EGFP-filamin A in podosomes than in invadopodia. Furthermore, the cell extensions in 43B cells were also replenished with new molecules, which may, at least in part, indicate their active involvement in cell migration and invasion in EMT-experienced 43B cells.

8 DISCUSSION

8.1. Snail-dependent and -independent EMT in oral SCC cells

Oral SCC is a highly invasive cancer with a poor prognosis (Greer 2006; Ziober et al. 2006). The mechanisms of oral SCC progression are known only partially, and due to the malignant nature of oral SCC, research focusing on its detection and molecular characteristics is required. One of the culprits of progression of carcinomas may be EMT (Guarino et al. 2007; Peinado et al. 2007; Yang et al. 2007; Yanjia and Xinchun 2007). The first aim of this study was to analyse the characteristics of cell lines obtained from the oral SCC primary tumour and from its recurrence. 43A cells showed an epithelial phenotype, i.e., round, flattened morphology, close contact with neighbouring cells and circumferential actin filaments. 43B cells were more fibroblastoid-like cells with less prominent cell-cell adhesions complexes and strong actin stress fibres. The majority of intermediate filaments in 43A cells were cytokeratins. Only in 43B cells did we detect prominent fibrillar arrays of vimentin filaments, which have previously been connected to a malignant phenotype of oral SCC (de Araujo et al. 1993; Islam et al. 2000). Since the intermediate filaments express distinct mechanical properties, these switches may affect the overall ability of the cells to change shape, migrate and establish cell-cell contacts (Savagner 2001).

The adherens junctions of 43A cells were enriched with E-cadherin, which is one of the classic epithelial hallmarks and is considered to be one of the tumour-suppressor genes (Vleminckx et al. 1991; Perl et al. 1998; Semb and Christofori 1998; Van Aken et al. 2001). Loss of E-cadherin is an indicator of poor prognosis in several cancers, including oral SCC (Schipper et al. 1991; Chow et al. 2001; Lim et al. 2004; Diniz-Freitas et al. 2006). 43B cells were devoid of E-cadherin, but showed N-cadherin immunoreactivity, suggestive of an E-cadherin/ N-cadherin switch (Islam et al. 1996; Cavallaro et al. 2002; Cavallaro and Christofori 2004; Maeda et al. 2005b). Furthermore, loss of E-cadherin and acquisition of fibroblastoid morphology indicated that 43B cells had experienced EMT. By failing to maintain the stable connections to other epithelial cells via E-cadherin, the EMT-driven cells may be released from their positions (Thiery 2002; Thiery 2003). Ectopic expression of Snail in 43A-SNA cells resulted in a highly similar, but even more

pronounced EMT relative to 43B cells. Immunolabellings and Western blots showed cadherin switching in conjunction with a morphological change to strictly fibroblastoid phenotype, drastic reduction of cytokeratins and accumulation of vimentin (Boyer et al. 1989). With these cell lines, we further studied the role of EMT in oral SCC.

E-cadherin is mainly downregulated in EMT through transcriptional repression (Van Aken et al. 2001; Christofori 2003). Northern blots showed that 43A cells expressed transcripts for ZEB-1 and Slug, whereas 43B cells expressed prominently ZEB-1, ZEB-2 and Slug. The transcription factors present in 43A-SNA cells, in addition to Snail, were similar to the EMT-driven 43B cells. These results suggested, first, that the faint expression of ZEB-1 or the strong expression of Slug was not sufficient to repress E-cadherin and induce EMT in 43A cells, second, that ZEB-1 and ZEB-2 were most probably responsible for the endogenous EMT in 43B cells, and third, that ectopic Snail could upregulate the levels of transcription factors ZEB-1 and ZEB-2 in 43A-SNA cells. Considering 43B cells, ZEB-2 is linked to lower survival rates in oral SCC (Maeda et al. 2005a). In other cell systems, Snail has been shown to stimulate expression of other transcription factors such as ZEB-1 or Ets-1 (Guaita et al. 2002; Taki et al. 2006). ZEB-2 is unable to induce the levels of ZEB-1 or Snail (Taki et al. 2006), suggesting that Snail is a stronger trigger for EMT. Slug has been considered a weaker repressor of E-cadherin than Snail (Bolós et al. 2003), a conclusion supported by our studies.

Next, we used the epithelial 43A and fibroblastoid 43B and 43A-SNA SCC cells expressing endogenous or exogenous EMT in search of new, potential signs of EMT. Loss of BM components is considered an important step towards tumour malignancy (Bosman et al. 1992; Ingber 2002; Kalluri 2003). Immunoprecipitations and immunofluorescence labellings showed that 43A cells prominently synthesized and secreted all chains of laminin-332 into the culture medium and ECM. In EMT-experienced 43B cells, synthesis of laminin α3 chain mRNA and protein ceased in early-passage cells, and the cells secreted laminin β3γ2 chains to the culture medium. Only unprocessed laminin γ2 chain was finally synthesized in late-passage 43B cells, but was not secreted. In 43A-SNA cells, we found neither synthesis nor secretion of laminin-332 chains. The polymerization of laminin chains is guided primarily by the α chain (Matsui et al. 1995b; Yurchenco et al. 1997). Apart from the α chain, it seems that β and γ chains may play roles in cancer. For

instance, in colorectal carcinoma, the budding cells in the invasive fronts have been shown to have immunoreactivity for laminin β3γ2 chains (Sordat et al. 1998). In their study, laminin α3 chain was only weakly present in fragmented BMs of poorly differentiated carcinomas and metastases. It was concluded that laminin β3γ2 chains could mark the transition from a stationary to an invading phenotype (Sordat et al. 1998). On the other hand, presence of laminin γ2 fragments in circulation of pancreatic carcinoma patients has been suggested to predict malignant tendency (Katayama et al. 2003; Miyazaki 2006). It seems that the expression of laminin γ2 chain could be regulated by β-catenin signalling, which represents one of the EMT pathways (Hlubek et al. 2001). However, it remains unclear how intracellular laminin chains affect cell functions. For instance, laminin γ2 chain harbours binding sites for EGF, through which it has been proposed to promote invasion and migration (Katoh et al. 2002). Our results showed that in EMT of oral SCC cells, the synthesis, secretion and deposition of laminin-332 chains were progressively downregulated. Furthermore, pancreatic carcinoma cells with endogenous Snail reactivity did not synthesize laminin-332, although this laminin was ubiquitously expressed in Snail-negative pancreatic carcinoma cells. Corroborating our findings concerning the effects of EMT on laminins, later studies have implicated ZEB-1 in downregulating the expression of laminin-332 in colorectal carcinoma (Spaderna et al. 2006).

Our results showed that the distribution and amount of integrin $\alpha_6\beta_4$, a receptor for laminin-332, were affected in EMT. Integrin $\alpha_6\beta_4$ is a part of the hemidesmosomal complex and is essential for a polarized phenotype and for organization and maintenance of the normal epithelial structure (Tamura et al. 1990; Litjens et al. 2006). 43A cells organized hemidesmosomal complexes with reactivity for integrin β_4 subunit and linker proteins HD1/ plectin and BP180 antigen. However, the amount of integrin β_4 subunit was highly reduced in 43B cells, and it was found only sparsely at the cell membrane in a streak-like distribution. HD1/ plectin had changed its normal localization and was now attached to other cytoplasmic fibres, probably vimentin, and BP180 was lost. In 43A-SNA cells, integrin $\alpha_6\beta_4$ was not detected at all. In the epidermis, integrin $\alpha_6\beta_4$ has been suggested to mediate mainly pro-adhesive signals. The cytoplasmic tail of integrin β_4 subunit enables the connection between Ck filaments and laminin-332 (Tamura et al. 1990; Nievers et al. 1999). The proteolytic cleavage of laminin α3 chain appears to induce a change towards a form that actively binds integrin $\alpha_6\beta_4$ and enables stable adhesion

(Goldfinger et al. 1999; Miyazaki 2006). Although some cancers have upregulated integrin $\alpha_6\beta_4$ levels, disappearance of integrin $\alpha_6\beta_4$ in conjunction with loss of BM components have been reported in invasive margins of oral SCC (Downer et al. 1993; Jones et al. 1993; Tani et al. 1996). Marked integrin $\alpha_6\beta_4$ loss or change in localization is more common in poorly differentiated tumours. For instance, in undifferentiated SCC of a mouse skin carcinogenesis model, integrin $\alpha_6\beta_4$ levels are highly reduced and the remaining protein dimer is aberrantly distributed, suggesting an altered function (Witkowski et al. 2000). Loss of integrin $\alpha_6\beta_4$ may also enhance the survival of colon and breast carcinoma cells when they have lost anchorage to laminin-332 (Bachelder et al. 1999; Guo and Giancotti 2004). Our findings suggested that as a result of EMT hemidesmosomal complexes are disintegrated in oral SCC cells. A recent study supports our results concerning the downregulation of integrin β_4 subunit in EMT (Yang et al. 2009). Thus, EMT affects the expression of both cytoplasmic and ECM proteins.

8.2. Expression of Snail protein in the tumour-stroma interface

Snail mRNA has been studied in cells and tumour samples via Northern blots, RT-PCR, *in situ* hybridization and microarray analysis. We produced two MAbs, 173CE2 and 173EC3, against Snail protein. In ELISA and Western blots of 43A-SNA cells, the MAbs specifically recognized a M_r 32 000 polypeptide, corresponding to the previously reported size of Snail protein (Batlle et al. 2000). The short, ca. 25-minute half-life of Snail protein sets a challenge for its detection. Furthermore, GSK3β-dependent phosphorylation influences the subcellular localization of Snail, and Snail is considered inactive in the cytoplasm (Domínguez et al. 2003; Zhou et al. 2004; Yang et al. 2005; Yook et al. 2005). We have also shown that Snail may control its own expression by binding to E-box motifs in its promoter (Peiró et al. 2006). Immunofluorescence analysis demonstrated a strong nuclear localization of Snail in 43A-SNA cells and a heterogeneous, yet nuclear localization in pancreatic carcinoma cells. Endogenous Snail immunoreactivity was detected, for instance, in human and mouse fibroblasts and in colon carcinoma cell lines.

During early-mid gastrulation of mouse development at E7.5, Snail protein localized to the mesoderm, parietal endoderm and ectoplacental cone. At E9.5, reactivity for Snail was detected in the neural crest cells migrating to branchial arches. During late embryogenesis

at E15.5, Snail reactivity was strong in the cartilage, lung mesenchyme and the upper layers of the dermis. After birth, the levels of Snail immunoreactivity were less intense, but still detectable in the lung and skin, where it was found around the mesenchymal cells near the hair follicle. These results are congruent with those gained from mRNA localization studies in the mouse (Nieto et al. 1992; Sefton et al. 1998). Our findings partly agree with others concerning the expression of Snail during hair follicle development. Mesenchymal cells required for hair growth reside at the dermal papilla (Jahoda et al. 1984). Mice overexpressing Snail transgene develop a thickened, hyperproliferative epidermis, suggesting that Snail plays a role in hair follicle morphogenesis (Jamora et al. 2005). However, by *in situ* hybridization, Snail was not detected in the cells of the epidermal-dermal interface as in our studies, but was located only transiently in the developing hair bud (Jamora et al. 2005).

To gain more information on the roles of Snail in skin and especially cell migration, we performed *in vivo* wound-healing assays. Cutaneous wound-healing requires rapid and transient events to restore the integrity of the skin. The migration of keratinocytes during re-epithelization involves morphological and functional changes that resemble EMT. Previously, expression of transcription factor Slug mRNA has been associated with wound-healing (Savagner et al. 2005). In their study, Slug induced cohesive cell migration, which could be interpreted as a partial EMT. Expression of Slug rose at wound margins after one day and fell after four days (Savagner et al. 2005). We found Snail protein at the margins of mouse skin wounds on days 2-7. Thereafter, the levels of Snail declined as the proliferation period was accomplished. The fibroblast-like cells that were infiltrating the granulation tissue showed prominent Snail reactivity. Therefore, both Snail and Slug seem to operate in wound-healing, although their reciprocal functions remain to be evaluated. To study the role of activated fibroblasts further, we analysed the expression of Snail in fibromatosis, fibrosarcoma and sarcoma samples; large numbers of Snail-positive cells were found throughout the lesions.

An inverse correlation between Snail and E-cadherin mRNA has been reported *in vivo* and *in vitro* in oral SCC, diffuse gastric, colorectal, hepatocellular and breast carcinomas (Yokoyama et al. 2001; Rosivatz et al. 2002; Fujita et al. 2003; Sugimachi et al. 2003; Pálmer et al. 2004; Moody et al. 2005; Peña et al. 2005). In invasive ductal breast

carcinoma, Snail mRNA expression is inversely correlated with the grade of differentiation and predicts the presence of lymph node metastasis (Blanco et al. 2002). In breast and ovarian carcinoma effusions, Snail mRNA corresponds to a shorter disease-free period and also shorter overall survival (Elloul et al. 2005). Furthermore, in chemically-induced mouse skin SCCs, Snail mRNA has been detected at the invasive fronts of the tumours (Cano et al. 2000). As stated above, Snail mRNA and protein levels do not always correlate since the protein is rather unstable and its localization and activity depend on its status of phosphorylation (Domínguez et al. 2003; Zhou et al. 2004). We also found that the levels of Snail mRNA and protein are dependent on the presence of serum. Furthermore, the mRNA from Snail retrogene may also interfere with PCR analyses (Locascio et al. 2002). In our study, colon carcinoma and cervical SCC specimens showed Snail immunoreactivity mainly at the invasive fronts of the tumours as well as in the stromal cells close to the tumour islets. Although the majority of Snail-positive cells showed an elongated phenotype, some cells demonstrated epithelioid characteristics, suggesting that they could be entering EMT. To analyse the relationship between Snail and E-cadherin, laryngeal SCC and colon adenocarcinoma sections were labelled with MAbs to Snail and E-cadherin. Snail reactivity was most commonly found at the edges of tumour cell islands and adjacent to the stroma, whereas E-cadherin in these cells was typically missing. Snail-positive, elongated cells were also detected in the centre of these tumours. Considering the findings of Snail immunoreactivity in stromal cells, the progression of a carcinoma lesion has been suggested to depend on the engagement of a reactive stroma that provides structural and vascular support for tumour growth and invasion (Liotta and Kohn 2001; Tlsty and Coussens 2006). The microenvironment of the tumour-host margin may even represent an active participant in the progression of a carcinoma (Moinfar et al. 2000; Liotta and Kohn 2001; Orimo et al. 2005). In addition to the carcinoma cells, many molecules and enzymes operating at the invasive front can also arise from the stroma (Stuelten et al. 2005). For instance, carcinoma-associated fibroblasts from a prostate tumour enhance the progression and growth of prostate carcinoma cells (Olumi et al. 1999), and stromal cells of breast carcinoma secrete MMP-2 and MMP-9 in response to stimuli from the tumour (Shekhar et al. 2001; Petersen et al. 2003; Stuelten et al. 2005). Importantly, oral SCCs and breast carcinomas could develop carcinoma-associated fibroblasts from their primary tumours through EMT (Petersen et al. 2003; Vered et al. 2010). These EMT-derived stromal cells can augment the growth and size of

the tumour or be highly tumourigenic and invasive themselves (Petersen et al. 2003; Galiè et al. 2005). It is therefore possible that the Snail-positive stromal cells in our studies, which most likely originated through EMT from the primary tumour, could represent cells migrating away from the tumour as well as contributing to the stromal reaction. The MAbs developed here have been used since to verify the role of Snail in other carcinomas. In oral SCC and colon adenocarcinoma (Francí et al. 2009; Franz et al. 2009), Snail was mainly located in the stroma of the invasive fronts, thus supporting our findings. In addition, a polyclonal antibody showed a correlation between high amounts of Snail-positive carcinoma cells, lymph node metastasis and poor prognosis in oral SCC (Schwock et al. 2010). The roles of Snail in other carcinomas remain to be established.

During this thesis project another group described a rat monoclonal antibody against human Snail (Rosivatz et al. 2006). In adenocarcinomas of the upper gastrointestinal tract, expression of Snail protein was limited (in 27/340; 7.9%). Tissue microarray samples showed a significantly more frequent expression of Snail in oesophageal carcinomas than in cardiac or gastric carcinomas (Rosivatz et al. 2006). Endogenous Snail localized to the cell nuclei, as in our studies. They reported Snail expression also in a subset of stromal cells, in which it was potentially connected to areas of mucosal erosion. Possibly related to the limits of using tissue microarrays, they did not report the presence or absence of Snail at the invasive fronts of these carcinomas.

8.3. EMT downregulates laminin α5 chain and upregulates laminin α4 chain in oral SCC cells

The results that showed downregulation of laminin-332 and its receptor integrin $\alpha_6\beta_4$ in EMT raised the question of whether other laminins could also be targeted by EMT. The oral epithelium has been shown to synthesize laminin chains α3, α5, β1, β2, β3, γ1 and γ2 (Kosmehl et al. 1999; Pakkala et al. 2002). We evaluated the effect of EMT on laminin-511 and laminin-411. Laminin α5 chain guides epithelial morphogenesis during development and is crucial, for instance, in the MET of kidney (Miner and Li 2000; Rebustini et al. 2007). Laminin-511 is ubiquitously expressed in normal epithelial BMs, but is lost in some carcinomas, including oral SCC and invasive colorectal carcinoma (Miner et al. 1995; Lohi et al. 1996; Miner et al. 1997; Kosmehl et al. 1999; Lohi et al.

2000; Brar et al. 2003). Laminin-411, on the other hand, is considered a mainly mesenchymal laminin and is suggested to participate in the progression of malignancy of breast cancer and glioma (Ljubimova et al. 2001; Ljubimova et al. 2004; Fujita et al. 2005). In Northern blots, the expression of laminin α5 chain mRNA was strong in 43A cells, but in EMT-experienced 43B cells the expression was less prominent and in 43A-SNA cells was absent altogether. Immunofluorescence studies and immunoprecipitations corroborated the findings, as laminin α5 was found together with laminin β1 and γ1 chains in 43A cell culture medium, whereas the secretion of laminin-511 chains was diminished in 43B cells and absent in 43A-SNA cells.

In contrast to laminin α5 chain, Northern blots did not detect any laminin α4 chain transcripts in 43A cells, whereas they were clearly present in 43B and 43A-SNA cells. Immunofluorescence labellings, immunoprecipitations and Western blots showed polypeptides corresponding to laminin-411 chains, but not laminin-421 chains, only in 43B and 43A-SNA cells. To further evaluate the role of EMT and especially Snail in the control of laminin chain expression, we used chromatin immunoprecipitations of 43A-SNA cells. As the transcriptional control of laminins is generally poorly known and the promoter sites not established (Aberdam et al. 2000; Virolle et al. 2002), we screened genomic regions 3000 bp upstream of both laminin α5 and α4 chain transcription start sites. MAb 173EC3 against Snail detected two regions upstream of laminin α5 chain gene and three regions upstream of laminin α4 chain gene that bound Snail. These regions contained E-box or Z-box motifs, which are the specific sequences bound by Snail and ZEB transcription factors (Mauhin et al. 1993; Postigo and Dean 1997; Verschueren et al. 1999). Thus, Snail may directly control the transcription of laminin α5 and α4 chains.

To assess the effects of EMT on different laminin receptors, we first turned to Lutheran. Lutheran is a specific receptor for α5 chain-containing laminins (Moulson et al. 2001; Parsons et al. 2001; Kikkawa et al. 2002), and in parallel studies we have shown their co-existence in normal oral BM (Willberg et al. 2007). Recently, we further demonstrated that human embryonic stem cells use Lutheran and integrin $\alpha_3\beta_1$ as receptors for laminin-511, and integrin $\alpha_6\beta_1$ as a receptor for laminin-411 (Vuoristo et al. 2009). 43A cells showed a strong expression of Lutheran in immunofluorescence labellings and immunoprecipitation, whereas 43B cells revealed a reduced, diffuse immunolabelling and

43A-SNA cells had no expression of Lutheran. Lutheran expression seems to follow laminin α5 chain levels, as in laminin α5 chain knock-out mice Lutheran expression is decreased and the cell surface distribution is non-polarized, whereas in laminin α5 chain overexpressing mice, also Lutheran levels are increased (Moulson et al. 2001). In skin tumours, Lutheran/ B-CAM expression has been found in SCC and basal cell carcinoma, but not in melanomas (Schön et al. 2000), suggesting an epithelial origin for Lutheran. Our results are in line with these findings, providing further evidence that also Lutheran is under the control of EMT.

Having observed that integrin $\alpha_6\beta_4$ complex is reduced in EMT, we investigated which other integrins could mediate adhesion to ECM. In immunohistochemical studies of oral SCC, loss of integrin $\alpha_6\beta_4$ has been connected to persisting expression of integrin α_6 subunit (Garzino-Demo et al. 1998). This could imply that upon dissociation of $\alpha_6\beta_4$ complex, integrin α_6 subunit recruits another β subunit. Immunolabellings and immunoprecipitations showed that the levels of integrin $\alpha_6\beta_4$ were strong in 43A cells, less intense in 43B cells, indicating some complex formation, and absent in 43A-SNA cells. Instead, 43A-SNA cells assembled integrin $\alpha_6\beta_1$, which is one of the few recognized receptors for laminin-411 (Kortesmaa et al. 2000; Fujiwara et al. 2001). Cancer cells have been shown to switch to expression of integrins favouring their survival and migration (Guo and Giancotti 2004). In agreement with our findings, integrin $\alpha_6\beta_4$ is replaced by $\alpha_6\beta_1$ in progression of prostate carcinoma (Cress et al. 1995). In addition, integrin $\alpha_6\beta_1$ is connected to an invasive phenotype, as it promotes survival and growth of metastatic breast carcinoma cells (Wewer et al. 1997a). In an EMT cell model of Ha-Ras-transformed mammary epithelial cells, expression of integrins $\alpha_5\beta_1$ and $\alpha_6\beta_1$ is upregulated (Maschler et al. 2005). The localization of α_5 and α_6 subunits, however, is depolarized and distributed at the entire cell surface as opposed to focal adhesions, questioning whether they are functional. Our results further showed that 43A-SNA cells upregulated the levels of integrin $\alpha_1\beta_1$, which is mainly a collagen-binding integrin and also related to a migratory phenotype (Hemler et al. 1984; Gardner et al. 1996). The levels of integrin $\alpha_1\beta_1$ rise in some malignancies such as invasive bladder carcinomas and mesenchymal tumours, fibrosarcoma and leiomyosarcoma (Miettinen et al. 1993; Liebert et al. 1994). We also detected neoexpression of ILK in focal adhesions of 43B and 43A-SNA cells. Ectopic ILK

induces cell invasion and tumourigenesis in nude mice (Novak et al. 1998; Janji et al. 1999). ILK may also initiate EMT and augment the levels of Snail through the GSK3β pathway (Somasiri et al. 2001; Tan et al. 2001). Our results suggest a feedback loop in which EMT upregulates ILK. This could be achieved, for instance, through EMT-induced engagement of potentially ILK-binding integrins $\alpha_6\beta_1$ and $\alpha_1\beta_1$, leading to activation of the TGF-β pathway and upregulation of ILK (Nieto 2002; Oloumi et al. 2004).

Laminin-411 and laminin-511 may have opposing effects on cell migration, as laminin-411 seems to promote monocyte migration through blood vessel walls into tissues and laminin-511 may determine their arrest (Pedraza et al. 2000). In our functional cell adhesion experiments, oral SCC cells adhered strongly to fibronectin and laminin-511, whereas adhesion to laminin-411 was minimal. Laminin-411 has previously been implicated in the detachment, migration and invasion of cancer cells, and suggested to belong to matricellular proteins that participate in modulation of anti-adhesive properties (Fujiwara et al. 2001; Murphy-Ullrich 2001; Bornstein and Sage 2002; Khazenzon et al. 2003; Vainionpää et al. 2007). There is also evidence that matricellular protein SPARC enables local tumour cell colonization and induces EMT in progression of melanoma (Bornstein and Sage 2002; Robert et al. 2006). When we used fibronectin or laminin-511 as adhesion substrates with increasing concentrations of laminin-411, laminin-411 significantly compromised the adhesion of 43A, 43B and 43A-SNA cells. Interference of laminin-411 or tenascin-C with adhesion to fibronectin has previously been detected with glioblastoma, breast and renal cell carcinoma cells (Huang et al. 2001; Vainionpää et al. 2007). Western blots and immunoprecipitations of 43B cells further showed co-precipitation of laminin-411 and fibronectin, indicating that they bind to each other. These results suggested that laminin-411 may modulate cell adhesion as an intermediary with other ECM proteins. The EMT-experienced oral SCC cells may control their microenvironment and gain access to distant sites by regulating the synthesis of ECM proteins that enhance their migration abilities.

8.4. Podosome-like structures of non-invasive oral SCC cells are replaced in EMT by actin comet-based invadopodia

Our observations suggest that 43A cells organize prominent hemidesmosomes and focal adhesions, whereas 43B and 43A-SNA cells organize mainly focal and fibrillar adhesions. We further found that EMT strongly potentiates the invasion abilities of oral SCC cells. Wound-healing and invasion assays combined with rhodamine phalloidin labellings revealed that 43A and mesenchymally transformed 43B cells assembled actin-based structures that resembled podosomes and invadopodia (Lehto et al. 1982; Linder and Aepfelbacher 2003; Weaver 2006; Linder 2007; Yilmaz and Christofori 2009). Podosomes of 43A cells were punctate structures, whereas 43B cell invadopodia had tail-like, curling actin assemblies. In wound-healing experiments and FESEM, 43B cells developed similar actin-rich protrusions from their cell membranes. 43A-SNA cells lacked such actin accumulations, although their invasion and migration competence was significantly higher than that of 43A or 43B cells. This could indicate that 43A-SNA cells employ an ameboid-type of movement, which has been detected during migration of highly malignant cancer cells (Friedl and Bröcker 2000; Wolf et al. 2003; Carragher et al. 2006). In such situation, the cells do not degrade their surrounding extracellular matrix substantially, but squeeze through the collagen networks.

To attain more knowledge about podosome-like structures and invadopodia in 43A and 43B cells, we first followed random cell migration with epifluorescence wide-field live-cell imaging. Confirming the results obtained with wound-healing experiments, 43A cells migrated in ten hours only marginally, whereas 43B cells had significantly longer migration trajectories and greater velocity. In contrast to many other cell models (Tarone et al. 1985; Hai et al. 2002; Moreau et al. 2003; Furmaniak-Kazmierczak et al. 2007), 43A and 43B cells assembled podosomes and invadopodia constitutively under normal cell culture conditions, without any need for stimulation with growth factors or tyrosine kinases. These structures organized independently of the ECM substrate coating and their morphology did not change when cell migration was stimulated with EGF. When the cells were seeded on fluorescently labelled gelatin, 43A and 43B cells formed the podosomes and invadopodia rapidly, in two hours, and degraded the underlying matrix possibly via MT1-MMP (Sato et al. 1997). 43B cells further formed actin-based, club-ended cell extensions in five hours, which also degraded the ECM. FESEM indicated 43A cells as

flat epithelioid cells with prominent lamellae, whereas 43B cells were covered with club-ended cell extensions that seemed to originate from the dorsal cell surfaces. These extensions were distinct from filopodia, which do not have such large endings (Faix and Rottner 2006; Yamaguchi and Condeelis 2007). 3D confocal microscopy and *in situ* gelatin zymography disclosed 43A podosomes as relatively large, ECM-protruding structures, whose volumes increased over time. 43B cells assembled greater numbers of invadopodia that were narrow tail-like structures with no specific tendency to increase in volume over time. With regard to their invasion capacities, 43B invadopodia degraded significantly larger areas of ECM per cell than 43A podosomes.

To gain more information about the structural proteins in podosomes and invadopodia, we used EGFP-actin transfections together with immunofluorescence labellings, immunoprecipitations and Western blots. In addition to hemidesmosomes in 43A cells, HD1/ plectin was found at the peripheral ring of 43A podosomes, but not in 43B invadopodia. HD1/ plectin is a linker protein that regulates also microtubule and actin dynamics through its different domains (Niessen et al. 1997; Sonnenberg and Liem 2007). As the binding sites of integrin β_4 subunit and actin seem to overlap, HD1/ plectin cannot bind both of these molecules simultaneously (Sonnenberg and Liem 2007). This could be the reason why HD1/ plectin localized with actin filaments in podosomes, but with Ck filaments in hemidesmosomes of 43A cells. HD1/ plectin and αII-spectrin belong to the spectraplakin superfamily and function as membrane anchoring and scaffolding molecules that crosslink actin to the cell membrane (Röper et al. 2002; Sonnenberg and Liem 2007). Similarly to HD1/ plectin, we detected αII-spectrin reactivity only at the podosome rings of 43A cells, not in 43B invadopodia. These proteins may be used to mediate protein recruitment and membrane scaffolding in 43A podosomes.

Other proteins that localized to 43A podosome rings, but not to 43B invadopodia were talin, FAK and pacsin 2. Talin is an important adaptor between integrins, mediators such as FAK, and the cytoskeleton, and it regulates actin assembly by capping the barbed filament ends (Critchley 2004; Le Clainche and Carlier 2008). Our results suggested that talin was replaced by tensin in 43B cell invadopodia and cell extensions. Previously, the talin-tensin switch has been found in maturing focal adhesions (McCleverty et al. 2007; Legate and Fässler 2009), in which they both bind integrin β_1 and β_5 subunits and mediate

adhesion to actin filaments. The talin-tensin switch has been suggested to transform a structural adhesion to an actively signalling one (Legate and Fässler 2009), which could be advantageous to rapidly migrating EMT-experienced 43B cells.

The results also showed pacsin 2 immunoreactivity together with its binding partner filamin A only in the 43A podosome ring and core, respectively, not in invadopodia. Filamin A, an actin crosslinking protein (van der Flier and Sonnenberg 2001b; Nikki et al. 2002), did not accumulate to 43B invadopodia until 15 hours after seeding, i.e., after the functional invadopodia had formed. This suggested that invadopodia can mature into actively degrading structures independent of filamin A. Filamin A overexpression did not recruit pacsin 2 to 43B invadopodia. As pacsin 2 has been implicated as a membrane-bending protein with a role in mediating endocytosis (Modregger et al. 2000; Qualmann and Kelly 2000; Halbach et al. 2007; Heath and Insall 2008), it may participate in the formation of podosome 3D structure and gather proteins for cytoplasmic import. Furthermore, by binding to filamin A, it may contribute to stabilization of the podosome in a time-dependent manner.

Integrin $\alpha_v\beta_5$ localized only to the sharp interface between the invadopodia head and the cell membrane. Integrin $\alpha_v\beta_5$, a vitronectin receptor, is linked to a mesenchymal phenotype, has been reported in EMT in normal tooth development and is required for invasion of human embryonal kidney cells undergoing EMT (Salmivirta et al. 1996; Yan and Shao 2006). In addition, integrin $\alpha_v\beta_5$ may have a role in endocytosis, as it mediates degradation and internalization of vitronectin in fibroblasts (Panetti and McKeown-Longo 1993). Integrin $\alpha_3\beta_1$, on the other hand, is able to bind multiple ligands, including fibronectin, type IV collagen and laminins (Belkin and Stepp 2000). We found integrin $\alpha_3\beta_1$ at the podosome rings of 43A cells. In 43B cells, the distribution of integrin $\alpha_3\beta_1$ was restricted to cover the cell membrane around the invadopodia and the cell extensions protruding from the cells. Although this integrin has been detected previously in invadopodia, a similar distribution has not been reported (Mueller et al. 1999). The localization of integrin $\alpha_3\beta_1$ in 43B cells could be explained partly by the fact that the morphology of 43B invadopodia is rather unique, as only one study has previously reported actin tails in invadopodia (Baldassarre et al. 2006). If this integrin is used in 43B cells in the docking of proteolytic enzymes to invadopodia (Mueller et al. 1999), its wide

distribution around the actin tails could explain the greater degrading activity of the invadopodia. However, it remains to be shown whether integrins *de facto* mediate invadopodia adhesion to ECM or function primarily as guiding or tethering proteins.

Time-lapse epifluorescence and TIRF microscopy with EGFP-actin and EGFP-cortactin-transfected cells disclosed 43A podosomes as highly stable structures with long life-spans. In contrast, 43B invadopodia had long, vigorously propelling tails that were attached by their heads to the basal cell membrane. Although predominantly long-lived, the actin tails were occasionally released from their attachment site and shuttled through the cytoplasm and new invadopodia developed. Migrating 43B cells showed club-ended extensions at the retracting cells as well as between the cell borders, suggesting that they are involved in maintenance of contacts between the cells and the ECM. Prolonged TIRF microscopy revealed halos of EGFP-actin in the immediate basal cell surface focal plane, correlating to a pool of monomeric actin (Destaing et al. 2003) surrounding 43A podosomes, but not in the vicinity of 43B invadopodia. In contrast to suggestions by Yamaguchi et al. (2005a), we could not detect migration of single podosomes or invadopodia, nor did we witness their fission from existing podosomes, thus concluding that they are formed *de novo* in 43A and 43B cells. Furthermore, when the actin filaments or microtubules were disrupted with cytochalasin B or demecolcine (Linder et al. 2000b), respectively, no new podosomes or invadopodia developed, suggesting that both networks are needed for their organization. As the growing heads of actin filaments in podosomes reach towards the membrane (Akisaka et al. 2008), they presumably provide the tension to create membrane protrusions. If implemented to cover the functions of actin comets in 43B invadopodia, they may be related to invasive abilities. In congruence, actin comets have been first discovered in intracellular bacteria, where they gather an actin polymerization machinery to produce movement (Gouin et al. 2005). These results are supported by our findings of several members of the actin treadmilling machinery, e.g., Arp 2/3, cortactin and vinculin, in both 43A podosomes and 43B invadopodia.

The formation and maintenance of function of both podosomes and invadopodia depend on continuous actin assembly (Linder et al. 2000a; Linder et al. 2000b; Yamaguchi et al. 2005a; Weaver 2006). FRAP experiments with EGFP-transfected cells showed significant differences between the turnover of fluorescent proteins in 43A podosomes and 43B

invadopodia. Actin, cortactin and filamin A were all rapidly organized to both podosomes and invadopodia, but the recovery times were always shorter in podosomes. Also the 43B cell extensions showed shuffling of actin molecules, indicating that they are actively regulated cell organs. FRAP experiments of osteoclast podosomes have shown that the recovery of actin to plateau is ca. 1-2 minutes (Ochoa et al. 2000; Destaing et al. 2003). As opposed to our study, osteoclast podosomes were photobleached in colonies of tens to hundreds of podosomes, and their results may be compromised by the diffusion distance of actin molecules being longer in such a setting. When bleaching is directed to a broader area, the phototoxicity also affects a larger cytoplasmic environment. Congruent with the slower recovery of 43B invadopodia compared with 43A podosomes, photobleaching of melanoma cell invadopodia have shown actin recovery of 3 minutes (Baldassarre et al. 2006). The life-spans of osteoclast podosomes have been reported to be 2-12 minutes, although they depend on the stage of podosome differentiation, i.e., whether the osteoclasts form podosome clusters, belts or rings (Kanehisa et al. 1990; Akisaka et al. 2001; Destaing et al. 2003). In this respect, the several-hour-long life-spans of oral SCC podosomes and invadopodia resemble characteristics reported for invadopodia (Yamaguchi et al. 2005a; Baldassarre et al. 2006). Taken together, 43A podosomes are complex structures with typical organization with a ring and core. Actin, cortactin and filamin A molecules present high turnover in these structures, indicating a strict regulation of podosome dynamics. The actin tail-embedded invadopodia in 43B cells are long-lived, but the reorganization of structural proteins is slower than in podosomes, possibly reflecting a more labile phenotype. As the 3D structure of invadopodia remains the same during their life-span, and regardless of their small size, invadopodia being able to degrade ECM in high amounts, it can be suggested that they may be used in invasion of oral SCC cells. The cell extensions in 43B cells harboured the same proteins as invadopodia and showed dynamic shuffling of actin molecules, suggesting that they also participate in the migration and invasion of EMT-experienced cells.

9 CONCLUSIONS

Invasion and metastasis of epithelial tumours remains the primary cause of treatment failure and death of cancer patients. Further insights into the mechanisms leading to malignancy are a prerequisite for identifying new, clinically valuable prognostic markers and developing new therapies. Emerging interest has focused on the involvement of EMT in pathological conditions, including cancer progression. The primary focus of this thesis was to study the role of EMT in oral SCC cell lines and in tumour samples.

As the role and localization of transcription factor Snail in cancer have remained undetermined due to lack of proper antibodies, we created two MAbs specific for Snail. The MAbs showed endogenous and exogenous Snail in the nuclei of murine and human fibroblasts and in many human carcinoma cells. Snail was detected at the stroma and invasive margins of colon adenocarcinoma and cervical and laryngeal SCC. It also localized to activated fibroblastoid cells in wound borders and was found in fibromatosis, fibrosarcoma and sarcoma samples.

In oral SCC cells, EMT not only downregulated E-cadherin at the adherens junction, but upregulated N-cadherin and induced a vast cytoskeletal change by downregulating cytokeratin expression profile, upregulating vimentin intermediate filaments and dissociating hemidesmosomal complexes. E-cadherin repressors ZEB-1 and ZEB-2 were most likely responsible for the endogenous EMT, and Snail was further found to induce these transcription factors in the exogenous EMT. In addition, EMT affected the expression and distribution of a variety of integrins, namely $\alpha_1\beta_1$, $\alpha_3\beta_1$, $\alpha_6\beta_1$, $\alpha_6\beta_4$ and $\alpha_v\beta_5$, which operate in the adhesion, proliferation and migration of normal and malignant cells. EMT also progressively downregulated the expression of epithelial BM components laminin-332 and laminin-511 and upregulated the expression of mesenchymal laminin-411. The results showed that Snail can directly bind the promoter sites of laminin α5 and α4 chains and control their transcription. Laminin-411 may hinder the binding of cells to other ECM components and thus elicit migration of cancer cells. EMT gave rise to a highly migratory and invasive phenotype in oral SCC cells. EMT induced a switch in the adhesion and invasion machinery, changing from assembly of podosome-like structures to actin comet-embedded invadopodia. Previously unidentified structural proteins, e.g., HD1/ plectin, αII-spectrin, pacsin 2 and filamin A, that were detected in podosomes or invadopodia depict and emphasize their differences as

mediators of cancer development. Compared with podosomes, invadopodia had a less regulated and less stable appearance. Invadopodia were more numerous, degraded greater amounts of ECM and, through cellular extensions, probed their immediate environment, thus presenting qualities that EMT-experienced carcinoma cells could exploit in migration and invasion.

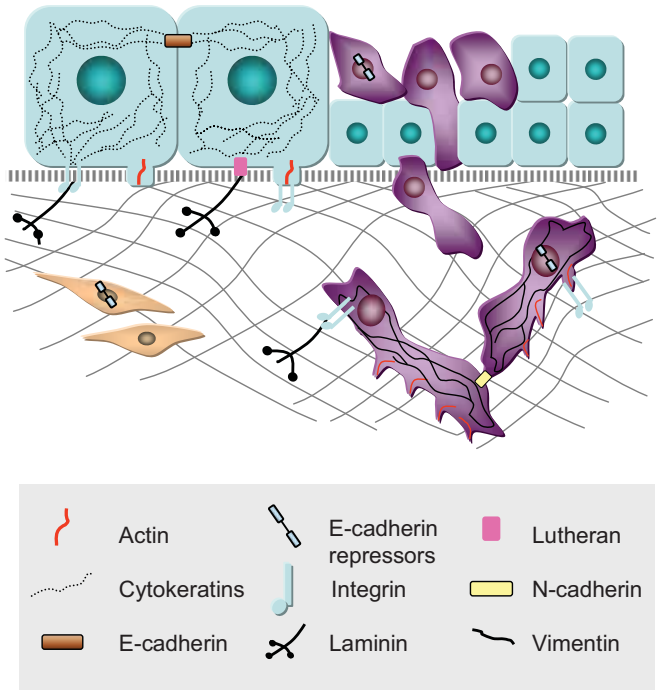


Figure 10. *A schematic model of EMT in oral SCC cells. Further details are described in the text.*

The principal findings of this study suggest that EMT affects the transcription, synthesis and secretion of laminins-332, -411 and -511 in addition to the levels and distribution of their specific receptors. The oral SCC cell lines can be used in the future to further evaluate the roles of EMT in the progression of malignancy, as well as in studies of the function of podosomes and invadopodia in cell migration and invasion. The MAbs created in this study revealed Snail protein in invasive fronts of carcinomas and in the tumour-stroma compartment. They can thus be used to detect Snail and to predict the presence of EMT and malignant phenotype in cell lines and patient samples. More thorough understanding of the pathomechanisms of cancer will pave the way for novel, effective cancer treatment modalities.

10 ACKNOWLEDGEMENTS

This study was conducted at the Institute of Biomedicine / Anatomy, University of Helsinki. My work was supported by the Biomedicum Helsinki Foundation, the Finnish Medical Foundation Duodecim, the Finnish-Norwegian Medical Foundation, the Helsinki Biomedical Graduate School, the K. Albin Johansson Foundation, the Mary and Georg C Ehrnrooth Foundation, the University of Helsinki Chancellor's Fund and the University of Helsinki Medical Fund.

My deepest gratitude goes to the following persons:

My supervisor, Professor Ismo Virtanen, who passed away during the final stages of this thesis. I thank him for guidance during these years and for continuous new ideas. His broad knowledge of science never ceased to amaze me. He will be missed.

Reviewers of this thesis, Professor Tuula Salo and Professor Veli-Jukka Uitto, for your careful review and useful comments.

Carol Ann Pelli, for author-editing.

Co-authors in Finland and abroad, for participating in this work. Especially, Professor Reidar Grenman, for providing the magnificent cell lines that made this study possible. Professor Antonio García de Herreros and Dr. Clara Francí, for valuable constructs and fruitful collaboration. Professor Yrjö T. Konttinen, for allowing me to use the facilities in your laboratory and for your advice and interest in my work. Dr. Mari Ainola, for invaluable help with the chromatin immunoprecipitation experiments and for good questions, good suggestions and a biochemical perspective. Drs. Mika Hukkanen and Mikko Liljeström, for providing me with exciting methods to adopt, for expertise in cell imaging, for critical reading of the manuscripts and most importantly, for your sinister sense of humour that saved many days.

Colleagues Docent Heikki Hervonen, Docent Nils Bäck, Professor Pertti Panula, Professor Elina Ikonen, Docent Matti Korhonen, Suvi Viranta-Kovanen, Anna Meuronen, Ville

Sallinen, Jukka Pajarinen, Ariel Noro, Eeva Castrén, Sofia Franssi, Sanna Vuoristo and Outi Heikkilä, for sharing your opinions and experiences with teaching or scientific work. Colleagues Noora Skants and Sissi Katz, for many shared hours inside and outside of work and for friendship, advice and support.

Personnel of the Institute of Biomedicine / Anatomy: Pipsa Kaipainen, for help with the countless experiments, hands-on training and insightful discussions. Marja-Leena Piironen and Hanna Wennäkoski, for help with cell culture and immunolabellings, and for knowledge about the multitude of antibodies. Outi Rauanheimo, for kind words and expertise in secretarial and administrative tasks. Reijo Karppinen and Hannu Kamppinen, for the introduction into the interesting world of photography and image processing. Paula Hasenson, Anne Reijula, Kaisu Laine, Pirjo Salminen, Eija Kaila, Erkki Hänninen, Pauliina Porola and Anna Uro, for help in the laboratory and indispensable coffee breaks.

Educational staff of the Institute of Biomedicine: Aulis “Muumi” Martonen, Ritva Henriksson and Katriina Laurén, for your everyday input on behalf of the students and teachers. I also thank all students at the Faculty of Medicine who I have had the opportunity to teach during these years; while teaching you, I have learnt a great deal, particularly about myself. I very much appreciate your special way of acknowledging my work in 2008.

My parents, to whom I dedicate this book. I admire your interest in science, culture and music; it has greatly enriched my childhood and my adult life. I thank you for your belief in me and unwavering encouragement. I also thank my brother Mikko and my sister-in-law Carolina for many joyful moments, Mikko for being a trustworthy advisor and Carolina for excellent cooking. My godparents Raija and Pentti Hornamo are thanked for positive life-long support.

Noora Lylykangas, for a long friendship and several life-saving discussions over a cup of tea. Our adorable godchildren Joel Kuhlberg, Lenni Hirvonen and Kerttu Kujala as well as their families, for letting us into their lives. My in-laws Pirjo-Liisa and Timo Volanen, for accepting me into their family, for stimulating discussions and for sharing many

meaningful events. I thank all of my friends, relatives and in-laws for being there for me during these years.

My dear husband Jussi, the light of my life, I thank you for every day you have spent with me. I cherish your love, rationality and technical point of view, and your truly incredible sense of humour.

Minna Takkunen

11 REFERENCES

Aberdam D, Virolle T, Simon-Assmann P. Transcriptional regulation of laminin gene expression. Microsc Res Tech 2000 51:228-237.

Airenne T, Haakana H, Sainio K, Kallunki T, Kallunki P, Sariola H, Tryggvason K. Structure of the human laminin gamma 2 chain gene (LAMC2): alternative splicing with different tissue distribution of two transcripts. Genomics 1996 32:54-64.

Akashi T, Ito E, Eishi Y, Koike M, Nakamura K, Burgeson RE. Reduced expression of laminin alpha 3 and alpha 5 chains in non-small cell lung cancers. Jpn J Cancer Res 2001 92:293-301.

Akisaka T, Yoshida H, Inoue S, Shimizu K. Organization of cytoskeletal F-actin, G-actin, and gelsolin in the adhesion structures in cultured osteoclast. J Bone Miner Res 2001 16:1248-1255.

Akisaka T, Yoshida H, Suzuki R, Takama K. Adhesion structures and their cytoskeleton-membrane interactions at podosomes of osteoclasts in culture. Cell Tissue Res 2008 331:625-641.

Alberga A, Boulay JL, Kempe E, Dennefeld C, Haenlin M. The snail gene required for mesoderm formation in Drosophila is expressed dynamically in derivatives of all three germ layers. Development 1991 111:983-992.

Artym VV, Kindzelskii AL, Chen WT, Petty HR. Molecular proximity of seprase and the urokinase-type plasminogen activator receptor on malignant melanoma cell membranes: dependence on beta1 integrins and the cytoskeleton. Carcinogenesis 2002 23:1593-1601.

Aszódi A, Legate KR, Nakchbandi I, Fässler R. What mouse mutants teach us about extracellular matrix function. Annu Rev Cell Dev Biol 2006 22:591-621.

Aumailley M, Bruckner-Tuderman L, Carter WG, Deutzmann R, Edgar D, Ekblom P, Engel J, Engvall E, Hohenester E, Jones JC, Kleinman HK, Marinkovich MP, Martin GR, Mayer U, Meneguzzi G, Miner JH, Miyazaki K, Patarroyo M, Paulsson M, Quaranta V, Sanes JR, Sasaki T, Sekiguchi K, Sorokin LM, Talts JF, Tryggvason K, Uitto J, Virtanen I, von der Mark K, Wewer UM, Yamada Y, Yurchenco PD. A simplified laminin nomenclature. Matrix Biol 2005 24:326-332.

Aumailley M, El Khal A, Knoss N, Tunggal L. Laminin 5 processing and its integration into the ECM. Matrix Biol 2003 22:49-54.

Bachelder RE, Marchetti A, Falcioni R, Soddu S, Mercurio AM. Activation of p53 function in carcinoma cells by the alpha6beta4 integrin. J Biol Chem 1999 274:20733-20737.

Baldassarre M, Ayala I, Beznoussenko G, Giacchetti G, Machesky LM, Luini A, Buccione R. Actin dynamics at sites of extracellular matrix degradation. Eur J Cell Biol 2006 85:1217-1231.

Baldassarre M, Pompeo A, Beznoussenko G, Castaldi C, Cortellino S, McNiven MA, Luini A, Buccione R. Dynamin participates in focal extracellular matrix degradation by invasive cells. Mol Biol Cell 2003 14:1074-1084.

Barrallo-Gimeno A, Nieto MA. The Snail genes as inducers of cell movement and survival: implications in development and cancer. Development 2005 132:3151-3161.

Batlle E, Sancho E, Francí C, Domínguez D, Monfar M, Baulida J, García de Herreros A. The transcription factor snail is a repressor of E-cadherin gene expression in epithelial tumour cells. Nat Cell Biol 2000 2:84-89.

Behrens J. Cadherins and catenins: role in signal transduction and tumor progression. Cancer Metastasis Rev 1999 18:15-30.

Belkin AM, Stepp MA. Integrins as receptors for laminins. Microsc Res Tech 2000 51:280-301.

Bershadsky A, Chausovsky A, Becker E, Lyubimova A, Geiger B. Involvement of microtubules in the control of adhesion-dependent signal transduction. Curr Biol 1996 6:1279-1289.

Blanco MJ, Moreno-Bueno G, Sarrio D, Locascio A, Cano A, Palacios J, Nieto MA. Correlation of Snail expression with histological grade and lymph node status in breast carcinomas. Oncogene 2002 21:3241-3246.

Blose SH, Meltzer DI, Feramisco JR. 10-Nm Filaments are Induced to Collapse in Living Cells Microinjected with Monoclonal and Polyclonal Antibodies Against Tubulin. J Cell Biol 1984 98:847-858.

Bolós V, Peinado H, Pérez-Moreno MA, Fraga MF, Esteller M, Cano A. The transcription factor Slug represses E-cadherin expression and induces epithelial to mesenchymal transitions: a comparison with Snail and E47 repressors. J Cell Sci 2003 116:499-511.

Bornstein P, Sage EH. Matricellular proteins: extracellular modulators of cell function. Curr Opin Cell Biol 2002 14:608-616.

Borza DB, Bondar O, Ninomiya Y, Sado Y, Naito I, Todd P, Hudson BG. The NC1 domain of collagen IV encodes a novel network composed of the alpha 1, alpha 2, alpha 5, and alpha 6 chains in smooth muscle basement membranes. J Biol Chem 2001 276:28532-28540.

Bosman FT, Havenith MG, Visser R, Cleutjens JP. Basement membranes in neoplasia. Prog Histochem Cytochem 1992 24:1-92.

Boulay JL, Dennefeld C, Alberga A. The Drosophila developmental gene snail encodes a protein with nucleic acid binding fingers. Nature 1987 330:395-398.

Boussif O, Lezoualc'h F, Zanta MA, Mergny MD, Scherman D, Demeneix B, Behr JP. A versatile vector for gene and oligonucleotide transfer into cells in culture and in vivo: polyethylenimine. Proc Natl Acad Sci U S A 1995 92:7297-7301.

Bowden ET, Barth M, Thomas D, Glazer RI, Mueller SC. An invasion-related complex of cortactin, paxillin and PKCmu associates with invadopodia at sites of extracellular matrix degradation. Oncogene 1999 18:4440-4449.

Boyer B, Tucker GC, Valles AM, Franke WW, Thiery JP. Rearrangements of desmosomal and cytoskeletal proteins during the transition from epithelial to fibroblastoid organization in cultured rat bladder carcinoma cells. J Cell Biol 1989 109:1495-1509.

Brar PK, Dalkin BL, Weyer C, Sallam K, Virtanen I, Nagle RB. Laminin alpha-1, alpha-3, and alpha-5 chain expression in human prepubertal [correction of prepubetal] benign prostate glands and adult benign and malignant prostate glands. Prostate 2003 55:65-70.

Bretscher MS, Aguado-Velasco C. Membrane traffic during cell locomotion. Curr Opin Cell Biol 1998 10:537-541.

Burgeson RE, Chiquet M, Deutzmann R, Ekblom P, Engel J, Kleinman H, Martin GR, Meneguzzi G, Paulsson M, Sanes J. A new nomenclature for the laminins. Matrix Biol 1994 14:209-211.

Bussemakers MJ, Giroldi LA, van Bokhoven A, Schalken JA. Transcriptional regulation of the human E-cadherin gene in human prostate cancer cell lines: characterization of the human E-cadherin gene promoter. Biochem Biophys Res Commun 1994 203:1284-1290.

Caligaris-Cappio F, Bergui L, Tesio L, Corbascio G, Tousco F, Marchisio PC. Cytoskeleton organization is aberrantly rearranged in the cells of B chronic lymphocytic leukemia and hairy cell leukemia. Blood 1986 67:233-239.

Campbell IG, Foulkes WD, Senger G, Trowsdale J, Garin-Chesa P, Rettig WJ. Molecular cloning of the B-CAM cell surface glycoprotein of epithelial cancers: a novel member of the immunoglobulin superfamily. Cancer Res 1994 54:5761-5765.

Cano A, Pérez-Moreno MA, Rodrigo I, Locascio A, Blanco MJ, del Barrio MG, Portillo F, Nieto MA. The transcription factor snail controls epithelial-mesenchymal transitions by repressing E-cadherin expression. Nat Cell Biol 2000 2:76-83.

Carragher NO, Walker SM, Scott Carragher LA, Harris F, Sawyer TK, Brunton VG, Ozanne BW, Frame MC. Calpain 2 and Src dependence distinguishes mesenchymal and amoeboid modes of tumour cell invasion: a link to integrin function. Oncogene 2006 25:5726-5740.

Carter WG, Ryan MC, Gahr PJ. Epiligrin, a new cell adhesion ligand for integrin alpha 3 beta 1 in epithelial basement membranes. Cell 1991 65:599-610.

Carver EA, Jiang R, Lan Y, Oram KF, Gridley T. The mouse snail gene encodes a key regulator of the epithelial-mesenchymal transition. Mol Cell Biol 2001 21:8184-8188.

Cavallaro U, Christofori G. Cell adhesion and signalling by cadherins and Ig-CAMs in cancer. Nat Rev Cancer 2004 4:118-132.

Cavallaro U, Schaffhauser B, Christofori G. Cadherins and the tumour progression: is it all in a switch? Cancer Lett 2002 176:123-128.

Champliaud MF, Virtanen I, Tiger CF, Korhonen M, Burgeson R, Gullberg D. Posttranslational modifications and beta/gamma chain associations of human laminin alpha1 and laminin alpha5 chains: purification of laminin-3 from placenta. Exp Cell Res 2000 259:326-335.

Chellaiah M, Kizer N, Silva M, Alvarez U, Kwiatkowski D, Hruska KA. Gelsolin deficiency blocks podosome assembly and produces increased bone mass and strength. J Cell Biol 2000 148:665-678.

Chen Q, Lipkina G, Song Q, Kramer RH. Promoter methylation regulates cadherin switching in squamous cell carcinoma. Biochem Biophys Res Commun 2004 315:850-856.

Chen WT, Kelly T. Seprase complexes in cellular invasiveness. Cancer Metastasis Rev 2003 22:259-269.

Chen WT, Lee CC, Goldstein L, Bernier S, Liu CH, Lin CY, Yeh Y, Monsky WL, Kelly T, Dai M. Membrane proteases as potential diagnostic and therapeutic targets for breast malignancy. Breast Cancer Res Treat 1994 31:217-226.

Chen WT, Olden K, Bernard BA, Chu FF. Expression of transformation-associated protease(s) that degrade fibronectin at cell contact sites. J Cell Biol 1984 98:1546-1555.

Cheresh DA, Spiro RC. Biosynthetic and functional properties of an Arg-Gly-Asp-directed receptor involved in human melanoma cell attachment to vitronectin, fibrinogen, and von Willebrand factor. J Biol Chem 1987 262:17703-17711.

Chomczynski P, Sacchi N. Single-step method of RNA isolation by acid guanidinium thiocyanate-phenol-chloroform extraction. Anal Biochem 1987 162:156-159.

Chow V, Yuen AP, Lam KY, Tsao GS, Ho WK, Wei WI. A comparative study of the clinicopathological significance of E-cadherin and catenins (alpha, beta, gamma) expression in the surgical management of oral tongue carcinoma. J Cancer Res Clin Oncol 2001 127:59-63.

Christiansen JJ, Rajasekaran AK. Reassessing epithelial to mesenchymal transition as a prerequisite for carcinoma invasion and metastasis. Cancer Res 2006 66:8319-8326.

Christofori G. Changing neighbours, changing behaviour: cell adhesion molecule-mediated signalling during tumour progression. EMBO J 2003 22:2318-2323.

Clark ES, Whigham AS, Yarbrough WG, Weaver AM. Cortactin is an essential regulator of matrix metalloproteinase secretion and extracellular matrix degradation in invadopodia. Cancer Res 2007 67:4227-4235.

Clark RA, Folkvord JM, Nielsen LD. Either exogenous or endogenous fibronectin can promote adherence of human endothelial cells. J Cell Sci 1986 82:263-280.

Colognato H, Yurchenco PD. Form and function: the laminin family of heterotrimers. Dev Dyn 2000 218:213-234.

Comijn J, Berx G, Vermassen P, Verschueren K, van Grunsven L, Bruyneel E, Mareel M, Huylebroeck D, van Roy F. The two-handed E box binding zinc finger protein SIP1 downregulates E-cadherin and induces invasion. Mol Cell 2001 7:1267-1278.

Condeelis J, Segall JE. Intravital imaging of cell movement in tumours. Nat Rev Cancer 2003 3:921-930.

Coopman PJ, Do MT, Thompson EW, Mueller SC. Phagocytosis of cross-linked gelatin matrix by human breast carcinoma cells correlates with their invasive capacity. Clin Cancer Res 1998 4:507-515.

Cress AE, Rabinovitz I, Zhu W, Nagle RB. The alpha 6 beta 1 and alpha 6 beta 4 integrins in human prostate cancer progression. Cancer Metastasis Rev 1995 14:219-228.

Critchley DR. Cytoskeletal proteins talin and vinculin in integrin-mediated adhesion. Biochem Soc Trans 2004 32:831-836.

Danjo Y, Gipson IK. Actin 'purse string' filaments are anchored by E-cadherin-mediated adherens junctions at the leading edge of the epithelial wound, providing coordinated cell movement. J Cell Sci 1998 111 (Pt 22):3323-3332.

de Araujo VC, Pinto Júnior DS, de Sousa SO, Nunes FD, de Araujo NS. Vimentin in oral squamous cell carcinoma. Eur Arch Otorhinolaryngol 1993 250:105-109.

De Craene B, Gilbert B, Stove C, Bruyneel E, van Roy F, Berx G. The transcription factor snail induces tumor cell invasion through modulation of the epithelial cell differentiation program. Cancer Res 2005a 65:6237-6244.

De Craene B, van Roy F, Berx G. Unraveling signalling cascades for the Snail family of transcription factors. Cell Signal 2005b 17:535-547.

de Iongh RU, Wederell E, Lovicu FJ, McAvoy JW. Transforming growth factor-beta-induced epithelial-mesenchymal transition in the lens: a model for cataract formation. Cells Tissues Organs 2005 179:43-55.

De Leeuw WJ, Berx G, Vos CB, Peterse JL, Van de Vijver MJ, Litvinov S, Van Roy F, Cornelisse CJ, Cleton-Jansen AM. Simultaneous loss of E-cadherin and catenins in invasive lobular breast cancer and lobular carcinoma in situ. J Pathol 1997 183:404-411.

Delaissé JM, Engsig MT, Everts V, del Carmen Ovejero M, Ferreras M, Lund L, Vu TH, Werb Z, Winding B, Lochter A, Karsdal MA, Troen T, Kirkegaard T, Lenhard T, Heegaard AM, Neff L, Baron R, Foged NT. Proteinases in bone resorption: obvious and less obvious roles. Clin Chim Acta 2000 291:223-234.

Deryugina EI, Ratnikov B, Monosov E, Postnova TI, DiScipio R, Smith JW, Strongin AY. MT1-MMP initiates activation of pro-MMP-2 and integrin alphavbeta3 promotes maturation of MMP-2 in breast carcinoma cells. Exp Cell Res 2001 263:209-223.

Destaing O, Saltel F, Geminard JC, Jurdic P, Bard F. Podosomes display actin turnover and dynamic self-organization in osteoclasts expressing actin-green fluorescent protein. Mol Biol Cell 2003 14:407-416.

Diniz-Freitas M, García-Caballero T, Antúnez-López J, Gándara-Rey JM, García-García A. Reduced E-cadherin expression is an indicator of unfavourable prognosis in oral squamous cell carcinoma. Oral Oncol 2006 42:190-200.

Doi M, Thyboll J, Kortesmaa J, Jansson K, Iivanainen A, Parvardeh M, Timpl R, Hedin U, Swedenborg J, Tryggvason K. Recombinant human laminin-10 (alpha5beta1gamma1). Production, purification, and migration-promoting activity on vascular endothelial cells. J Biol Chem 2002 277:12741-12748.

Domínguez D, Montserrat-Sentís B, Virgós-Soler A, Guaita S, Grueso J, Porta M, Puig I, Baulida J, Francí C, García de Herreros A. Phosphorylation regulates the subcellular location and activity of the snail transcriptional repressor. Mol Cell Biol 2003 23:5078-5089.

Dong R, Cwynarski K, Entwistle A, Marelli-Berg F, Dazzi F, Simpson E, Goldman JM, Melo JV, Lechler RI, Bellantuono I, Ridley A, Lombardi G. Dendritic cells from CML patients have altered actin organization, reduced antigen processing, and impaired migration. Blood 2003 101:3560-3567.

Downer CS, Watt FM, Speight PM. Loss of alpha 6 and beta 4 integrin subunits coincides with loss of basement membrane components in oral squamous cell carcinomas. J Pathol 1993 171:183-190.

Durkin ME, Loechel F, Mattei MG, Gilpin BJ, Albrechtsen R, Wewer UM. Tissue-specific expression of the human laminin alpha5-chain, and mapping of the gene to human chromosome 20q13.2-13.3 and to distal mouse chromosome 2 near the locus for the ragged (Ra) mutation. FEBS Lett 1997 411:296-300.

Eger A, Aigner K, Sonderegger S, Dampier B, Oehler S, Schreiber M, Berx G, Cano A, Beug H, Foisner R. DeltaEF1 is a transcriptional repressor of E-cadherin and regulates epithelial plasticity in breast cancer cells. Oncogene 2005 24:2375-2385.

El Nemer W, Gane P, Colin Y, Bony V, Rahuel C, Galactéros F, Cartron JP, Le Van Kim C. The Lutheran blood group glycoproteins, the erythroid receptors for laminin, are adhesion molecules. J Biol Chem 1998 273:16686-16693.

Elloul S, Elstrand MB, Nesland JM, Trope CG, Kvalheim G, Goldberg I, Reich R, Davidson B. Snail, Slug, and Smad-interacting protein 1 as novel parameters of disease aggressiveness in metastatic ovarian and breast carcinoma. Cancer 2005 103:1631-1643.

Engvall E, Davis GE, Dickerson K, Ruoslahti E, Varon S, Manthorpe M. Mapping of domains in human laminin using monoclonal antibodies: localization of the neurite-promoting site. J Cell Biol 1986 103:2457-2465.

Engvall E, Ruoslahti E. Binding of soluble form of fibroblast surface protein, fibronectin, to collagen. Int J Cancer 1977 20:1-5.

Entschladen F, Drell TL,4th, Lang K, Masur K, Palm D, Bastian P, Niggemann B, Zaenker KS. Analysis methods of human cell migration. Exp Cell Res 2005 307:418-426.

Erickson AC, Couchman JR. Still more complexity in mammalian basement membranes. J Histochem Cytochem 2000 48:1291-1306.

Evans JG, Correia I, Krasavina O, Watson N, Matsudaira P. Macrophage podosomes assemble at the leading lamella by growth and fragmentation. J Cell Biol 2003 161:697-705.

Faix J, Rottner K. The making of filopodia. Curr Opin Cell Biol 2006 18:18-25.

Ferletta M, Ekblom P. Identification of laminin-10/11 as a strong cell adhesive complex for a normal and a malignant human epithelial cell line. J Cell Sci 1999 112 (Pt 1):1-10.

Fidler IJ. The pathogenesis of cancer metastasis: the 'seed and soil' hypothesis revisited. Nat Rev Cancer 2003 3:453-458.

Filenius S, Hormia M, Rissanen J, Burgeson RE, Yamada Y, Araki-Sasaki K, Nakamura M, Virtanen I, Tervo T. Laminin synthesis and the adhesion characteristics of immortalized human corneal epithelial cells to laminin isoforms. Exp Eye Res 2001 72:93-103.

Finnish Cancer Registry. Cancer in Finland 2004 and 2005. Cancer Society of Finland Publication No. 72, Helsinki, 2007.

Flug M, Köpf-Maier P. The basement membrane and its involvement in carcinoma cell invasion. Acta Anat (Basel) 1995 152:69-84.

Fort P, Marty L, Piechaczyk M, el Sabrouty S, Dani C, Jeanteur P, Blanchard JM. Various rat adult tissues express only one major mRNA species from the glyceraldehyde-3-phosphate-dehydrogenase multigenic family. Nucleic Acids Res 1985 13:1431-1442.

Fradet Y, Cordon-Cardo C, Thomson T, Daly ME, Whitmore WF,Jr, Lloyd KO, Melamed MR, Old LJ. Cell surface antigens of human bladder cancer defined by mouse monoclonal antibodies. Proc Natl Acad Sci U S A 1984 81:224-228.

Francí C, Gallén M, Alameda F, Baró T, Iglesias M, Virtanen I, García de Herreros A. Snail1 protein in the stroma as a new putative prognosis marker for colon tumours. PLoS One 2009 4:e5595.

Franz M, Spiegel K, Umbreit C, Richter P, Codina-Canet C, Berndt A, Altendorf-Hofmann A, Koscielny S, Hyckel P, Kosmehl H, Virtanen I, Berndt A. Expression of Snail is associated with myofibroblast phenotype development in oral squamous cell carcinoma. Histochem Cell Biol 2009 131:651-660.

Friedl P, Bröcker EB. The biology of cell locomotion within three-dimensional extracellular matrix. Cell Mol Life Sci 2000 57:41-64.

Friedl P, Wolf K. Tumour-cell invasion and migration: diversity and escape mechanisms. Nat Rev Cancer 2003 3:362-374.

Frieser M, Nöckel H, Pausch F, Röder C, Hahn A, Deutzmann R, Sorokin LM. Cloning of the mouse laminin alpha 4 cDNA. Expression in a subset of endothelium. Eur J Biochem 1997 246:727-735.

Fujita M, Khazenzon NM, Bose S, Sekiguchi K, Sasaki T, Carter WG, Ljubimov AV, Black KL, Ljubimova JY. Overexpression of beta1-chain-containing laminins in capillary basement membranes of human breast cancer and its metastases. Breast Cancer Res 2005 7:R411-21.

Fujita N, Jaye DL, Kajita M, Geigerman C, Moreno CS, Wade PA. MTA3, a Mi-2/NuRD complex subunit, regulates an invasive growth pathway in breast cancer. Cell 2003 113:207-219.

Fujiwara H, Kikkawa Y, Sanzen N, Sekiguchi K. Purification and characterization of human laminin-8. Laminin-8 stimulates cell adhesion and migration through alpha3beta1 and alpha6beta1 integrins. J Biol Chem 2001 276:17550-17558.

Furmaniak-Kazmierczak E, Crawley SW, Carter RL, Maurice DH, Côté GP. Formation of extracellular matrix-digesting invadopodia by primary aortic smooth muscle cells. Circ Res 2007 100:1328-1336.

Gabbert HE, Mueller W, Schneiders A, Meier S, Moll R, Birchmeier W, Hommel G. Prognostic value of E-cadherin expression in 413 gastric carcinomas. Int J Cancer 1996 69:184-189.

Gaidano G, Bergui L, Schena M, Gaboli M, Cremona O, Marchisio PC, Caligaris-Cappio F. Integrin distribution and cytoskeleton organization in normal and malignant monocytes. Leukemia 1990 4:682-687.

Gailit J, Welch MP, Clark RA. TGF-beta 1 stimulates expression of keratinocyte integrins during re-epithelialization of cutaneous wounds. J Invest Dermatol 1994 103:221-227.

Galiè M, Sorrentino C, Montani M, Micossi L, Di Carlo E, D'Antuono T, Calderan L, Marzola P, Benati D, Merigo F, Orlando F, Smorlesi A, Marchini C, Amici A, Sbarbati A. Mammary carcinoma provides highly tumourigenic and invasive reactive stromal cells. Carcinogenesis 2005 26:1868-1878.

Galliano MF, Aberdam D, Aguzzi A, Ortonne JP, Meneguzzi G. Cloning and complete primary structure of the mouse laminin alpha 3 chain. Distinct expression pattern of the laminin alpha 3A and alpha 3B chain isoforms. J Biol Chem 1995 270:21820-21826.

Gálvez BG, Matías-Román S, Albar JP, Sánchez-Madrid F, Arroyo AG. Membrane type 1-matrix metalloproteinase is activated during migration of human endothelial cells and modulates endothelial motility and matrix remodeling. J Biol Chem 2001 276:37491-37500.

Gardner H, Kreidberg J, Koteliansky V, Jaenisch R. Deletion of integrin alpha 1 by homologous recombination permits normal murine development but gives rise to a specific deficit in cell adhesion. Dev Biol 1996 175:301-313.

Garzino-Demo P, Carrozzo M, Trusolino L, Savoia P, Gandolfo S, Marchisio PC. Altered expression of alpha 6 integrin subunit in oral squamous cell carcinoma and oral potentially malignant lesions. Oral Oncol 1998 34:204-210.

Gavazzi I, Nermut MV, Marchisio PC. Ultrastructure and gold-immunolabelling of cell-substratum adhesions (podosomes) in RSV-transformed BHK cells. J Cell Sci 1989 94 (Pt 1):85-99.

Geberhiwot T, Assefa D, Kortesmaa J, Ingerpuu S, Pedraza C, Wondimu Z, Charo J, Kiessling R, Virtanen I, Tryggvason K, Patarroyo M. Laminin-8 (alpha4beta1gamma1) is synthesized by lymphoid cells, promotes lymphocyte migration and costimulates T cell proliferation. J Cell Sci 2001 114:423-433.

Geberhiwot T, Ingerpuu S, Pedraza C, Neira M, Lehto U, Virtanen I, Kortesmaa J, Tryggvason K, Engvall E, Patarroyo M. Blood platelets contain and secrete laminin-8 (alpha4beta1gamma1) and adhere to laminin-8 via alpha6beta1 integrin. Exp Cell Res 1999 253:723-732.

Geiger B, Bershadsky A. Exploring the neighborhood: adhesion-coupled cell mechanosensors. Cell 2002 110:139-142.

Geiger B, Bershadsky A, Pankov R, Yamada KM. Transmembrane crosstalk between the extracellular matrix--cytoskeleton crosstalk. Nat Rev Mol Cell Biol 2001 2:793-805.

Ghersi G, Dong H, Goldstein LA, Yeh Y, Hakkinen L, Larjava HS, Chen WT. Regulation of fibroblast migration on collagenous matrix by a cell surface peptidase complex. J Biol Chem 2002 277:29231-29241.

Giancotti FG, Ruoslahti E. Integrin signaling. Science 1999 285:1028-1032.

Gimona M, Buccione R. Adhesions that mediate invasion. Int J Biochem Cell Biol 2006 38:1875-1892.

Goldfinger LE, Hopkinson SB, deHart GW, Collawn S, Couchman JR, Jones JC. The alpha3 laminin subunit, alpha6beta4 and alpha3beta1 integrin coordinately regulate wound healing in cultured epithelial cells and in the skin. J Cell Sci 1999 112 (Pt 16):2615-2629.

Gonzalez AM, Gonzales M, Herron GS, Nagavarapu U, Hopkinson SB, Tsuruta D, Jones JC. Complex interactions between the laminin alpha 4 subunit and integrins regulate endothelial cell behavior in vitro and angiogenesis in vivo. Proc Natl Acad Sci U S A 2002 99:16075-16080.

Gouin E, Welch MD, Cossart P. Actin-based motility of intracellular pathogens. Curr Opin Microbiol 2005 8:35-45.

Grau Y, Carteret C, Simpson P. Mutations and Chromosomal Rearrangements Affecting the Expression of Snail, a Gene Involved in Embryonic Patterning in Drosophila melanogaster. Genetics 1984 108:347-360.

Greer RO. Pathology of malignant and premalignant oral epithelial lesions. Otolaryngol Clin North Am 2006 39:249-75, v.

Grimes HL, Chan TO, Zweidler-McKay PA, Tong B, Tsichlis PN. The Gfi-1 proto-oncoprotein contains a novel transcriptional repressor domain, SNAG, and inhibits G1 arrest induced by interleukin-2 withdrawal. Mol Cell Biol 1996 16:6263-6272.

Grooteclaes ML, Frisch SM. Evidence for a function of CtBP in epithelial gene regulation and anoikis. Oncogene 2000 19:3823-3828.

Guaita S, Puig I, Francí C, Garrido M, Domínguez D, Batlle E, Sancho E, Dedhar S, De Herreros AG, Baulida J. Snail induction of epithelial to mesenchymal transition in tumor cells is accompanied by MUC1 repression and ZEB1 expression. J Biol Chem 2002 277:39209-39216.

Guarino M, Rubino B, Ballabio G. The role of epithelial-mesenchymal transition in cancer pathology. Pathology 2007 39:305-318.

Gullberg D, Tiger CF, Velling T. Laminins during muscle development and in muscular dystrophies. Cell Mol Life Sci 1999 56:442-460.

Guo W, Giancotti FG. Integrin signalling during tumour progression. Nat Rev Mol Cell Biol 2004 5:816-826.

Gustafsson E, Fässler R. Insights into extracellular matrix functions from mutant mouse models. Exp Cell Res 2000 261:52-68.

Hagedorn H, Schreiner M, Wiest I, Tubel J, Schleicher ED, Nerlich AG. Defective basement membrane in laryngeal carcinomas with heterogeneous loss of distinct components. Hum Pathol 1998 29:447-454.

Hai CM, Hahne P, Harrington EO, Gimona M. Conventional protein kinase C mediates phorbol-dibutyrate-induced cytoskeletal remodeling in a7r5 smooth muscle cells. Exp Cell Res 2002 280:64-74.

Haikonen J, Rantanen V, Pekkola K, Kulmala J, Grenman R. Does skin fibroblast radiosensitivity predict squamous cancer cell radiosensitivity of the same individual? Int J Cancer 2003 103:784-788.

Halbach A, Morgelin M, Baumgarten M, Milbrandt M, Paulsson M, Plomann M. PACSIN 1 forms tetramers via its N-terminal F-BAR domain. FEBS J 2007 274:773-782.

Hanahan D, Weinberg RA. The hallmarks of cancer. Cell 2000 100:57-70.

Hannigan GE, Leung-Hagesteijn C, Fitz-Gibbon L, Coppolino MG, Radeva G, Filmus J, Bell JC, Dedhar S. Regulation of cell adhesion and anchorage-dependent growth by a new beta 1-integrin-linked protein kinase. Nature 1996 379:91-96.

Hay ED. The mesenchymal cell, its role in the embryo, and the remarkable signaling mechanisms that create it. Dev Dyn 2005 233:706-720.

Hayashi Y, Kim KH, Fujiwara H, Shimono C, Yamashita M, Sanzen N, Futaki S, Sekiguchi K. Identification and recombinant production of human laminin alpha4 subunit splice variants. Biochem Biophys Res Commun 2002 299:498-504.

Hazan RB, Phillips GR, Qiao RF, Norton L, Aaronson SA. Exogenous expression of N-cadherin in breast cancer cells induces cell migration, invasion, and metastasis. J Cell Biol 2000 148:779-790.

Hazan RB, Qiao R, Keren R, Badano I, Suyama K. Cadherin switch in tumor progression. Ann N Y Acad Sci 2004 1014:155-163.

Heath RJ, Insall RH. F-BAR domains: multifunctional regulators of membrane curvature. J Cell Sci 2008 121:1951-1954.

Hemler ME, Sanchez-Madrid F, Flotte TJ, Krensky AM, Burakoff SJ, Bhan AK, Springer TA, Strominger JL. Glycoproteins of 210,000 and 130,000 m.w. on activated T cells: cell distribution and antigenic relation to components on resting cells and T cell lines. J Immunol 1984 132:3011-3018.

Hernandez-Barrantes S, Toth M, Bernardo MM, Yurkova M, Gervasi DC, Raz Y, Sang QA, Fridman R. Binding of active (57 kDa) membrane type 1-matrix metalloproteinase (MT1-MMP) to tissue inhibitor of metalloproteinase (TIMP)-2 regulates MT1-MMP processing and pro-MMP-2 activation. J Biol Chem 2000 275:12080-12089.

Hieda Y, Nishizawa Y, Uematsu J, Owaribe K. Identification of a new hemidesmosomal protein, HD1: a major, high molecular mass component of isolated hemidesmosomes. J Cell Biol 1992 116:1497-1506.

Hirohashi S. Inactivation of the E-cadherin-mediated cell adhesion system in human cancers. Am J Pathol 1998 153:333-339.

Hlubek F, Jung A, Kotzor N, Kirchner T, Brabletz T. Expression of the invasion factor laminin gamma2 in colorectal carcinomas is regulated by beta-catenin. Cancer Res 2001 61:8089-8093.

Hood JD, Cheresh DA. Role of integrins in cell invasion and migration. Nat Rev Cancer 2002 2:91-100.

Huang W, Chiquet-Ehrismann R, Moyano JV, Garcia-Pardo A, Orend G. Interference of tenascin-C with syndecan-4 binding to fibronectin blocks cell adhesion and stimulates tumor cell proliferation. Cancer Res 2001 61:8586-8594.

Hynes RO. Integrins: bidirectional, allosteric signaling machines. Cell 2002 110:673-687.

Iivanainen A, Kortesmaa J, Sahlberg C, Morita T, Bergmann U, Thesleff I, Tryggvason K. Primary structure, developmental expression, and immunolocalization of the murine laminin alpha4 chain. J Biol Chem 1997 272:27862-27868.

Iivanainen A, Sainio K, Sariola H, Tryggvason K. Primary structure and expression of a novel human laminin alpha 4 chain. FEBS Lett 1995 365:183-188.

Ikenouchi J, Matsuda M, Furuse M, Tsukita S. Regulation of tight junctions during the epithelium-mesenchyme transition: direct repression of the gene expression of claudins/occludin by Snail. J Cell Sci 2003 116:1959-1967.

Ingber DE. Cancer as a disease of epithelial-mesenchymal interactions and extracellular matrix regulation. Differentiation 2002 70:547-560.

Islam S, Carey TE, Wolf GT, Wheelock MJ, Johnson KR. Expression of N-cadherin by human squamous carcinoma cells induces a scattered fibroblastic phenotype with disrupted cell-cell adhesion. J Cell Biol 1996 135:1643-1654.

Islam S, Kim JB, Trendel J, Wheelock MJ, Johnson KR. Vimentin expression in human squamous carcinoma cells: relationship with phenotypic changes and cadherin-based cell adhesion. J Cell Biochem 2000 78:141-150.

Iwano M, Plieth D, Danoff TM, Xue C, Okada H, Neilson EG. Evidence that fibroblasts derive from epithelium during tissue fibrosis. J Clin Invest 2002 110:341-350.

Jacobsen LB, Calvin SA, Colvin KE, Wright M. FuGENE 6 Transfection Reagent: the gentle power. Methods 2004 33:104-112.

Jahoda CA, Horne KA, Oliver RF. Induction of hair growth by implantation of cultured dermal papilla cells. Nature 1984 311:560-562.

Jamora C, Lee P, Kocieniewski P, Azhar M, Hosokawa R, Chai Y, Fuchs E. A signaling pathway involving TGF-beta2 and snail in hair follicle morphogenesis. PLoS Biol 2005 3:e11.

Janji B, Melchior C, Gouon V, Vallar L, Kieffer N. Autocrine TGF-beta-regulated expression of adhesion receptors and integrin-linked kinase in HT-144 melanoma cells correlates with their metastatic phenotype. Int J Cancer 1999 83:255-262.

Jiang R, Lan Y, Norton CR, Sundberg JP, Gridley T. The Slug gene is not essential for mesoderm or neural crest development in mice. Dev Biol 1998 198:277-285.

Johnson KR, Lewis JE, Li D, Wahl J, Soler AP, Knudsen KA, Wheelock MJ. P- and E-cadherin are in separate complexes in cells expressing both cadherins. Exp Cell Res 1993 207:252-260.

Jones J, Sugiyama M, Watt FM, Speight PM. Integrin expression in normal, hyperplastic, dysplastic, and malignant oral epithelium. J Pathol 1993 169:235-243.

Kalluri R. Basement membranes: structure, assembly and role in tumour angiogenesis. Nat Rev Cancer 2003 3:422-433.

Kalluri R, Neilson EG. Epithelial-mesenchymal transition and its implications for fibrosis. J Clin Invest 2003 112:1776-1784.

Kanazawa T, Watanabe T, Kazama S, Tada T, Koketsu S, Nagawa H. Poorly differentiated adenocarcinoma and mucinous carcinoma of the colon and rectum show higher rates of loss of heterozygosity and loss of E-cadherin expression due to methylation of promoter region. Int J Cancer 2002 102:225-229.

Kanehisa J, Yamanaka T, Doi S, Turksen K, Heersche JN, Aubin JE, Takeuchi H. A band of F-actin containing podosomes is involved in bone resorption by osteoclasts. Bone 1990 11:287-293.

Kannan S, Balaram P, Chandran GJ, Pillai MR, Mathew B, Nalinakumari KR, Nair MK. Alterations in expression of basement membrane proteins during tumour progression in oral mucosa. Histopathology 1994 24:531-537.

Katayama M, Hirai S, Kamihagi K, Nakagawa K, Yasumoto M, Kato I. Soluble E-cadherin fragments increased in circulation of cancer patients. Br J Cancer 1994 69:580-585.

Katayama M, Sanzen N, Funakoshi A, Sekiguchi K. Laminin gamma2-chain fragment in the circulation: a prognostic indicator of epithelial tumor invasion. Cancer Res 2003 63:222-229.

Katayama M, Sekiguchi K. Laminin-5 in epithelial tumour invasion. J Mol Histol 2004 35:277-286.

Katoh K, Nakanishi Y, Akimoto S, Yoshimura K, Takagi M, Sakamoto M, Hirohashi S. Correlation between laminin-5 gamma2 chain expression and epidermal growth factor receptor expression and its clinicopathological significance in squamous cell carcinoma of the tongue. Oncology 2002 62:318-326.

Kelly T, Yan Y, Osborne RL, Athota AB, Rozypal TL, Colclasure JC, Chu WS. Proteolysis of extracellular matrix by invadopodia facilitates human breast cancer cell invasion and is mediated by matrix metalloproteinases. Clin Exp Metastasis 1998 16:501-512.

Khazenzon NM, Ljubimov AV, Lakhter AJ, Fujita M, Fujiwara H, Sekiguchi K, Sorokin LM, Petäjäniemi N, Virtanen I, Black KL, Ljubimova JY. Antisense inhibition of laminin-8 expression reduces invasion of human gliomas in vitro. Mol Cancer Ther 2003 2:985-994.

Khoshnoodi J, Pedchenko V, Hudson BG. Mammalian collagen IV. Microsc Res Tech 2008 71:357-370.

Kikkawa Y, Miner JH. Review: Lutheran/B-CAM: a laminin receptor on red blood cells and in various tissues. Connect Tissue Res 2005 46:193-199.

Kikkawa Y, Moulson CL, Virtanen I, Miner JH. Identification of the binding site for the Lutheran blood group glycoprotein on laminin alpha 5 through expression of chimeric laminin chains in vivo. J Biol Chem 2002 277:44864-44869.

Kikkawa Y, Sanzen N, Fujiwara H, Sonnenberg A, Sekiguchi K. Integrin binding specificity of laminin-10/11: laminin-10/11 are recognized by alpha 3 beta 1, alpha 6 beta 1 and alpha 6 beta 4 integrins. J Cell Sci 2000 113 (Pt 5):869-876.

Kirtschig G, Marinkovich MP, Burgeson RE, Yancey KB. Anti-basement membrane autoantibodies in patients with anti-epiligrin cicatricial pemphigoid bind the alpha subunit of laminin 5. J Invest Dermatol 1995 105:543-548.

Knöll R, Postel R, Wang J, Krätzner R, Hennecke G, Vacaru AM, Vakeel P, Schubert C, Murthy K, Rana BK, Kube D, Knöll G, Schäfer K, Hayashi T, Holm T, Kimura A, Schork N, Toliat MR, Nürnberg P, Schultheiss HP, Schaper W, Schaper J, Bos E, Den Hertog J, van Eeden FJ, Peters PJ, Hasenfuss G, Chien KR, Bakkers J. Laminin-alpha4 and integrin-linked kinase mutations cause human cardiomyopathy via simultaneous defects in cardiomyocytes and endothelial cells. Circulation 2007 116:515-525.

Kortesmaa J, Doi M, Patarroyo M, Tryggvason K. Chondroitin sulphate modification in the alpha4 chain of human recombinant laminin-8 (alpha4beta1gamma1). Matrix Biol 2002 21:483-486.

Kortesmaa J, Yurchenco P, Tryggvason K. Recombinant laminin-8 (alpha(4)beta(1)gamma(1)). Production, purification,and interactions with integrins. J Biol Chem 2000 275:14853-14859.

Koshikawa N, Moriyama K, Takamura H, Mizushima H, Nagashima Y, Yanoma S, Miyazaki K. Overexpression of laminin gamma2 chain monomer in invading gastric carcinoma cells. Cancer Res 1999 59:5596-5601.

Kosmehl H, Berndt A, Strassburger S, Borsi L, Rousselle P, Mandel U, Hyckel P, Zardi L, Katenkamp D. Distribution of laminin and fibronectin isoforms in oral mucosa and oral squamous cell carcinoma. Br J Cancer 1999 81:1071-1079.

Krafchak CM, Pawar H, Moroi SE, Sugar A, Lichter PR, Mackey DA, Mian S, Nairus T, Elner V, Schteingart MT, Downs CA, Kijek TG, Johnson JM, Trager EH, Rozsa FW, Mandal MN, Epstein MP, Vollrath D, Ayyagari R, Boehnke M, Richards JE. Mutations in TCF8 cause posterior polymorphous corneal dystrophy and ectopic expression of COL4A3 by corneal endothelial cells. Am J Hum Genet 2005 77:694-708.

Kramer RH, Shen X, Zhou H. Tumor cell invasion and survival in head and neck cancer. Cancer Metastasis Rev 2005 24:35-45.

Kurrey NK, K A, Bapat SA. Snail and Slug are major determinants of ovarian cancer invasiveness at the transcription level. Gynecol Oncol 2005 97:155-165.

Köhler G, Milstein C. Continuous cultures of fused cells secreting antibody of predefined specificity. Nature 1975 256:495-497.

Lakkakorpi PT, Väänänen HK. Kinetics of the osteoclast cytoskeleton during the resorption cycle in vitro. J Bone Miner Res 1991 6:817-826.

Larue L, Ohsugi M, Hirchenhain J, Kemler R. E-cadherin null mutant embryos fail to form a trophectoderm epithelium. Proc Natl Acad Sci U S A 1994 91:8263-8267.

Lauffenburger DA, Horwitz AF. Cell migration: a physically integrated molecular process. Cell 1996 84:359-369.

Le Clainche C, Carlier MF. Regulation of actin assembly associated with protrusion and adhesion in cell migration. Physiol Rev 2008 88:489-513.

Lefebvre O, Sorokin L, Kedinger M, Simon-Assmann P. Developmental expression and cellular origin of the laminin alpha2, alpha4, and alpha5 chains in the intestine. Dev Biol 1999 210:135-150.

Legate KR, Fässler R. Mechanisms that regulate adaptor binding to beta-integrin cytoplasmic tails. J Cell Sci 2009 122:187-198.

Lehto VP, Hovi T, Vartio T, Badley RA, Virtanen I. Reorganization of cytoskeletal and contractile elements during transition of human monocytes into adherent macrophages. Lab Invest 1982 47:391-399.

Leivo I, Engvall E. Merosin, a protein specific for basement membranes of Schwann cells, striated muscle, and trophoblast, is expressed late in nerve and muscle development. Proc Natl Acad Sci U S A 1988 85:1544-1548.

Li F, Zhang Y, Wu C. Integrin-linked kinase is localized to cell-matrix focal adhesions but not cell-cell adhesion sites and the focal adhesion localization of integrin-linked kinase is regulated by the PINCH-binding ANK repeats. J Cell Sci 1999 112 (Pt 24):4589-4599.

Li J, Tzu J, Chen Y, Zhang YP, Nguyen NT, Gao J, Bradley M, Keene DR, Oro AE, Miner JH, Marinkovich MP. Laminin-10 is crucial for hair morphogenesis. EMBO J 2003 22:2400-2410.

Li S, Harrison D, Carbonetto S, Fässler R, Smyth N, Edgar D, Yurchenco PD. Matrix assembly, regulation, and survival functions of laminin and its receptors in embryonic stem cell differentiation. J Cell Biol 2002 157:1279-1290.

Libby RT, Champliaud MF, Claudepierre T, Xu Y, Gibbons EP, Koch M, Burgeson RE, Hunter DD, Brunken WJ. Laminin expression in adult and developing retinae: evidence of two novel CNS laminins. J Neurosci 2000 20:6517-6528.

Liebert M, Washington R, Stein J, Wedemeyer G, Grossman HB. Expression of the VLA beta 1 integrin family in bladder cancer. Am J Pathol 1994 144:1016-1022.

Lim SC, Zhang S, Ishii G, Endoh Y, Kodama K, Miyamoto S, Hayashi R, Ebihara S, Cho JS, Ochiai A. Predictive markers for late cervical metastasis in stage I and II invasive squamous cell carcinoma of the oral tongue. Clin Cancer Res 2004 10:166-172.

Linder S. The matrix corroded: podosomes and invadopodia in extracellular matrix degradation. Trends Cell Biol 2007 17:107-117.

Linder S, Aepfelbacher M. Podosomes: adhesion hot-spots of invasive cells. Trends Cell Biol 2003 13:376-385.

Linder S, Higgs H, Hüfner K, Schwarz K, Pannicke U, Aepfelbacher M. The polarization defect of Wiskott-Aldrich syndrome macrophages is linked to dislocalization of the Arp2/3 complex. J Immunol 2000a 165:221-225.

Linder S, Hüfner K, Wintergerst U, Aepfelbacher M. Microtubule-dependent formation of podosomal adhesion structures in primary human macrophages. J Cell Sci 2000b 113 Pt 23:4165-4176.

Linder S, Nelson D, Weiss M, Aepfelbacher M. Wiskott-Aldrich syndrome protein regulates podosomes in primary human macrophages. Proc Natl Acad Sci U S A 1999 96:9648-9653.

Liotta LA. Tumor invasion and metastases: role of the basement membrane. Warner-Lambert Parke-Davis Award lecture. Am J Pathol 1984 117:339-348.

Liotta LA, Kohn EC. The microenvironment of the tumour-host interface. Nature 2001 411:375-379.

Litjens SH, de Pereda JM, Sonnenberg A. Current insights into the formation and breakdown of hemidesmosomes. Trends Cell Biol 2006 16:376-383.

Ljubimova JY, Fugita M, Khazenzon NM, Das A, Pikul BB, Newman D, Sekiguchi K, Sorokin LM, Sasaki T, Black KL. Association between laminin-8 and glial tumor grade, recurrence, and patient survival. Cancer 2004 101:604-612.

Ljubimova JY, Lakhter AJ, Loksh A, Yong WH, Riedinger MS, Miner JH, Sorokin LM, Ljubimov AV, Black KL. Overexpression of alpha4 chain-containing laminins in human glial tumors identified by gene microarray analysis. Cancer Res 2001 61:5601-5610.

Locascio A, Vega S, de Frutos CA, Manzanares M, Nieto MA. Biological potential of a functional human SNAIL retrogene. J Biol Chem 2002 277:38803-38809.

Lohi J, Oivula J, Kivilaakso E, Kiviluoto T, Fröjdman K, Yamada Y, Burgeson RE, Leivo I, Virtanen I. Basement membrane laminin-5 is deposited in colorectal adenomas and carcinomas and serves as a ligand for alpha3beta1 integrin. APMIS 2000 108:161-172.

Lohi J, Tani T, Leivo I, Linnala A, Kangas L, Burgeson RE, Lehto VP, Virtanen I. Expression of laminin in renal-cell carcinomas, renal-cell carcinoma cell lines and xenografts in nude mice. Int J Cancer 1996 68:364-371.

Maeda G, Chiba T, Okazaki M, Satoh T, Taya Y, Aoba T, Kato K, Kawashiri S, Imai K. Expression of SIP1 in oral squamous cell carcinomas: implications for E-cadherin expression and tumor progression. Int J Oncol 2005a 27:1535-1541.

Maeda M, Johnson KR, Wheelock MJ. Cadherin switching: essential for behavioral but not morphological changes during an epithelium-to-mesenchyme transition. J Cell Sci 2005b 118:873-887.

Marchisio PC, Bergui L, Corbascio GC, Cremona O, D'Urso N, Schena M, Tesio L, Caligaris-Cappio F. Vinculin, talin, and integrins are localized at specific adhesion sites of malignant B lymphocytes. Blood 1988 72:830-833.

Marchisio PC, Cirillo D, Naldini L, Primavera MV, Teti A, Zambonin-Zallone A. Cell-substratum interaction of cultured avian osteoclasts is mediated by specific adhesion structures. J Cell Biol 1984 99:1696-1705.

Marinkovich MP, Lunstrum GP, Burgeson RE. The anchoring filament protein kalinin is synthesized and secreted as a high molecular weight precursor. J Biol Chem 1992 267:17900-17906.

Martin KJ, Kwan CP, Nagasaki K, Zhang X, O'Hare MJ, Kaelin CM, Burgeson RE, Pardee AB, Sager R. Down-regulation of laminin-5 in breast carcinoma cells. Mol Med 1998 4:602-613.

Martin P. Wound healing--aiming for perfect skin regeneration. Science 1997 276:75-81.

Maschler S, Wirl G, Spring H, Bredow DV, Sordat I, Beug H, Reichmann E. Tumor cell invasiveness correlates with changes in integrin expression and localization. Oncogene 2005 24:2032-2041.

Matsui C, Nelson CF, Hernandez GT, Herron GS, Bauer EA, Hoeffler WK. Gamma 2 chain of laminin-5 is recognized by monoclonal antibody GB3. J Invest Dermatol 1995a 105:648-652.

Matsui C, Wang CK, Nelson CF, Bauer EA, Hoeffler WK. The assembly of laminin-5 subunits. J Biol Chem 1995b 270:23496-23503.

Mauhin V, Lutz Y, Dennefeld C, Alberga A. Definition of the DNA-binding site repertoire for the Drosophila transcription factor SNAIL. Nucleic Acids Res 1993 21:3951-3957.

McCleverty CJ, Lin DC, Liddington RC. Structure of the PTB domain of tensin1 and a model for its recruitment to fibrillar adhesions. Protein Sci 2007 16:1223-1229.

McLean WH, Irvine AD, Hamill KJ, Whittock NV, Coleman-Campbell CM, Mellerio JE, Ashton GS, Dopping-Hepenstal PJ, Eady RA, Jamil T, Phillips RJ, Shabbir SG, Haroon TS, Khurshid K, Moore JE, Page B, Darling J, Atherton DJ, Van Steensel MA, Munro CS, Smith FJ, McGrath JA. An unusual N-terminal deletion of the laminin alpha3a isoform leads to the chronic granulation tissue disorder laryngo-onycho-cutaneous syndrome. Hum Mol Genet 2003 12:2395-2409.

Mehrotra R, Yadav S. Oral squamous cell carcinoma: etiology, pathogenesis and prognostic value of genomic alterations. Indian J Cancer 2006 43:60-66.

Meng X, Klement JF, Leperi DA, Birk DE, Sasaki T, Timpl R, Uitto J, Pulkkinen L. Targeted inactivation of murine laminin gamma2-chain gene recapitulates human junctional epidermolysis bullosa. J Invest Dermatol 2003 121:720-731.

Merker HJ. Morphology of the basement membrane. Microsc Res Tech 1994 28:95-124.

Miettinen M, Castello R, Wayner E, Schwarting R. Distribution of VLA integrins in solid tumors. Emergence of tumor-type-related expression. Patterns in carcinomas and sarcomas. Am J Pathol 1993 142:1009-1018.

Miner JH, Cunningham J, Sanes JR. Roles for laminin in embryogenesis: exencephaly, syndactyly, and placentopathy in mice lacking the laminin alpha5 chain. J Cell Biol 1998 143:1713-1723.

Miner JH, Lewis RM, Sanes JR. Molecular cloning of a novel laminin chain, alpha 5, and widespread expression in adult mouse tissues. J Biol Chem 1995 270:28523-28526.

Miner JH, Li C. Defective glomerulogenesis in the absence of laminin alpha5 demonstrates a developmental role for the kidney glomerular basement membrane. Dev Biol 2000 217:278-289.

Miner JH, Patton BL. Laminin-11. Int J Biochem Cell Biol 1999 31:811-816.

Miner JH, Patton BL, Lentz SI, Gilbert DJ, Snider WD, Jenkins NA, Copeland NG, Sanes JR. The laminin alpha chains: expression, developmental transitions, and chromosomal locations of alpha1-5, identification of heterotrimeric laminins 8-11, and cloning of a novel alpha3 isoform. J Cell Biol 1997 137:685-701.

Miner JH, Yurchenco PD. Laminin functions in tissue morphogenesis. Annu Rev Cell Dev Biol 2004 20:255-284.

Miyazaki K. Laminin-5 (laminin-332): Unique biological activity and role in tumor growth and invasion. Cancer Sci 2006 97:91-98.

Miyazaki K, Kikkawa Y, Nakamura A, Yasumitsu H, Umeda M. A large cell-adhesive scatter factor secreted by human gastric carcinoma cells. Proc Natl Acad Sci U S A 1993 90:11767-11771.

Mizushima H, Koshikawa N, Moriyama K, Takamura H, Nagashima Y, Hirahara F, Miyazaki K. Wide distribution of laminin-5 gamma 2 chain in basement membranes of various human tissues. Horm Res 1998 50 Suppl 2:7-14.

Mizutani K, Miki H, He H, Maruta H, Takenawa T. Essential role of neural Wiskott-Aldrich syndrome protein in podosome formation and degradation of extracellular matrix in src-transformed fibroblasts. Cancer Res 2002 62:669-674.

Modregger J, Ritter B, Witter B, Paulsson M, Plomann M. All three PACSIN isoforms bind to endocytic proteins and inhibit endocytosis. J Cell Sci 2000 113 Pt 24:4511-4521.

Moinfar F, Man YG, Arnould L, Bratthauer GL, Ratschek M, Tavassoli FA. Concurrent and independent genetic alterations in the stromal and epithelial cells of mammary carcinoma: implications for tumorigenesis. Cancer Res 2000 60:2562-2566.

Monsky WL, Lin CY, Aoyama A, Kelly T, Akiyama SK, Mueller SC, Chen WT. A potential marker protease of invasiveness, seprase, is localized on invadopodia of human malignant melanoma cells. Cancer Res 1994 54:5702-5710.

Moody SE, Perez D, Pan TC, Sarkisian CJ, Portocarrero CP, Sterner CJ, Notorfrancesco KL, Cardiff RD, Chodosh LA. The transcriptional repressor Snail promotes mammary tumor recurrence. Cancer Cell 2005 8:197-209.

Moreau V, Tatin F, Varon C, Anies G, Savona-Baron C, Génot E. Cdc42-driven podosome formation in endothelial cells. Eur J Cell Biol 2006 85:319-325.

Moreau V, Tatin F, Varon C, Génot E. Actin can reorganize into podosomes in aortic endothelial cells, a process controlled by Cdc42 and RhoA. Mol Cell Biol 2003 23:6809-6822.

Mould AP, Humphries MJ. Regulation of integrin function through conformational complexity: not simply a knee-jerk reaction? Curr Opin Cell Biol 2004 16:544-551.

Moulson CL, Li C, Miner JH. Localization of Lutheran, a novel laminin receptor, in normal, knockout, and transgenic mice suggests an interaction with laminin alpha5 in vivo. Dev Dyn 2001 222:101-114.

Mueller SC, Ghersi G, Akiyama SK, Sang QX, Howard L, Pineiro-Sanchez M, Nakahara H, Yeh Y, Chen WT. A novel protease-docking function of integrin at invadopodia. J Biol Chem 1999 274:24947-24952.

Mulrooney J, Foley K, Vineberg S, Barreuther M, Grabel L. Phosphorylation of the beta1 integrin cytoplasmic domain: toward an understanding of function and mechanism. Exp Cell Res 2000 258:332-341.

Murphy-Ullrich JE. The de-adhesive activity of matricellular proteins: is intermediate cell adhesion an adaptive state? J Clin Invest 2001 107:785-790.

Mühle C, Neuner A, Park J, Pacho F, Jiang Q, Waddington SN, Schneider H. Evaluation of prenatal intra-amniotic LAMB3 gene delivery in a mouse model of Herlitz disease. Gene Ther 2006 13:1665-1676.

Myllyharju J, Kivirikko KI. Collagens, modifying enzymes and their mutations in humans, flies and worms. Trends Genet 2004 20:33-43.

Määttä M, Bützow R, Luostarinen J, Petäjäniemi N, Pihlajaniemi T, Salo S, Miyazaki K, Autio-Harmainen H, Virtanen I. Differential expression of laminin isoforms in ovarian epithelial carcinomas suggesting different origin and providing tools for differential diagnosis. J Histochem Cytochem 2005 53:1293-1300.

Määttä M, Virtanen I, Burgeson R, Autio-Harmainen H. Comparative analysis of the distribution of laminin chains in the basement membranes in some malignant epithelial tumors: the alpha1 chain of laminin shows a selected expression pattern in human carcinomas. J Histochem Cytochem 2001 49:711-726.

Nagle RB, Böcker W, Davis JR, Heid HW, Kaufmann M, Lucas DO, Jarasch ED. Characterization of breast carcinomas by two monoclonal antibodies distinguishing myoepithelial from luminal epithelial cells. J Histochem Cytochem 1986 34:869-881.

Nakahara H, Howard L, Thompson EW, Sato H, Seiki M, Yeh Y, Chen WT. Transmembrane/cytoplasmic domain-mediated membrane type 1-matrix metalloprotease docking to invadopodia is required for cell invasion. Proc Natl Acad Sci U S A 1997 94:7959-7964.

Nakamura F, Pudas R, Heikkinen O, Permi P, Kilpeläinen I, Munday AD, Hartwig JH, Stossel TP, Ylänne J. The structure of the GPIb-filamin A complex. Blood 2006 107:1925-1932.

Newby AC, Zaltsman AB. Molecular mechanisms in intimal hyperplasia. J Pathol 2000 190:300-309.

Nieman MT, Prudoff RS, Johnson KR, Wheelock MJ. N-cadherin promotes motility in human breast cancer cells regardless of their E-cadherin expression. J Cell Biol 1999 147:631-644.

Niessen CM, Hulsman EH, Rots ES, Sánchez-Aparicio P, Sonnenberg A. Integrin alpha 6 beta 4 forms a complex with the cytoskeletal protein HD1 and induces its redistribution in transfected COS-7 cells. Mol Biol Cell 1997 8:555-566.

Nieto MA. The snail superfamily of zinc-finger transcription factors. Nat Rev Mol Cell Biol 2002 3:155-166.

Nieto MA, Bennett MF, Sargent MG, Wilkinson DG. Cloning and developmental expression of Sna, a murine homologue of the Drosophila snail gene. Development 1992 116:227-237.

Nieto MA, Sargent MG, Wilkinson DG, Cooke J. Control of cell behavior during vertebrate development by Slug, a zinc finger gene. Science 1994 264:835-839.

Nievers MG, Schaapveld RQ, Sonnenberg A. Biology and function of hemidesmosomes. Matrix Biol 1999 18:5-17.

Niimi T, Kumagai C, Okano M, Kitagawa Y. Differentiation-dependent expression of laminin-8 (alpha 4 beta 1 gamma 1) mRNAs in mouse 3T3-L1 adipocytes. Matrix Biol 1997 16:223-230.

Nikki M, Meriläinen J, Lehto VP. FAP52 regulates actin organization via binding to filamin. J Biol Chem 2002 277:11432-11440.

Novak A, Hsu SC, Leung-Hagesteijn C, Radeva G, Papkoff J, Montesano R, Roskelley C, Grosschedl R, Dedhar S. Cell adhesion and the integrin-linked kinase regulate the LEF-1 and beta-catenin signaling pathways. Proc Natl Acad Sci U S A 1998 95:4374-4379.

Ochoa GC, Slepnev VI, Neff L, Ringstad N, Takei K, Daniell L, Kim W, Cao H, McNiven M, Baron R, De Camilli P. A functional link between dynamin and the actin cytoskeleton at podosomes. J Cell Biol 2000 150:377-389.

Ohkubo T, Ozawa M. The transcription factor Snail downregulates the tight junction components independently of E-cadherin downregulation. J Cell Sci 2004 117:1675-1685.

Oloumi A, McPhee T, Dedhar S. Regulation of E-cadherin expression and beta-catenin/Tcf transcriptional activity by the integrin-linked kinase. Biochim Biophys Acta 2004 1691:1-15.

Olumi AF, Grossfeld GD, Hayward SW, Carroll PR, Tlsty TD, Cunha GR. Carcinoma-associated fibroblasts direct tumor progression of initiated human prostatic epithelium. Cancer Res 1999 59:5002-5011.

Ono Y, Nakanishi Y, Ino Y, Niki T, Yamada T, Yoshimura K, Saikawa M, Nakajima T, Hirohashi S. Clinocopathologic significance of laminin-5 gamma2 chain expression in squamous cell carcinoma of the tongue: immunohistochemical analysis of 67 lesions. Cancer 1999 85:2315-2321.

Orian-Rousseau V, Aberdam D, Rousselle P, Messent A, Gavrilovic J, Meneguzzi G, Kedinger M, Simon-Assmann P. Human colonic cancer cells synthesize and adhere to laminin-5. Their adhesion to laminin-5 involves multiple receptors among which is integrin alpha2beta1. J Cell Sci 1998 111 (Pt 14):1993-2004.

Orimo A, Gupta PB, Sgroi DC, Arenzana-Seisdedos F, Delaunay T, Naeem R, Carey VJ, Richardson AL, Weinberg RA. Stromal fibroblasts present in invasive human breast carcinomas promote tumor growth and angiogenesis through elevated SDF-1/CXCL12 secretion. Cell 2005 121:335-348.

Otey CA, Carpén O. Alpha-actinin revisited: a fresh look at an old player. Cell Motil Cytoskeleton 2004 58:104-111.

Owaribe K, Nishizawa Y, Franke WW. Isolation and characterization of hemidesmosomes from bovine corneal epithelial cells. Exp Cell Res 1991 192:622-630.

Pakkala T, Virtanen I, Oksanen J, Jones JC, Hormia M. Function of laminins and laminin-binding integrins in gingival epithelial cell adhesion. J Periodontol 2002 73:709-719.

Palazzo AF, Gundersen GG. Microtubule-actin cross-talk at focal adhesions. Sci STKE 2002 2002:PE31.

Pálmer HG, Larriba MJ, García JM, Ordóñez-Morán P, Peña C, Peiró S, Puig I, Rodríguez R, de la Fuente R, Bernad A, Pollán M, Bonilla F, Gamallo C, de Herreros AG, Muñoz A. The transcription factor SNAIL represses vitamin D receptor expression and responsiveness in human colon cancer. Nat Med 2004 10:917-919.

Panetti TS, McKeown-Longo PJ. The alpha v beta 5 integrin receptor regulates receptor-mediated endocytosis of vitronectin. J Biol Chem 1993 268:11492-11495.

Parkin DM, Bray F, Ferlay J, Pisani P. Global cancer statistics, 2002. CA Cancer J Clin 2005 55:74-108.

Parsons SF, Lee G, Spring FA, Willig TN, Peters LL, Gimm JA, Tanner MJ, Mohandas N, Anstee DJ, Chasis JA. Lutheran blood group glycoprotein and its newly characterized mouse homologue specifically bind alpha5 chain-containing human laminin with high affinity. Blood 2001 97:312-320.

Parsons SF, Mallinson G, Daniels GL, Green CA, Smythe JS, Anstee DJ. Use of domain-deletion mutants to locate Lutheran blood group antigens to each of the five immunoglobulin superfamily domains of the Lutheran glycoprotein: elucidation of the molecular basis of the Lu(a)/Lu(b) and the Au(a)/Au(b) polymorphisms. Blood 1997 89:4219-4225.

Parsons SF, Mallinson G, Holmes CH, Houlihan JM, Simpson KL, Mawby WJ, Spurr NK, Warne D, Barclay AN, Anstee DJ. The Lutheran blood group glycoprotein, another member of the immunoglobulin superfamily, is widely

expressed in human tissues and is developmentally regulated in human liver. Proc Natl Acad Sci U S A 1995 92:5496-5500.

Pasqualini R, Bodorova J, Ye S, Hemler ME. A study of the structure, function and distribution of beta 5 integrins using novel anti-beta 5 monoclonal antibodies. J Cell Sci 1993 105 (Pt 1):101-111.

Patarroyo M, Tryggvason K, Virtanen I. Laminin isoforms in tumor invasion, angiogenesis and metastasis. Semin Cancer Biol 2002 12:197-207.

Patton BL, Cunningham JM, Thyboll J, Kortesmaa J, Westerblad H, Edström L, Tryggvason K, Sanes JR. Properly formed but improperly localized synaptic specializations in the absence of laminin alpha4. Nat Neurosci 2001 4:597-604.

Pedraza C, Geberhiwot T, Ingerpuu S, Assefa D, Wondimu Z, Kortesmaa J, Tryggvason K, Virtanen I, Patarroyo M. Monocytic cells synthesize, adhere to, and migrate on laminin-8 (alpha 4 beta 1 gamma 1). J Immunol 2000 165:5831-5838.

Peinado H, Olmeda D, Cano A. Snail, Zeb and bHLH factors in tumour progression: an alliance against the epithelial phenotype? Nat Rev Cancer 2007 7:415-428.

Peiró S, Escrivà M, Puig I, Barberà MJ, Dave N, Herranz N, Larriba MJ, Takkunen M, Francí C, Muñoz A, Virtanen I, Baulida J, García de Herreros A. Snail1 transcriptional repressor binds to its own promoter and controls its expression. Nucleic Acids Res 2006 34:2077-2084.

Peña C, García JM, Silva J, García V, Rodríguez R, Alonso I, Millán I, Salas C, de Herreros AG, Muñoz A, Bonilla F. E-cadherin and vitamin D receptor regulation by SNAIL and ZEB1 in colon cancer: clinicopathological correlations. Hum Mol Genet 2005 14:3361-3370.

Pérez-Pomares JM, Muñoz-Chápuli R. Epithelial-mesenchymal transitions: a mesodermal cell strategy for evolutive innovation in Metazoans. Anat Rec 2002 268:343-351.

Perl AK, Wilgenbus P, Dahl U, Semb H, Christofori G. A causal role for E-cadherin in the transition from adenoma to carcinoma. Nature 1998 392:190-193.

Petersen OW, Nielsen HL, Gudjonsson T, Villadsen R, Rank F, Niebuhr E, Bissell MJ, Rønnov-Jessen L. Epithelial to mesenchymal transition in human breast cancer can provide a nonmalignant stroma. Am J Pathol 2003 162:391-402.

Petäjäniemi N, Korhonen M, Kortesmaa J, Tryggvason K, Sekiguchi K, Fujiwara H, Sorokin L, Thornell LE, Wondimu Z, Assefa D, Patarroyo M, Virtanen I. Localization of laminin alpha4-chain in developing and adult human tissues. J Histochem Cytochem 2002 50:1113-1130.

Pfaff M, Jurdic P. Podosomes in osteoclast-like cells: structural analysis and cooperative roles of paxillin, proline-rich tyrosine kinase 2 (Pyk2) and integrin alphaVbeta3. J Cell Sci 2001 114:2775-2786.

Pitiyage G, Tilakaratne WM, Tavassoli M, Warnakulasuriya S. Molecular markers in oral epithelial dysplasia: review. J Oral Pathol Med 2009 38:737-752.

Pollard TD, Blanchoin L, Mullins RD. Molecular mechanisms controlling actin filament dynamics in nonmuscle cells. Annu Rev Biophys Biomol Struct 2000 29:545-576.

Pollard TD, Borisy GG. Cellular motility driven by assembly and disassembly of actin filaments. Cell 2003 112:453-465.

Postigo AA. Opposing functions of ZEB proteins in the regulation of the TGFbeta/BMP signaling pathway. EMBO J 2003 22:2443-2452.

Postigo AA, Dean DC. ZEB, a vertebrate homolog of Drosophila Zfh-1, is a negative regulator of muscle differentiation. EMBO J 1997 16:3935-3943.

Postigo AA, Dean DC. Differential expression and function of members of the zfh-1 family of zinc finger/homeodomain repressors. Proc Natl Acad Sci U S A 2000 97:6391-6396.

Postigo AA, Sheppard AM, Mucenski ML, Dean DC. c-Myb and Ets proteins synergize to overcome transcriptional repression by ZEB. EMBO J 1997 16:3924-3934.

Pouliot N, Connolly LM, Moritz RL, Simpson RJ, Burgess AW. Colon cancer cells adhesion and spreading on autocrine laminin-10 is mediated by multiple integrin receptors and modulated by EGF receptor stimulation. Exp Cell Res 2000 261:360-371.

Pouliot N, Nice EC, Burgess AW. Laminin-10 mediates basal and EGF-stimulated motility of human colon carcinoma cells via alpha(3)beta(1) and alpha(6)beta(4) integrins. Exp Cell Res 2001 266:1-10.

Prater CA, Plotkin J, Jaye D, Frazier WA. The properdin-like type I repeats of human thrombospondin contain a cell attachment site. J Cell Biol 1991 112:1031-1040.

Pulkkinen L, Uitto J. Mutation analysis and molecular genetics of epidermolysis bullosa. Matrix Biol 1999 18:29-42.

Pytela R, Pierschbacher MD, Ruoslahti E. A 125/115-kDa cell surface receptor specific for vitronectin interacts with the arginine-glycine-aspartic acid adhesion sequence derived from fibronectin. Proc Natl Acad Sci U S A 1985a 82:5766-5770.

Pytela R, Pierschbacher MD, Ruoslahti E. Identification and isolation of a 140 kd cell surface glycoprotein with properties expected of a fibronectin receptor. Cell 1985b 40:191-198.

Qualmann B, Kelly RB. Syndapin isoforms participate in receptor-mediated endocytosis and actin organization. J Cell Biol 2000 148:1047-1062.

Rabut G, Ellenberg J. Photobleaching techniques to study mobility and molecular dynamics of proteins in live cells: FRAP, iFRAP, and FLIP. In: Live cell imaging: A laboratory manual. Cold Spring Harbor Laboratory Press, New York, 2005:101-126.

Rahuel C, Le Van Kim C, Mattei MG, Cartron JP, Colin Y. A unique gene encodes spliceoforms of the B-cell adhesion molecule cell surface glycoprotein of epithelial cancer and of the Lutheran blood group glycoprotein. Blood 1996 88:1865-1872.

Raines EW. The extracellular matrix can regulate vascular cell migration, proliferation, and survival: relationships to vascular disease. Int J Exp Pathol 2000 81:173-182.

Ramirez F. Pathophysiology of the microfibril/elastic fiber system: introduction. Matrix Biol 2000 19:455-456.

Rebustini IT, Patel VN, Stewart JS, Layvey A, Georges-Labouesse E, Miner JH, Hoffman MP. Laminin alpha5 is necessary for submandibular gland epithelial morphogenesis and influences FGFR expression through beta1 integrin signaling. Dev Biol 2007 308:15-29.

Richards A, Al-Imara L, Pope FM. The complete cDNA sequence of laminin alpha 4 and its relationship to the other human laminin alpha chains. Eur J Biochem 1996 238:813-821.

Richards A, Luccarini C, Pope FM. The structural organisation of LAMA4, the gene encoding laminin alpha4. Eur J Biochem 1997 248:15-23.

Richards AJ, al-Imara L, Carter NP, Lloyd JC, Leversha MA, Pope FM. Localization of the gene (LAMA4) to chromosome 6q21 and isolation of a partial cDNA encoding a variant laminin A chain. Genomics 1994 22:237-239.

Ridley AJ, Schwartz MA, Burridge K, Firtel RA, Ginsberg MH, Borisy G, Parsons JT, Horwitz AR. Cell migration: integrating signals from front to back. Science 2003 302:1704-1709.

Riethmacher D, Brinkmann V, Birchmeier C. A targeted mutation in the mouse E-cadherin gene results in defective preimplantation development. Proc Natl Acad Sci U S A 1995 92:855-859.

Riou P, Saffroy R, Chenailler C, Franc B, Gentile C, Rubinstein E, Resink T, Debuire B, Piatier-Tonneau D, Lemoine A. Expression of T-cadherin in tumor cells influences invasive potential of human hepatocellular carcinoma. FASEB J 2006 20:2291-2301.

Robert G, Gaggioli C, Bailet O, Chavey C, Abbe P, Aberdam E, Sabatie E, Cano A, García de Herreros A, Ballotti R, Tartare-Deckert S. SPARC represses E-cadherin and induces mesenchymal transition during melanoma development. Cancer Res 2006 66:7516-7523.

Rosivatz E, Becker I, Bamba M, Schott C, Diebold J, Mayr D, Höfler H, Becker KF. Neoexpression of N-cadherin in E-cadherin positive colon cancers. Int J Cancer 2004 111:711-719.

Rosivatz E, Becker I, Specht K, Fricke E, Luber B, Busch R, Höfler H, Becker KF. Differential expression of the epithelial-mesenchymal transition regulators snail, SIP1, and twist in gastric cancer. Am J Pathol 2002 161:1881-1891.

Rosivatz E, Becker KF, Kremmer E, Schott C, Blechschmidt K, Höfler H, Sarbia M. Expression and nuclear localization of Snail, an E-cadherin repressor, in adenocarcinomas of the upper gastrointestinal tract. Virchows Arch 2006 448:277-287.

Rousselle P, Aumailley M. Kalinin is more efficient than laminin in promoting adhesion of primary keratinocytes and some other epithelial cells and has a different requirement for integrin receptors. J Cell Biol 1994 125:205-214.

Rousselle P, Lunstrum GP, Keene DR, Burgeson RE. Kalinin: an epithelium-specific basement membrane adhesion molecule that is a component of anchoring filaments. J Cell Biol 1991 114:567-576.

Rozen S, Skaletsky H. Primer3 on the WWW for general users and for biologist programmers. Methods Mol Biol 2000 132:365-386.

Ruoslahti E, Giancotti FG. Integrins and tumor cell dissemination. Cancer Cells 1989 1:119-126.

Ryan MC, Tizard R, VanDevanter DR, Carter WG. Cloning of the LamA3 gene encoding the alpha 3 chain of the adhesive ligand epiligrin. Expression in wound repair. J Biol Chem 1994 269:22779-22787.

Röper K, Gregory SL, Brown NH. The 'spectraplakins': cytoskeletal giants with characteristics of both spectrin and plakin families. J Cell Sci 2002 115:4215-4225.

Salmivirta K, Gullberg D, Hirsch E, Altruda F, Ekblom P. Integrin subunit expression associated with epithelial-mesenchymal interactions during murine tooth development. Dev Dyn 1996 205:104-113.

Sambrook J, Russell DW. Analysis of gene expression in cultured mammalian cells. In: Molecular Cloning: A Laboratory Manual. Cold Spring Harbor Laboratory Press, New York, 2001:17.4-17.9.

Sánchez-Martín M, Pérez-Losada J, Rodríguez-García A, González-Sánchez B, Korf BR, Kuster W, Moss C, Spritz RA, Sánchez-Garcia I. Deletion of the SLUG (SNAI2) gene results in human piebaldism. Am J Med Genet A 2003 122A:125-132.

Sánchez-Martín M, Rodríguez-García A, Pérez-Losada J, Sagrera A, Read AP, Sánchez-Garcia I. SLUG (SNAI2) deletions in patients with Waardenburg disease. Hum Mol Genet 2002 11:3231-3236.

Sasaki T, Mann K, Timpl R. Modification of the laminin alpha 4 chain by chondroitin sulfate attachment to its N-terminal domain. FEBS Lett 2001 505:173-178.

Sasaki T, Timpl R. Domain IVa of laminin alpha5 chain is cell-adhesive and binds beta1 and alphaVbeta3 integrins through Arg-Gly-Asp. FEBS Lett 2001 509:181-185.

Sato T, del Carmen Ovejero M, Hou P, Heegaard AM, Kumegawa M, Foged NT, Delaissé JM. Identification of the membrane-type matrix metalloproteinase MT1-MMP in osteoclasts. J Cell Sci 1997 110 (Pt 5):589-596.

Savagner P. Leaving the neighborhood: molecular mechanisms involved during epithelial-mesenchymal transition. Bioessays 2001 23:912-923.

Savagner P, Kusewitt DF, Carver EA, Magnino F, Choi C, Gridley T, Hudson LG. Developmental transcription factor slug is required for effective re-epithelialization by adult keratinocytes. J Cell Physiol 2005 202:858-866.

Schipper JH, Frixen UH, Behrens J, Unger A, Jahnke K, Birchmeier W. E-cadherin expression in squamous cell carcinomas of head and neck: inverse correlation with tumor dedifferentiation and lymph node metastasis. Cancer Res 1991 51:6328-6337.

Schuuring E, Verhoeven E, Litvinov S, Michalides RJ. The product of the EMS1 gene, amplified and overexpressed in human carcinomas, is homologous to a v-src substrate and is located in cell-substratum contact sites. Mol Cell Biol 1993 13:2891-2898.

Schön M, Klein CE, Hogenkamp V, Kaufmann R, Wienrich BG, Schön MP. Basal-cell adhesion molecule (B-CAM) is induced in epithelial skin tumors and inflammatory epidermis, and is expressed at cell-cell and cell-substrate contact sites. J Invest Dermatol 2000 115:1047-1053.

Sefton M, Sánchez S, Nieto MA. Conserved and divergent roles for members of the Snail family of transcription factors in the chick and mouse embryo. Development 1998 125:3111-3121.

Semb H, Christofori G. The tumor-suppressor function of E-cadherin. Am J Hum Genet 1998 63:1588-1593.

Shekhar MP, Werdell J, Santner SJ, Pauley RJ, Tait L. Breast stroma plays a dominant regulatory role in breast epithelial growth and differentiation: implications for tumor development and progression. Cancer Res 2001 61:1320-1326.

Shimoyama Y, Hirohashi S. Expression of E- and P-cadherin in gastric carcinomas. Cancer Res 1991 51:2185-2192.

Shimoyama Y, Hirohashi S, Hirano S, Noguchi M, Shimosato Y, Takeichi M, Abe O. Cadherin cell-adhesion molecules in human epithelial tissues and carcinomas. Cancer Res 1989 49:2128-2133.

Simpson P. Maternal-Zygotic Gene Interactions during Formation of the Dorsoventral Pattern in Drosophila Embryos. Genetics 1983 105:615-632.

Sixt M, Engelhardt B, Pausch F, Hallmann R, Wendler O, Sorokin LM. Endothelial cell laminin isoforms, laminins 8 and 10, play decisive roles in T cell recruitment across the blood-brain barrier in experimental autoimmune encephalomyelitis. J Cell Biol 2001 153:933-946.

Somasiri A, Howarth A, Goswami D, Dedhar S, Roskelley CD. Overexpression of the integrin-linked kinase mesenchymally transforms mammary epithelial cells. J Cell Sci 2001 114:1125-1136.

Sonnenberg A, Janssen H, Hogervorst F, Calafat J, Hilgers J. A complex of platelet glycoproteins Ic and IIa identified by a rat monoclonal antibody. J Biol Chem 1987 262:10376-10383.

Sonnenberg A, Liem RK. Plakins in development and disease. Exp Cell Res 2007 313:2189-2203.

Sordat I, Bosman FT, Dorta G, Rousselle P, Aberdam D, Blum AL, Sordat B. Differential expression of laminin-5 subunits and integrin receptors in human colorectal neoplasia. J Pathol 1998 185:44-52.

Spaderna S, Schmalhofer O, Hlubek F, Berx G, Eger A, Merkel S, Jung A, Kirchner T, Brabletz T. A transient, EMT-linked loss of basement membranes indicates metastasis and poor survival in colorectal cancer. Gastroenterology 2006 131:830-840.

Spinardi L, Einheber S, Cullen T, Milner TA, Giancotti FG. A recombinant tail-less integrin beta 4 subunit disrupts hemidesmosomes, but does not suppress alpha 6 beta 4-mediated cell adhesion to laminins. J Cell Biol 1995 129:473-487.

Spinardi L, Marchisio PC. Podosomes as smart regulators of cellular adhesion. Eur J Cell Biol 2006 85:191-194.

Spinardi L, Rietdorf J, Nitsch L, Bono M, Tacchetti C, Way M, Marchisio PC. A dynamic podosome-like structure of epithelial cells. Exp Cell Res 2004 295:360-374.

Stewart DM, Tian L, Nelson DL. Linking cellular activation to cytoskeletal reorganization: Wiskott-Aldrich syndrome as a model. Curr Opin Allergy Clin Immunol 2001 1:525-533.

Stuelten CH, DaCosta Byfield S, Arany PR, Karpova TS, Stetler-Stevenson WG, Roberts AB. Breast cancer cells induce stromal fibroblasts to express MMP-9 via secretion of TNF-alpha and TGF-beta. J Cell Sci 2005 118:2143-2153.

Sugimachi K, Tanaka S, Kameyama T, Taguchi K, Aishima S, Shimada M, Sugimachi K, Tsuneyoshi M. Transcriptional repressor snail and progression of human hepatocellular carcinoma. Clin Cancer Res 2003 9:2657-2664.

Sugiyama S, Utani A, Yamada S, Kozak CA, Yamada Y. Cloning and expression of the mouse laminin gamma 2 (B2t) chain, a subunit of epithelial cell laminin. Eur J Biochem 1995 228:120-128.

Takagi T, Moribe H, Kondoh H, Higashi Y. DeltaEF1, a zinc finger and homeodomain transcription factor, is required for skeleton patterning in multiple lineages. Development 1998 125:21-31.

Takebayashi S, Ogawa T, Jung KY, Muallem A, Mineta H, Fisher SG, Grenman R, Carey TE. Identification of new minimally lost regions on 18q in head and neck squamous cell carcinoma. Cancer Res 2000 60:3397-3403.

Taki M, Verschueren K, Yokoyama K, Nagayama M, Kamata N. Involvement of Ets-1 transcription factor in inducing matrix metalloproteinase-2 expression by epithelial-mesenchymal transition in human squamous carcinoma cells. Int J Oncol 2006 28:487-496.

Talts JF, Sasaki T, Miosge N, Gohring W, Mann K, Mayne R, Timpl R. Structural and functional analysis of the recombinant G domain of the laminin alpha4 chain and its proteolytic processing in tissues. J Biol Chem 2000 275:35192-35199.

Tamura RN, Rozzo C, Starr L, Chambers J, Reichardt LF, Cooper HM, Quaranta V. Epithelial integrin alpha 6 beta 4: complete primary structure of alpha 6 and variant forms of beta 4. J Cell Biol 1990 111:1593-1604.

Tan C, Costello P, Sanghera J, Domínguez D, Baulida J, de Herreros AG, Dedhar S. Inhibition of integrin linked kinase (ILK) suppresses beta-catenin-Lef/Tcf-dependent transcription and expression of the E-cadherin repressor, snail, in APC-/- human colon carcinoma cells. Oncogene 2001 20:133-140.

Tani T, Karttunen T, Kiviluoto T, Kivilaakso E, Burgeson RE, Sipponen P, Virtanen I. Alpha 6 beta 4 integrin and newly deposited laminin-1 and laminin-5 form the adhesion mechanism of gastric carcinoma. Continuous expression of laminins but not that of collagen VII is preserved in invasive parts of the carcinomas: implications for acquisition of the invading phenotype. Am J Pathol 1996 149:781-793.

Tani T, Lehto VP, Virtanen I. Expression of laminins 1 and 10 in carcinoma cells and comparison of their roles in cell adhesion. Exp Cell Res 1999 248:115-121.

Tani T, Lumme A, Linnala A, Kivilaakso E, Kiviluoto T, Burgeson RE, Kangas L, Leivo I, Virtanen I. Pancreatic carcinomas deposit laminin-5, preferably adhere to laminin-5, and migrate on the newly deposited basement membrane. Am J Pathol 1997 151:1289-1302.

Tarin D, Thompson EW, Newgreen DF. The fallacy of epithelial mesenchymal transition in neoplasia. Cancer Res 2005 65:5996-6000; discussion 6000-1.

Tarone G, Cirillo D, Giancotti FG, Comoglio PM, Marchisio PC. Rous sarcoma virus-transformed fibroblasts adhere primarily at discrete protrusions of the ventral membrane called podosomes. Exp Cell Res 1985 159:141-157.

Tartakoff AM. Perturbation of vesicular traffic with the carboxylic ionophore monensin. Cell 1983 32:1026-1028.

Teti A, Migliaccio S, Taranta A, Bernardini S, De Rossi G, Luciani M, Iacobini M, De Felice L, Boldrini R, Bosman C, Corsi A, Bianco P. Mechanisms of osteoclast dysfunction in human osteopetrosis: abnormal osteoclastogenesis and lack of osteoclast-specific adhesion structures. J Bone Miner Res 1999 14:2107-2117.

Thiery JP. Epithelial-mesenchymal transitions in tumour progression. Nat Rev Cancer 2002 2:442-454.

Thiery JP. Epithelial-mesenchymal transitions in development and pathologies. Curr Opin Cell Biol 2003 15:740-746.

Thompson EW, Newgreen DF, Tarin D. Carcinoma invasion and metastasis: a role for epithelial-mesenchymal transition? Cancer Res 2005 65:5991-5; discussion 5995.

Thyboll J, Kortesmaa J, Cao R, Soininen R, Wang L, Iivanainen A, Sorokin L, Risling M, Cao Y, Tryggvason K. Deletion of the laminin alpha4 chain leads to impaired microvessel maturation. Mol Cell Biol 2002 22:1194-1202.

Tiger CF, Champliaud MF, Pedrosa-Domellof F, Thornell LE, Ekblom P, Gullberg D. Presence of laminin alpha5 chain and lack of laminin alpha1 chain during human muscle development and in muscular dystrophies. J Biol Chem 1997 272:28590-28595.

Timpl R, Brown JC. Supramolecular assembly of basement membranes. Bioessays 1996 18:123-132.

Timpl R, Rohde H, Robey PG, Rennard SI, Foidart JM, Martin GR. Laminin--a glycoprotein from basement membranes. J Biol Chem 1979 254:9933-9937.

Tlsty TD, Coussens LM. Tumor stroma and regulation of cancer development. Annu Rev Pathol 2006 1:119-150.

Tomita K, van Bokhoven A, van Leenders GJ, Ruijter ET, Jansen CF, Bussemakers MJ, Schalken JA. Cadherin switching in human prostate cancer progression. Cancer Res 2000 60:3650-3654.

Toth M, Chvyrkova I, Bernardo MM, Hernandez-Barrantes S, Fridman R. Pro-MMP-9 activation by the MT1-MMP/MMP-2 axis and MMP-3: role of TIMP-2 and plasma membranes. Biochem Biophys Res Commun 2003 308:386-395.

Tran NL, Nagle RB, Cress AE, Heimark RL. N-Cadherin expression in human prostate carcinoma cell lines. An epithelial-mesenchymal transformation mediating adhesion withStromal cells. Am J Pathol 1999 155:787-798.

Turner DL, Weintraub H. Expression of achaete-scute homolog 3 in Xenopus embryos converts ectodermal cells to a neural fate. Genes Dev 1994 8:1434-1447.

Udani M, Zen Q, Cottman M, Leonard N, Jefferson S, Daymont C, Truskey G, Telen MJ. Basal cell adhesion molecule/lutheran protein. The receptor critical for sickle cell adhesion to laminin. J Clin Invest 1998 101:2550-2558.

Vainionpää N, Lehto VP, Tryggvason K, Virtanen I. Alpha4 chain laminins are widely expressed in renal cell carcinomas and have a de-adhesive function. Lab Invest 2007 87:780-791.

Wallquist W, Plantman S, Thams S, Thyboll J, Kortesmaa J, Lannergren J, Domogatskaya A, Ogren SO, Risling M, Hammarberg H, Tryggvason K, Cullheim S. Impeded interaction between Schwann cells and axons in the absence of laminin alpha4. J Neurosci 2005 25:3692-3700.

Van Aken E, De Wever O, Correia da Rocha AS, Mareel M. Defective E-cadherin/catenin complexes in human cancer. Virchows Arch 2001 439:725-751.

Van de Putte T, Maruhashi M, Francis A, Nelles L, Kondoh H, Huylebroeck D, Higashi Y. Mice lacking ZFHX1B, the gene that codes for Smad-interacting protein-1, reveal a role for multiple neural crest cell defects in the etiology of Hirschsprung disease-mental retardation syndrome. Am J Hum Genet 2003 72:465-470.

van der Flier A, Sonnenberg A. Function and interactions of integrins. Cell Tissue Res 2001a 305:285-298.

van der Flier A, Sonnenberg A. Structural and functional aspects of filamins. Biochim Biophys Acta 2001b 1538:99-117.

Vandewalle C, Comijn J, De Craene B, Vermassen P, Bruyneel E, Andersen H, Tulchinsky E, Van Roy F, Berx G. SIP1/ZEB2 induces EMT by repressing genes of different epithelial cell-cell junctions. Nucleic Acids Res 2005 33:6566-6578.

Wang J, Hoshijima M, Lam J, Zhou Z, Jokiel A, Dalton ND, Hultenby K, Ruiz-Lozano P, Ross J,Jr, Tryggvason K, Chien KR. Cardiomyopathy associated with microcirculation dysfunction in laminin alpha4 chain-deficient mice. J Biol Chem 2006 281:213-220.

Watt FM. Role of integrins in regulating epidermal adhesion, growth and differentiation. EMBO J 2002 21:3919-3926.

Watt FM, Hotchin NA. Kalinin, epiligrin and GB3 antigen: kalinepiligrinin-3? Curr Biol 1992 2:106-107.

Weaver AM. Invadopodia: specialized cell structures for cancer invasion. Clin Exp Metastasis 2006 23:97-105.

Weaver AM. Invadopodia. Curr Biol 2008 18:R362-4.

Vega S, Morales AV, Ocaña OH, Valdés F, Fabregat I, Nieto MA. Snail blocks the cell cycle and confers resistance to cell death. Genes Dev 2004 18:1131-1143.

Wehrle-Haller B, Imhof B. The inner lives of focal adhesions. Trends Cell Biol 2002 12:382-389.

Wehrle-Haller B, Imhof BA. Actin, microtubules and focal adhesion dynamics during cell migration. Int J Biochem Cell Biol 2003 35:39-50.

Weinberg RA. The Biology of Cancer. Garland Science, Taylor & Francis Group, New York, 2007.

Verrando P, Hsi BL, Yeh CJ, Pisani A, Serieys N, Ortonne JP. Monoclonal antibody GB3, a new probe for the study of human basement membranes and hemidesmosomes. Exp Cell Res 1987 170:116-128.

Verschueren K, Remacle JE, Collart C, Kraft H, Baker BS, Tylzanowski P, Nelles L, Wuytens G, Su MT, Bodmer R, Smith JC, Huylebroeck D. SIP1, a novel zinc finger/homeodomain repressor, interacts with Smad proteins and binds to 5'-CACCT sequences in candidate target genes. J Biol Chem 1999 274:20489-20498.

Wewer UM, Shaw LM, Albrechtsen R, Mercurio AM. The integrin alpha 6 beta 1 promotes the survival of metastatic human breast carcinoma cells in mice. Am J Pathol 1997a 151:1191-1198.

Wewer UM, Thornell LE, Loechel F, Zhang X, Durkin ME, Amano S, Burgeson RE, Engvall E, Albrechtsen R, Virtanen I. Extrasynaptic location of laminin beta 2 chain in developing and adult human skeletal muscle. Am J Pathol 1997b 151:621-631.

Vicovac L, Aplin JD. Epithelial-mesenchymal transition during trophoblast differentiation. Acta Anat (Basel) 1996 156:202-216.

Willberg J, Hormia M, Takkunen M, Kikkawa Y, Sekiguchi K, Virtanen I. Lutheran blood group antigen as a receptor for alpha5 laminins in gingival epithelia. J Periodontol 2007 78:1810-1818.

Willis BC, duBois RM, Borok Z. Epithelial origin of myofibroblasts during fibrosis in the lung. Proc Am Thorac Soc 2006 3:377-382.

Virolle T, Coraux C, Ferrigno O, Cailleteau L, Ortonne JP, Pognonec P, Aberdam D. Binding of USF to a non-canonical E-box following stress results in a cell-specific derepression of the lama3 gene. Nucleic Acids Res 2002 30:1789-1798.

Virtanen I, Gullberg D, Rissanen J, Kivilaakso E, Kiviluoto T, Laitinen LA, Lehto VP, Ekblom P. Laminin alpha1-chain shows a restricted distribution in epithelial basement membranes of fetal and adult human tissues. Exp Cell Res 2000 257:298-309.

Virtanen I, Miettinen M, Lehto VP, Kariniemi AL, Paasivuo R. Diagnostic application of monoclonal antibodies to intermediate filaments. Ann N Y Acad Sci 1985 455:635-648.

Witkowski CM, Bowden GT, Nagle RB, Cress AE. Altered surface expression and increased turnover of the alpha6beta4 integrin in an undifferentiated carcinoma. Carcinogenesis 2000 21:325-330.

Vleminckx K, Vakaet L,Jr, Mareel M, Fiers W, van Roy F. Genetic manipulation of E-cadherin expression by epithelial tumor cells reveals an invasion suppressor role. Cell 1991 66:107-119.

Wolf K, Mazo I, Leung H, Engelke K, von Andrian UH, Deryugina EI, Strongin AY, Bröcker EB, Friedl P. Compensation mechanism in tumor cell migration: mesenchymal-amoeboid transition after blocking of pericellular proteolysis. J Cell Biol 2003 160:267-277.

Wondimu Z, Geberhiwot T, Ingerpuu S, Juronen E, Xie X, Lindbom L, Doi M, Kortesmaa J, Thyboll J, Tryggvason K, Fadeel B, Patarroyo M. An endothelial laminin isoform, laminin 8 (alpha4beta1gamma1), is secreted by blood neutrophils, promotes neutrophil migration and extravasation, and protects neutrophils from apoptosis. Blood 2004 104:1859-1866.

Vuoristo S, Virtanen I, Takkunen M, Palgi J, Kikkawa Y, Rousselle P, Sekiguchi K, Tuuri T, Otonkoski T. Laminin isoforms in human embryonic stem cells: Synthesis, receptor usage and growth support. J Cell Mol Med 2009 13:2622-2633.

Yamaguchi H, Condeelis J. Regulation of the actin cytoskeleton in cancer cell migration and invasion. Biochim Biophys Acta 2007 1773:642-652.

Yamaguchi H, Lorenz M, Kempiak S, Sarmiento C, Coniglio S, Symons M, Segall J, Eddy R, Miki H, Takenawa T, Condeelis J. Molecular mechanisms of invadopodium formation: the role of the N-WASP-Arp2/3 complex pathway and cofilin. J Cell Biol 2005a 168:441-452.

Yamaguchi H, Wyckoff J, Condeelis J. Cell migration in tumors. Curr Opin Cell Biol 2005b 17:559-564.

Yamamoto H, Itoh F, Iku S, Hosokawa M, Imai K. Expression of the gamma(2) chain of laminin-5 at the invasive front is associated with recurrence and poor prognosis in human esophageal squamous cell carcinoma. Clin Cancer Res 2001 7:896-900.

Yan W, Shao R. Transduction of a mesenchyme-specific gene periostin into 293T cells induces cell invasive activity through epithelial-mesenchymal transformation. J Biol Chem 2006 281:19700-19708.

Yang MH, Chang SY, Chiou SH, Liu CJ, Chi CW, Chen PM, Teng SC, Wu KJ. Overexpression of NBS1 induces epithelial-mesenchymal transition and co-expression of NBS1 and Snail predicts metastasis of head and neck cancer. Oncogene 2007 26:1459-1467.

Yang X, Pursell B, Lu S, Chang TK, Mercurio AM. Regulation of beta 4-integrin expression by epigenetic modifications in the mammary gland and during the epithelial-to-mesenchymal transition. J Cell Sci 2009 122:2473-2480.

Yang Z, Rayala S, Nguyen D, Vadlamudi RK, Chen S, Kumar R. Pak1 phosphorylation of snail, a master regulator of epithelial-to-mesenchyme transition, modulates snail's subcellular localization and functions. Cancer Res 2005 65:3179-3184.

Yanjia H, Xinchun J. The role of epithelial-mesenchymal transition in oral squamous cell carcinoma and oral submucous fibrosis. Clin Chim Acta 2007 383:51-56.

Yilmaz M, Christofori G. EMT, the cytoskeleton, and cancer cell invasion. Cancer Metastasis Rev 2009 28:15-33.

Ylikoski J, Pirvola U, Närvänen O, Virtanen I. Nonerythroid spectrin (fodrin) is a prominent component of the cochlear hair cells. Hear Res 1990 43:199-203.

Ylänne J, Virtanen I. The Mr 140,000 fibronectin receptor complex in normal and virus-transformed human fibroblasts and in fibrosarcoma cells: identical localization and function. Int J Cancer 1989 43:1126-1136.

Yokoyama K, Kamata N, Fujimoto R, Tsutsumi S, Tomonari M, Taki M, Hosokawa H, Nagayama M. Increased invasion and matrix metalloproteinase-2 expression by Snail-induced mesenchymal transition in squamous cell carcinomas. Int J Oncol 2003 22:891-898.

Yokoyama K, Kamata N, Hayashi E, Hoteiya T, Ueda N, Fujimoto R, Nagayama M. Reverse correlation of E-cadherin and snail expression in oral squamous cell carcinoma cells in vitro. Oral Oncol 2001 37:65-71.

Yook JI, Li XY, Ota I, Fearon ER, Weiss SJ. Wnt-dependent regulation of the E-cadherin repressor snail. J Biol Chem 2005 280:11740-11748.

Yurchenco PD, Amenta PS, Patton BL. Basement membrane assembly, stability and activities observed through a developmental lens. Matrix Biol 2004 22:521-538.

Yurchenco PD, Quan Y, Colognato H, Mathus T, Harrison D, Yamada Y, O'Rear JJ. The alpha chain of laminin-1 is independently secreted and drives secretion of its beta- and gamma-chain partners. Proc Natl Acad Sci U S A 1997 94:10189-10194.

Zaidel-Bar R, Cohen M, Addadi L, Geiger B. Hierarchical assembly of cell-matrix adhesion complexes. Biochem Soc Trans 2004 32:416-420.

Zambonin-Zallone A, Teti A, Grano M, Rubinacci A, Abbadini M, Gaboli M, Marchisio PC. Immunocytochemical distribution of extracellular matrix receptors in human osteoclasts: a beta 3 integrin is colocalized with vinculin and talin in the podosomes of osteoclastoma giant cells. Exp Cell Res 1989 182:645-652.

Zamir E, Geiger B. Molecular complexity and dynamics of cell-matrix adhesions. J Cell Sci 2001 114:3583-3590.

Zeisberg M, Kalluri R. The role of epithelial-to-mesenchymal transition in renal fibrosis. J Mol Med 2004 82:175-181.

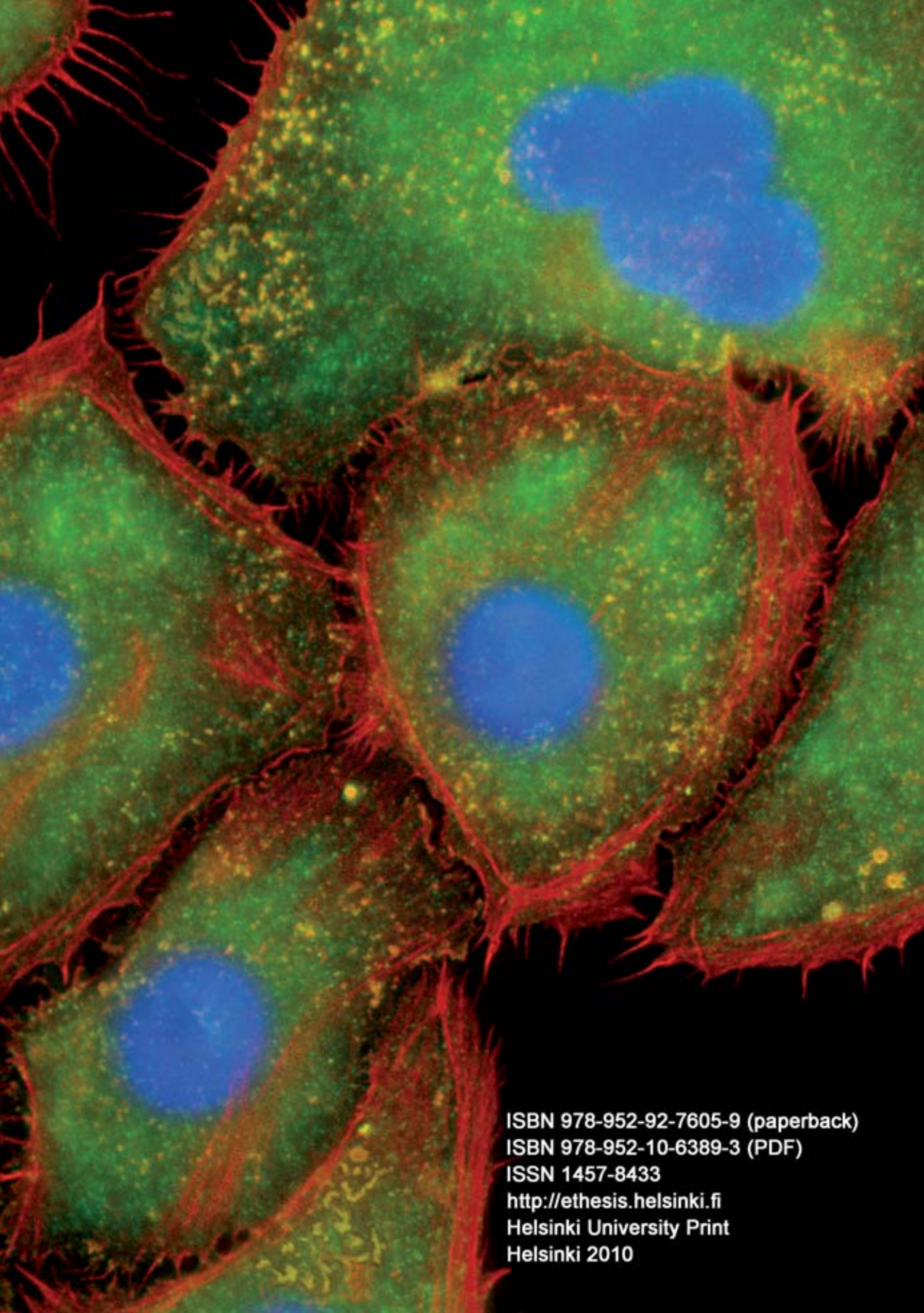
Zhou BP, Deng J, Xia W, Xu J, Li YM, Gunduz M, Hung MC. Dual regulation of Snail by GSK-3beta-mediated phosphorylation in control of epithelial-mesenchymal transition. Nat Cell Biol 2004 6:931-940.

Zhu J, Yu D, Zeng XC, Zhou K, Zhan X. Receptor-mediated endocytosis involves tyrosine phosphorylation of cortactin. J Biol Chem 2007 282:16086-16094.

Ziober AF, Falls EM, Ziober BL. The extracellular matrix in oral squamous cell carcinoma: friend or foe? Head Neck 2006 28:740-749.

Zweier C, Albrecht B, Mitulla B, Behrens R, Beese M, Gillessen-Kaesbach G, Rott HD, Rauch A. "Mowat-Wilson" syndrome with and without Hirschsprung disease is a distinct, recognizable multiple congenital anomalies-mental retardation syndrome caused by mutations in the zinc finger homeo box 1B gene. Am J Med Genet 2002 108:177-181.

12 ORIGINAL PUBLICATIONS



ISBN 978-952-92-7605-9 (paperback)
ISBN 978-952-10-6389-3 (PDF)
ISSN 1457-8433
http://ethesis.helsinki.fi
Helsinki University Print
Helsinki 2010